

THE UNIVERSITY OF CALGARY

**HYDRAULICS OF PIVOTING SHARP CRESTED WEIRS**

BY

LJILJANA BOZIC

A THESIS

SUBMITTED TO THE FACULTY OF GRADUATE STUDIES  
IN PARTIAL FULFILLMENT OF THE REQUIREMENTS FOR THE  
DEGREE OF MASTER OF SCIENCE IN ENGINEERING

DEPARTMENT OF CIVIL ENGINEERING

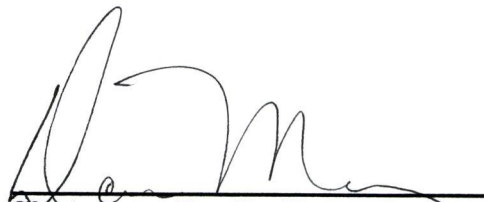
CALGARY, ALBERTA

JANUARY, 1991

© LJILJANA BOZIC, 1991

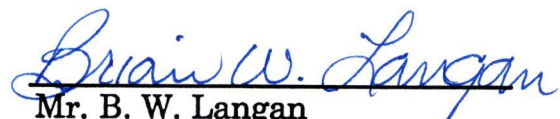
THE UNIVERSITY OF CALGARY  
FACULTY OF GRADUATE STUDIES

The undersigned certify that they have read, and recommend to the Faculty of Graduate Studies for acceptance, a thesis entitled "Hydraulics of Pivoting Sharp Crested Weirs" , submitted by Ljiljana Bozic in partial fulfillment of the requirements for the degree of Master of Science in Engineering.




---

Chairman, Dr. D. H. Manz  
Department of Civil Engineering



---

Mr. B. W. Langan  
Department of Civil Engineering



---

Dr. J. S. deKrasinski,  
Department of Mechanical  
Engineering

## ABSTRACT

This study is concerned with the hydraulic characteristics of pivoting sharp crested rectangular weirs operating under free and submerged outlet conditions in rectangular open channels. The study was initiated as the irrigation practices used in Southern Alberta require that the hydraulics of weir-type check structures be known over the entire range of their operation. A literature search, however, showed that a study which considers combined effects of weir and channel geometry, weir inclination and submergence on a single weir could not be found.

The data required for this study were collected in an extensive experimental program, conducted in the experimental flume on nine model weirs. The flume and model weirs were designed so that the variety of flow conditions can be simulated. The data were used to determine the values of effective discharge coefficients, inclination coefficients and submergence coefficients for a variety of flow conditions. An equation which assumes that the effects of geometry, inclination and submergence are multiplicative was used in the analysis. The results of the analysis are presented here and the applicability of equation used is commented upon.

## ACKNOWLEDGEMENTS

I wish to express my gratitude to my supervisor, Dr. D. H. Manz, for his support throughout the course of this study. I am indebted to him for his continuous availability and genuine interest during the last two years. He suggested the topic of this research, and our discussions were essential for the completion of the thesis.

Special thanks go to Mr. D. Anson, the technician responsible for the hydraulics laboratory whose help in the experimental course of work was invaluable and much appreciated.

I wish to extend my appreciation to the Faculty, staff and fellow graduate students of the Department of Civil Engineering for making my studies productive and enjoyable.

The financial support from the University of Calgary is gratefully acknowledged.

## TABLE OF CONTENTS

ABSTRACT .....	iii
ACKNOWLEDGEMENTS.....	iv
TABLE OF CONTENTS .....	v
LIST OF TABLES .....	viii
LIST OF FIGURES.....	xi
NOTATION .....	xvi

### Chapter 1

#### PROBLEM DEFINITION

1.1	Introduction.....	1
1.2	Literature Review .....	5
1.2.1	The Bazin's Equation .....	5
1.2.2	The Equations of Francis, La Sia and King .....	10
1.2.3	The Rehboch's Equation .....	11
1.2.4	The Rouse's Equation .....	12
1.2.5	The Equation Proposed by MIS USSR .....	12
1.2.6	The Herschel's Equation .....	15
1.2.7	The MIS USSR Equation .....	16
1.2.8	The Equation Proposed by D. Manz .....	18

1.3	Conclusion .....	19
1.4	Objectives of the Study .....	20

## Chapter 2

### LABORATORY SET-UP AND EXPERIMENTAL PROCEDURE

2.1	Design Criteria .....	21
2.2	Apparatus Layout .....	22
2.2.1	Experimental Flume .....	22
2.2.2	Supply System .....	25
2.2.3	Model Weirs .....	25
2.2.4	Downstream Control and Measuring Devices .....	27
2.3	Experimental Procedure .....	27
2.3.1	General.....	27
2.3.2	Experimental Runs for Unsubmerged Flow .....	28
2.3.3	Experimental Runs for Submerged Flow .....	28
2.3.4	Measurement Procedure .....	29
2.3.5	Entrance conditions .....	31

## Chapter 3

### DATA OBSERVATIONS AND ANALYSIS

3.1	Introduction .....	32
3.2	Unsubmerged Flow .....	32

3.3	Submerged Flow .....	85
3.4	Error Analysis .....	100
Chapter 4		
	DISCUSSION OF RESULTS .....	103
Chapter 5		
	CONCLUSIONS AND RECOMMENDATIONS	
5.1	Conclusions .....	106
5.2	Recommendations .....	117
	REFERENCES .....	118
	APPENDIX A.....	122
	APPENDIX B.....	127

## LIST OF TABLES

TABLE		PAGE
Table 1	Inclination coefficients (Bazin).....	8
Table 2	Length and width of model weirs.....	26
Table 3	Example of worksheet with unsubmerged flow data.....	34
Table 4	Example of worksheet with unsubmerged flow data summary...	43
Table 5	Values of $K_1$ for weir length 75 mm, and width 270 mm .....	54
Table 6	Values of $K_1$ for weir length 155 mm, and width 270 mm .....	54
Table 7	Values of $K_1$ for weir length 230 mm, and width 270 mm .....	55
Table 8	Values of $K_1$ for weir length 75 mm, and width 420 mm .....	55
Table 9	Values of $K_1$ for weir length 155 mm, and width 420 mm .....	56
Table 10	Values of $K_1$ for weir length 230 mm, and width 420 mm .....	56
Table 11	Values of $K_1$ for weir length 75 mm, and width 570 mm .....	57
Table 12	Values of $K_1$ for weir length 155 mm, and width 570 mm .....	57
Table 13	Values of $K_1$ for weir length 230 mm, and width 570 mm .....	58
Table 14	Example of worksheet with data summary and $K_0$ .....	67
Table 15	Values of $K_0$ for weir length 75 mm, and width 270 mm .....	75
Table 16	Values of $K_0$ for weir length 155 mm, and width 270 mm .....	75
Table 17	Values of $K_0$ for weir length 230 mm, and width 270 mm .....	76
Table 18	Values of $K_0$ for weir length 75 mm, and width 420 mm .....	76



Table 19	Values of $K_0$ for weir length 155 mm, and width 420 mm .....	77
Table 20	Values of $K_0$ for weir length 230 mm, and width 420 mm .....	77
Table 21	Values of $K_0$ for weir length 75 mm, and width 570 mm .....	78
Table 22	Values of $K_0$ for weir length 155 mm, and width 570 mm .....	78
Table 23	Values of $K_0$ for weir length 230 mm, and width 570 mm .....	79
Table 24	Example of worksheet with submerged flow data .....	86
Table 25	Example of worksheet with submerged flow data summary and calculated exponents $m$ , $b$ and coefficients $K_2$ .....	89
Table 26	Values of $m$ , $b$ , and $R$ for weir of length 75 mm and width 420 mm .....	95
Table 27	Values of $m$ , $b$ , and $R$ for weir of length 155 mm and width 420 mm .....	96
Table 28	Values of $m$ , $b$ , and $R$ for weir of length 75 mm and width 570 mm .....	96
Table 29	Values of $m$ , $b$ , and $R$ for weir of length 155 mm and width 570 mm .....	96
Table 30	Values of $m$ , $b$ , and $R$ for weir of length 75 mm and width 270 mm .....	97
Table 31	Values of $m$ , $b$ , and $R$ for weir of length 155 mm and width 270 mm .....	97
Table 32	Values of $m$ , $b$ , and $R$ for weir of length 230 mm and width 270 mm .....	97

Table 33	Error analysis for unsubmerged flow over weir .....	101
Table 34	$K_0$ range for different weir widths .....	108

## LIST OF FIGURES

FIGURE	PAGE
Fig.1	Installation with pivoting sharp crested rectangular weir operating under free flow conditions .....2
Fig.2	Installation with pivoting sharp crested rectangular weir operating under submerged flow conditions.....2
Fig.3	Weir in operation.....4
Fig.4	Free nappe.....7
Fig.5	Depressed nappe.....7
Fig.6	Clinging nappe.....7
Fig.7	Contracted flow over weir.....8
Fig.8	Frontally inclined weir.....13
Fig. 9	Weir inclined backwards.....14
Fig.10	Submerged weir.....16
Fig.11	Submerged weir - relative drop in water level.....17
Fig.12	Experimental flume layout.....23
Fig.13	Experimental flume - detail with the model weir.....24
Fig.14	Q vs $H_1$ for weir length 155 mm, width 420 mm and inclination of $\theta=24.8^\circ$ , $\theta=31.1^\circ$ , $\theta=37.8^\circ$ , and $\theta=45.2^\circ$ .....35
Fig.15	Q vs $H_1$ for weir length 155 mm, width 420 mm and inclination of $\theta=53.8^\circ$ , $\theta=64.6^\circ$ , and $\theta=90^\circ$ .....36

Fig.16	Q vs $H_1$ for weir length 75 mm, width 270 mm, and weir length 155 mm, width 420 mm .....	37
Fig.17	Q vs $H_1$ for weir length 230 mm, width 270 mm, and weir length 75 mm, width 420 mm .....	38
Fig.18	Q vs $H_1$ for weir length 155 mm, width 420 mm, and weir length 230 mm, width 420 mm.....	39
Fig.19	Q vs $H_1$ for weir length 75 mm, width 570 mm, and weir length 155 mm, width 570 mm.....	40
Fig.20	Q vs $H_1$ for weir length 230 mm, width 570 mm .....	41
Fig.21	Q vs $CxH_1^{1.5}$ for weir length 155 mm, width 420 mm, and inclination of $\theta=24.8^\circ$ , $\theta=31.1^\circ$ , $\theta=37.8^\circ$ , and $\theta=45.2^\circ$ .....	44
Fig.22	Q vs $CxH_1^{1.5}$ for weir length 155 mm, width 420 mm, and inclination $\theta=53.8^\circ$ , $\theta=64.6^\circ$ , and $\theta=90^\circ$ .....	45
Fig.23	Q vs $CxH_1^{1.5}$ for weir length 75 mm, width 270 mm, and weir length 155 mm, width 270 mm .....	46
Fig.24	Q vs $CxH_1^{1.5}$ for weir length 230 mm, width 270 mm, and weir length 75 mm, width 420 mm.....	47
Fig.25	Q vs $CxH_{11.5}^{1.5}$ for weir length 155 mm, width 420 mm, and weir length 230 mm, width 420 mm .....	48
Fig.26	Q v $CxH_1^{1.5}$ for weir length 75 mm, width 570 mm, and weir length 155 mm, width 570 mm .....	49
Fig.27	Q vs $CxH_1^{1.5}$ for weir length 230 mm, width 570 mm.....	50

Fig.28	$K_1$ vs $\theta$ for weir length 75 mm, width 270 mm .....	59
Fig.29	$K_1$ vs $\theta$ for weir length 155 mm, width 270 mm.....	59
Fig.30	$K_1$ vs $\theta$ for weir length 230 mm, width 270 mm.....	60
Fig.31	$K_1$ vs $\theta$ for weir length 75 mm, width 420 mm.....	60
Fig.32	$K_1$ vs $\theta$ for weir length 155 mm, width 420 mm.....	61
Fig.33	$K_1$ vs $\theta$ for weir length 230 mm, width 420 mm.....	61
Fig.34	$K_1$ vs $\theta$ for weir length 75 mm, width 570 mm.....	62
Fig.35	$K_1$ vs $\theta$ for weir length 155 mm, width 570 mm.....	62
Fig.36	$K_1$ vs $\theta$ for weir length 230 mm, width 570 mm.....	63
Fig.37	$Q$ vs $K_e \times C_x H_1^{1.5}$ for weir length 155 mm, width 420 mm, and inclination of $\theta=24.6^\circ, \theta=31.1^\circ, \theta=37.8^\circ, \theta=45.2^\circ$ .....	68
Fig.38	$Q$ vs $K_e \times C_x H_1^{1.5}$ for weir length 155 mm, width 420 mm, and inclination of $\theta=53.8^\circ, \theta=64.6^\circ$ , and $\theta=90^\circ$ .....	69
Fig.39	$Q$ vs $K_e \times C_x H_1^{1.5}$ for weir length 75 mm, width 270 mm, and weir length 155 mm, width 270 mm .....	70
Fig.40	$Q$ vs $K_e \times C_x H_1^{1.5}$ for weir length 230 mm, width 270 mm, and weir length 75 mm, width 420 mm .....	71
Fig.41	$Q$ vs $K_e \times C_x H_1^{1.5}$ for weir length 155 mm, width 420 mm, and weir length 230 mm, width 420 mm .....	72
Fig.42	$Q$ vs $K_e \times C_x H_1^{1.5}$ for weir length 75 mm, width 570 mm, and weir length 155 mm, width 570 mm .....	73
Fig.43	$Q$ vs $K_e \times C_x H_1^{1.5}$ for weir length 230 mm, width 570 mm .....	74

Fig.44	$K_\theta$ vs $\theta$ for weir length 75 mm, width 270 mm .....	80
Fig.45	$K_\theta$ vs $\theta$ for weir length 155 mm, width 270 mm .....	80
Fig.46	$K_\theta$ vs $\theta$ for weir length 230 mm, width 270 mm .....	81
Fig.47	$K_\theta$ vs $\theta$ for weir length 75 mm, width 420 mm.....	81
Fig.48	$K_\theta$ vs $\theta$ for weir length 155 mm, width 420 mm .....	82
Fig.49	$K_\theta$ vs $\theta$ for weir length 230 mm, width 420 mm .....	82
Fig.50	$K_\theta$ vs $\theta$ for weir length 75 mm, width 570 mm .....	83
Fig.51	$K_\theta$ vs $\theta$ for weir length 155 mm, width 570 mm .....	83
Fig.52	$K_\theta$ vs $\theta$ for weir length 230 mm, width 570 mm .....	84
Fig.53	Slope m and intercept b for weir length 155 mm, width 420 mm and inclination $\theta=24.6^\circ$ and $\theta=31.1^\circ$ .....	90
Fig.54	Slope m and intercept b for weir length 155 mm, width 420 mm and inclination $\theta=37.8^\circ$ and $\theta=45.2^\circ$ .....	91
Fig.55	Slope m and intercept b for weir length 155 mm, width 420 mm and inclination $\theta=53.8^\circ$ and $\theta=64.6^\circ$ .....	92
Fig.56	Slope m and intercept b for weir length 155 mm, width 420 mm and inclination $\theta=90^\circ$ .....	93
Fig.57	Slope m and intercept b for weir length 155 mm, width 420 mm and all angles of inclination .....	94
Fig.58	Surface jet observed on submerged weir of length 230 mm, and width 420 mm .....	99

Fig.59	Surface jet observed on submerged weir of length 230 mm, and width 570 mm .....	99
Fig.60	$K_\theta$ vs $\theta$ for weir width 270 mm .....	109
Fig.61	$K_\theta$ vs $\theta$ for weir width 420 mm .....	110
Fig.62	$K_\theta$ vs $\theta$ for weir width 570 mm .....	111
Fig.63	$K_\theta$ vs $\theta$ for weir length 75 mm .....	112
Fig.64	$K_\theta$ vs $\theta$ for weir length 155 mm.....	113
Fig.65	$K_\theta$ vs $\theta$ for weir length 230 mm .....	114
Fig.66	Surface jet observed on submerged weir of length 155 mm, and width 420 mm.....	125
Fig.67	Surface jet observed on submerged weir of length 155 mm, and width 570 mm .....	125
Fig.68	Surface jet observed on submerged weir of length 75 mm, and width 420 mm .....	126
Fig.69	Surface jet observed on submerged weir of length 155 mm, and width 270 mm .....	126

## NOTATION

$b$	- width of model weir
$B$	- width of experimental flume
$C$	- constant for one width of weir
$d_1$	- depth of flow upstream of weir
$d_2$	- depth of flow downstream of weir
$D_1, D_2, \dots, D_6$	- downstream depth readings
$D_{av}$	- average of downstream depth readings
$g$	- acceleration due to gravity
$H_1$	- upstream head over weir
$H_2$	- downstream head over weir
$K_1$	- discharge coefficient for unsubmerged flow over weir
$K_2$	- discharge coefficient for submerged flow over weir
$K_o$	- effective discharge coefficient
$K_\theta$	- inclination coefficient
$l$	- length of contracted flow
$L$	- length of model weir
$m$	- empirically determined exponential factor
$n$	- size of sample
$P$	- height of weir crest from channel bottom



$Q$	- discharge over weir
$U_1, U_2, U_3$	- upstream depth readings
$U_{av}$	- average of upstream depth readings
$x_i$	- independent variable
$y_i$	- dependent variable
$y_{intercept}$	- point at which line intercepts through the y-axis
$\beta_0$	- point at which line intercepts through y-axis
$\beta_1$	- amount of increase in the deterministic component of y for every one unit of increase in x, i.e. the slope of the line
$\xi$	- mass density of fluid
$\varepsilon$	- random error
$\sigma$	- surface tension of fluid
$\sigma_s$	- submergence coefficient in MIS USSR equation
$\theta$	- angle of weir inclination

## Chapter 1

### PROBLEM DEFINITION

#### 1.1 Introduction

The rectangular sharp crested pivoting weir is a hydraulic structure extensively used in irrigation for stream flow diversion. A sketch and photograph of typical pivoting weir in operation are shown on Fig.1, Fig.2 and Fig 3.

Check structures are used to increase the upstream depth of water to facilitate diversions through orifice-type outlets which otherwise might not have sufficient head to operate. If the check forms an inlet to a drop structure, the pivoting weir may be put on a fixed weir in order to avoid erosive water velocities in the upstream channel.

The standard rectangular pivoting sharp crested weir is a smooth plate with sharp top edge which ensures a line of contact with the flow. The weir crest is horizontal and located at height  $P$  above the channel bottom. The weir can be adjusted from the horizontal position to a near vertical position. The width of the approach channel is  $B$  and the width of the weir is  $b$ . When the weir is in a vertical position and weir width is sufficiently less than width of the approach channel, the sides of the stream may be fully contracted. This is

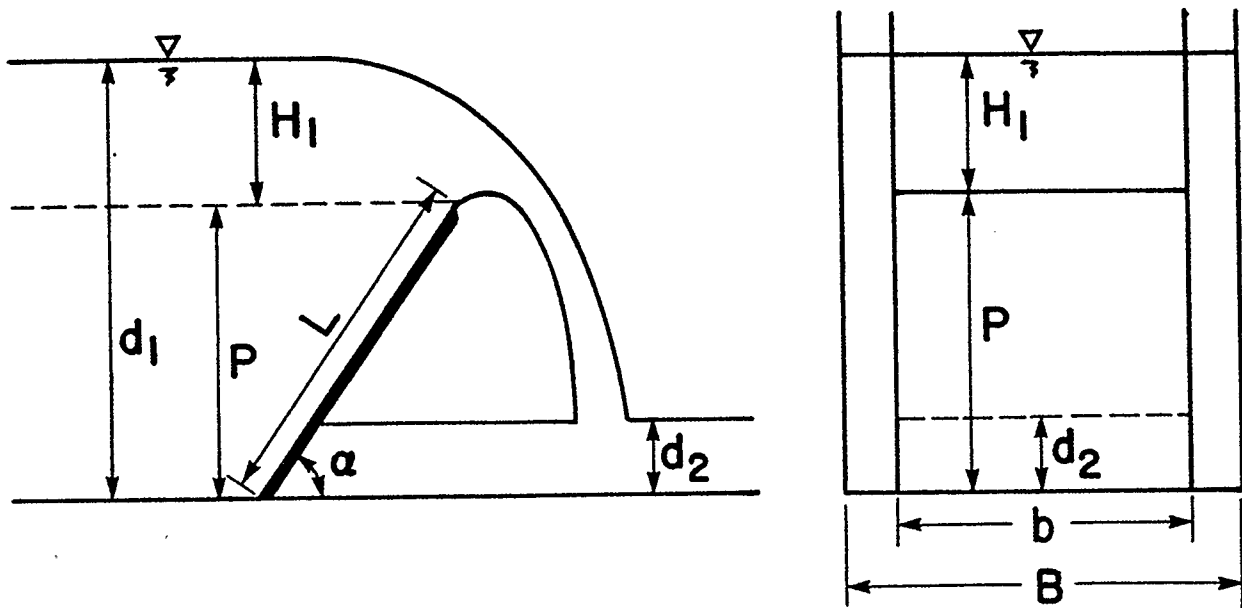


Fig.1 Installation with pivoting sharp crested rectangular weir operating under free flow conditions

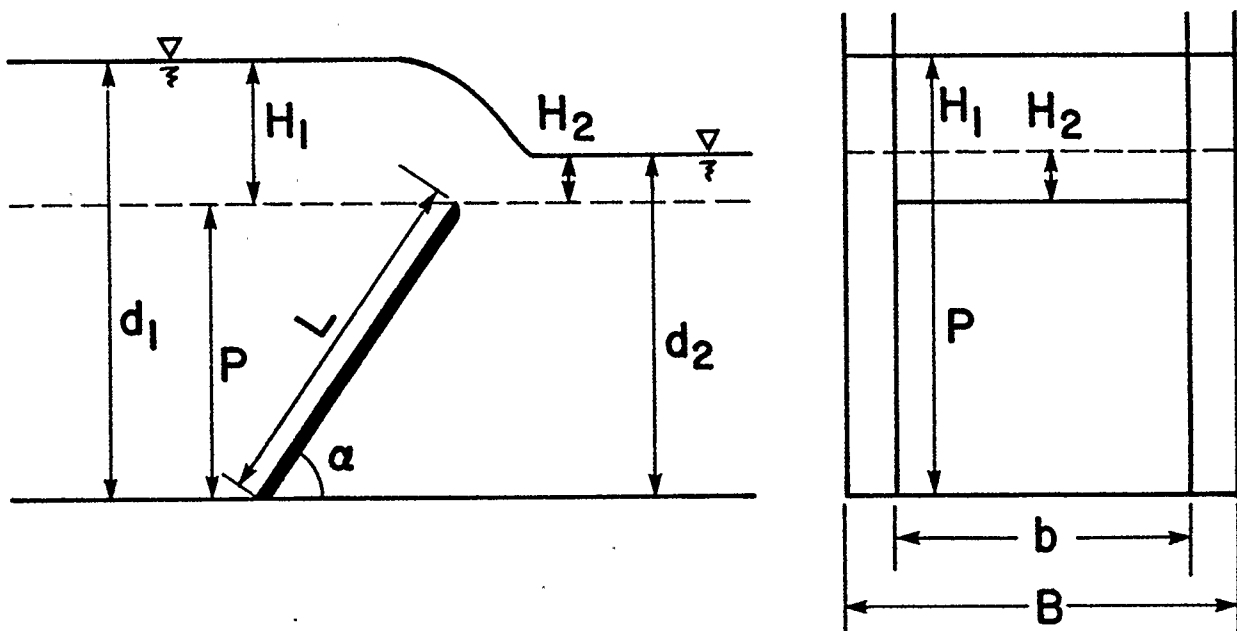


Fig.2 Installation with pivoting sharp crested rectangular weir operating under submerged conditions

called a weir with end contractions. If the approach channel and weir are of same width and shape, the water flows over the weir without being deflected from the vertical planes. This is called a weir without end contractions or a suppressed weir. In case of an inclined weir, the stream of flow entering the weir is neither fully contracted nor suppressed but somewhere between, and the weir can not be considered to operate in either suppressed or contracted mode.

The weir operates under free flow conditions when the nappe is free and downstream depth of the flow does not affect the discharge over weir. The weir operates under submerged flow conditions when the nappe rises above the weir crest and the discharge is influenced by the downstream head over weir  $H_2$ .

The first weir-type structures have been designed in Europe in the beginning of nineteenth century and consequently prompted first studies dealing with the hydraulics of a weir. Since then a number of studies dealing with the factors influencing the discharge over weir have been reported. Different authors have proposed equations that describe the weir hydraulics, as will be discussed in part 1.2. Even though these studies make a significant contribution to understanding complexity of factors that influence the discharge characteristics of a weir, they simplify the actual hydraulics of flow and do not consider combined effects of several factors on a single weir. The influence of weir angle on discharge coefficient is still poorly defined and understood. Very few papers dealing with the weirs operating under

submerged flow conditions could be found, which is partly due to the limited use of submerged weirs and consequent lack of experimental data.

In recent years a great number of weir-type structures are being used in irrigation as check structures. Automatic operation of irrigation systems requires that the precise hydraulic characteristics of a weir over entire range of operation be known. Thus the need was created for a detailed study which adequately describes the flow over weir and does not simplify the complex hydraulic characteristics of a structure.



Fig. 3 Weir in operation

## 1.2 Literature Review

In this review only the published research on the hydraulic characteristics of vertical and inclined pivoting overshoot sharp crested weirs operating under free flow and submerged conditions relevant for this study is reported and commented upon.

### 1.2.1 The Bazin's Equation

The structures like the Poiree weir and Chanoine weir were created in France in nineteenth century and likely encouraged Bazin's research<sup>(8)</sup>. Bazin developed an equation for flow over weir in a form<sup>(8)</sup>:

$$Q = K_1 \times b \times \sqrt{2g} \times H_1^{1.5} \quad (1)$$

where:  $b$  = width of weir

$H_1$  = head over weir

$K_1$  = Bazin's discharge coefficient

Equation (1) was developed for steady flow conditions and constant head  $H_1$ .

Bazin found that discharge coefficient  $K_1$  is influenced by the velocity of

flow approaching the weir, longitudinal and lateral contractions of flow over weir, aeration of the nappe, inclination of the weir and the degree of submergence. He developed different expressions for the discharge coefficient considering the effects of a single factor on flow over weir.

#### (a) The Effect of the Approach Velocity

The Equation (1) is valid if the velocity of flow over weir is assumed to be zero. The approach velocity, however, may have values significantly different from zero. Bazin found that the values of discharge coefficient  $K_1$  when the velocity of approaching flow is significant may be determined using the relation<sup>(12)</sup>:

$$K_1 = 0.425 + 0.21 \times \frac{H_1^2}{(P + H_1)^2} \quad (2)$$

where  $P$  is a weir height, or the vertical distance from the channel bottom to the weir crest.

#### (b) The Effect of the Shape of a Nappe

Bazin's experimental analysis has shown that different shapes of a weir nappe greatly affect the values of a discharge coefficient<sup>(12)</sup>. Equation (1) is correct for a free nappe and atmospheric pressure under the nappe (Fig.4). In the case of an unstable depressed nappe (Fig.5), or clinging nappe (Fig.6) the values of  $K_1$  significantly increase, as a result of the instability of flow over

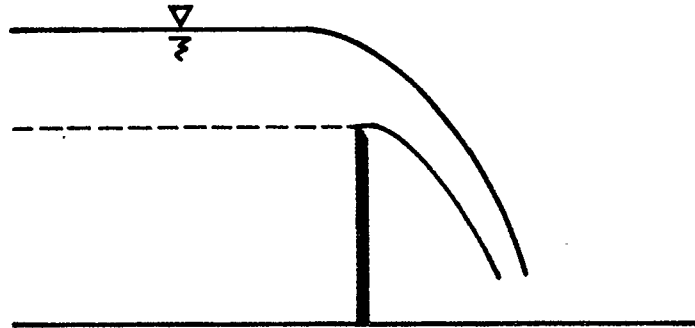


Fig.4 Free nappe

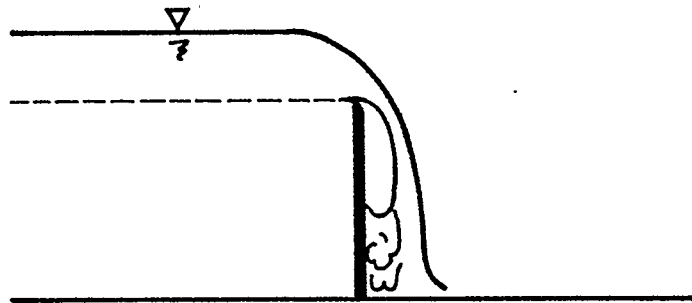


Fig.5 Depressed nappe

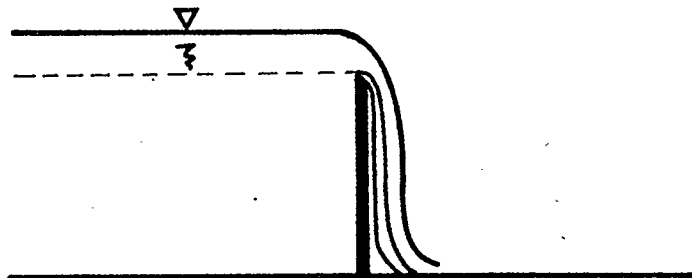


Fig.6 Clinging nappe



weir, pressure that is less than atmospheric and loss of energy of flow in turbulent fluctuations.

(c) Lateral Contraction of Flow

The equation (1) is correct if there is no lateral contraction of the flow over weir. In the case of contracted flow, the discharge over weir decreases and the Eq.(1) becomes<sup>(12)</sup>:

$$Q = K_1 \times \left(b - \frac{H_1}{5}\right) \times \sqrt{2g} \times H_1^{1.5} \quad (3)$$

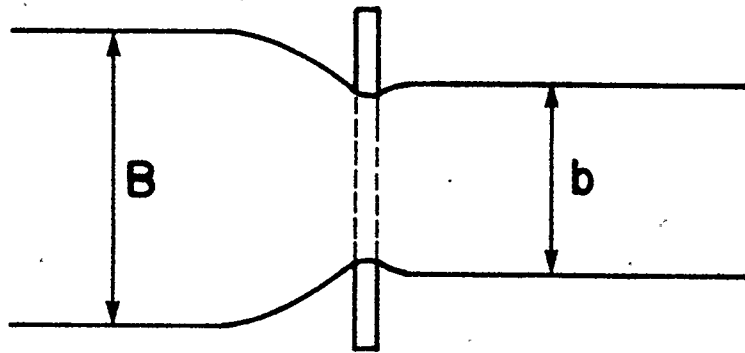


Fig 7. Contracted flow over weir

(d) Inclination of the Weir

Bazin found that for the case of inclined weir, the discharge coefficient has to be multiplied by a factor which depends on angle of inclination and is greater than unity<sup>(12)</sup> for frontally inclined weir and less than unity for weir inclined backwards, as shown in Table 1.

Inclination	Backwards	Frontally
1:4	*	1.09
1:2	0.93	1.12
1:1	0.93	1.10
3:2	0.94	1.07
3:1	0.96	1.04
vertical	1.00	1.00

Table 1. Inclination coefficients (Bazin)

### 1.2.2 The Equations of Francis, La Sia and King

Different equations for the discharge over sharp crested rectangular weir operating under free flow conditions and with lateral contractions of the flow were reported in a work done by Francis, La Sia and King<sup>(3)</sup>:

(a) Francis' Equation:

$$Q = 1.84 \times \left[ 1 + 0.259 \times \frac{H_1^2}{(H_1 + P)^2} \right] \times b \times H_1^{1.5} \quad (4)$$

(b) La Sia's Equation:

$$Q = 0.667 \times \left[ 0.615 + \frac{1}{1000H_1 + 1.6} \right] \times \left[ 1 + 0.5 \times \left( \frac{H_1}{H_1 + P} \right)^2 \right] \times b \times H_1^{1.5} \quad (5)$$

(c) King's Equation:

$$Q = 1.78 \times b \times H_1^{1.47} \times \left[ 1 + 0.56 \times \frac{H_1^2}{(H_1 + P)^2} \right] \quad (6)$$

where:  $b$  = width of the weir

$P$  = height of the weir crest from the channel bottom

A thorough analysis of the Eqs. (4), (5) and (6), however, shows that they do not represent any appreciable changes from Bazin's equation.

### 1.2.3 The Rehboch's Equation

Rehboch proposed an equation for discharge over weir which considers effects of viscosity and surface tension of the fluid<sup>(4),(28)</sup>

The equation was given in the form:

$$Q = 0.667 \times \left[ 0.611 + 0.075 \times \frac{H_1}{P} + \frac{0.36}{H_1 \sqrt{\left( \frac{\xi g}{\sigma} - 1 \right)}} \right] \times b \sqrt{2g} H_1^{1.5} \quad (7)$$

where  $\xi$  = mass density

$\sigma$  = surface tension of the fluid

When  $H_1$  is greater than the head corresponding to the minimum value of a discharge coefficient, the effect of surface tension can be neglected and the Eq.(7) reduces to<sup>(7)</sup>:

$$Q = 0.667 \times \left[ 0.611 + 0.075 \frac{H_1}{P} \right] \times b \sqrt{2g} H_1^{1.5} \quad (8)$$

It is apparent that Eq.(8) basically represents a different form of Bazin's equation. As argued by Kindswater and Carter in their paper<sup>(28)</sup>, the Rehboch's equation fails for high values of head/weir height ratios, since it gives values of  $K = \infty$  for a zero height weir.

### 1.2.4 The Rouse's Equation

Rouse improved the Eq.(8) by taking into account the fact that the critical depth of flow is established upstream of the weir. He gave the following equation for the discharge coefficient<sup>(28)</sup>:

$$K_1 = 1.06 \times \left(1 + \frac{P}{H_1}\right)^{1.5} \quad (9)$$

This equation, however, also fails for extreme values of  $H_1/P$  ratio.

Kandaswamy and Rouse<sup>(28)</sup> obtained discharge coefficients for a full range of operation of a weir by combining Eqs.(8) and (9) and fitting the experimental data:

$$K_1 = 1.06 \times \left[ \left( \frac{14.14P}{8.15P + H_1} \right)^{10} + \left( \frac{H_1}{H_1 + P} \right)^{15} \right]^{-0.1} \quad (10)$$

The Eq.10 gives better estimates of the flow over weir than Eq.8 and Eq.9, but it still can not be used for small weir heights.

### 1.2.5 The Equation Proposed by MIS USSR

In the work reported by Russian engineers<sup>(11)</sup> the Bazen's equation<sup>(8)</sup> for discharge coefficient was adjusted for relatively high velocity of the flow.

For the case of flow without side contractions, they proposed the

equation in a form:

$$K_1 = \left[ 0.405 + \frac{0.0027}{H_1} \right] \times \left[ 1 + 0.53 \times \left( \frac{H_1}{H_1 + P} \right)^2 \right] \quad (11)$$

For flow with side contractions, the expression for discharge coefficient was developed as:

$$K_1 = \left[ 0.405 + \frac{0.0027}{H_1} - 0.03 \times \left( 1 - \frac{b}{B} \right) \right] \times \left[ 1 + 0.55 \times \left( \frac{b}{B} \right)^2 \times \left( \frac{H_1}{H_1 + P} \right)^2 \right] \quad (12)$$

where  $b$  = length of contracted flow

$B$  = length of free flow

For the case of inclined weir, they have found that values of discharge coefficient change with the angle of inclination and are greater than unity for weirs inclined frontally and less than unity for weirs inclined backwards<sup>(28)</sup> (Fig.8 and 9). The values of  $K_1$  are close to those determined by Bazin.

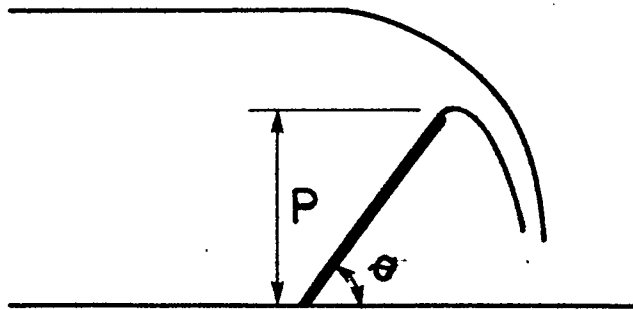


Fig.8 Frontally inclined weir

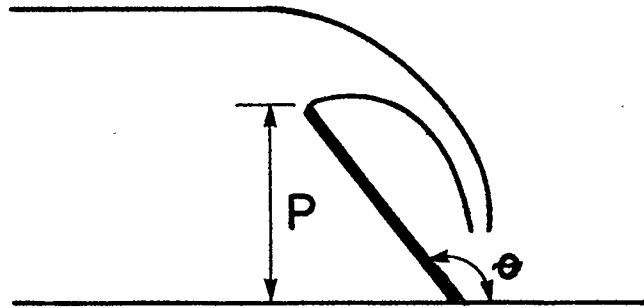


Fig. 9 Weir inclined backwards

#### Weirs Operating Under Submerged Flow Conditions

The weir is said to be submerged when the depth of flow on the downstream side of weir rises above the level of the crest. Weir submergence greatly influences the discharge and discharge coefficient. The equations developed for weirs operating under free flow conditions do not apply for submerged weirs. Submerged weirs cannot be used for discharge measurements.

There are not many studies dealing with the estimation of discharge over a submerged weir. The published research which is relevant for this study is discussed here.

### 1.2.6. The Herschel's Equation

In the work reported by Herschel and based on experiments conducted by Francis, Fteley and Stearns<sup>(17)</sup>, the method for estimating the discharge over

$$Q=3.33 \times b \times (nH_1)^{1.5}$$

a submerged weir without end contractions is given as in the Eq.13, where  $n$  is a multiplication factor which depends on ratio  $H_2/H_1$ ,  $H_2$  being the downstream head over weir (Fig.10).

When the downstream head equals zero,  $n$  equals unity and the weir is not submerged. When  $H_1 = H_2$ ,  $n$  equals zero and the discharge equals zero.

The Eq.13 does not predict discharge accurately for values of  $n$  less than 0.7.

The discharge over submerged weir can be regarded as composed of two portions. The discharge through the upper part is given by the equation for free flow over weir, the head being the difference between  $H_1$  and  $H_2$ :

$$Q_1 = K \times b \times \sqrt{2g(H_1 - H_2)^3} \quad (14)$$

The portion through the lower part is given by the equation for the submerged orifice in which  $H_2$  is the height and  $H_1 - H_2$  is the orifice head:

$$Q_2 = K \times b \times H_2 \times \sqrt{2g(H_1 - H_2)}$$



The described method, however, can not predict the discharge over the submerged weir accurately, as it is applicable only for suppressed weirs and does not consider the velocity of approach or inclination of the weir.

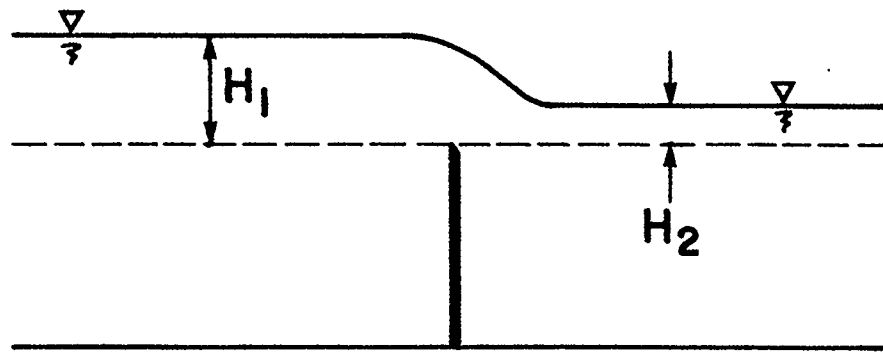


Fig.10 Submerged weir

#### 1.2.7. The MIS USSR Equation

The Russian engineers developed the expression for discharge coefficient in a form:

$$K_2 = K_1 \times \sigma, \quad (16)$$

where: -  $\sigma_s$  is a submergence coefficient that depends on relative depth of submergence  $H_1/P$  and relative drop in the water level  $(H_1-H_2)/P$  (refer to Fig.11)

-  $K_1$  is a discharge coefficient for free flow over weir, determined by Eq.11 or Eq.12 in the case of the flow with lateral contractions.

The submergence coefficient can be estimated using equation:

$$\sigma_s = 1.05 \times \left(1 + 0.2 \times \frac{H_2}{P}\right) \times \sqrt[3]{\frac{H_1 - H_2}{H_1}} \quad (17)$$

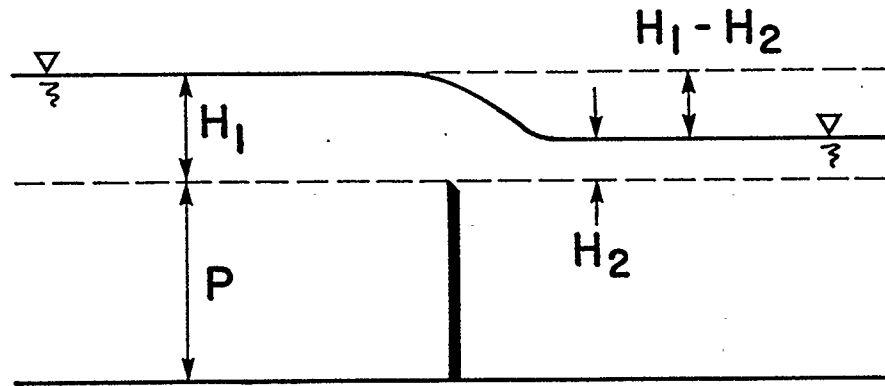


Fig.11 Submerged weir - relative drop in water level

This method gives somewhat better estimation of discharge over submerged weir than Herschel's method does for a range of  $0.15 < H_1/P < 1.6$ .

### 1.2.8 The Equation Proposed by D. Manz

Manz<sup>(16)</sup> proposed an equation developed by combining published research on the vertical and inclined sharp-crested weirs.

The equation considers combined effects of weir inlet conditions, submergence and weir inclination on a single weir<sup>(5)</sup>:

$$Q = K_e K_\theta K_2 \times b \times H^{1.5} \quad (18)$$

where:  $K_e$  = effective discharge coefficient which is a function of the ratio of weir width to width of the approach channel and upstream head above weir to weir height, as defined in the work performed by the Georgia Institute of Technology and reported by Bos<sup>(6)</sup>

$K_\theta$  = inclination coefficient which accounts for the weir angle as given by M. Bazen<sup>(2)</sup>

$K_2$  = submergence coefficient which accounts for weir submergence effects and is defined by Villemonte as<sup>(30)</sup>:

$$K_2 = \left[ 1 - \left( \frac{H_2}{H_1} \right)^{1.5} \right]^m \quad (19)$$

where:  $m$  = empirically determined exponential factor

This equation is a very important contribution to the research on weir hydraulics because it represents one of the first attempts to combine the

factors affecting a single weir, and it predicts flow with satisfactory accuracy to be used for design purposes. However, the equation is still in a preliminary form.

### 1.3 Conclusion

The most relevant studies that deal with the sharp crested overshoot pivoting weir are addressed in this chapter. The important factors that influence the flow over weir such as: the approach velocity, aeration of the nappe, inclination of a weir, degree of submergence and lateral contraction of the flow are discussed. The proposed equations are not at all satisfactory, as they anticipate coefficients which are deduced from experimental programs and hence the equations may be used only within the limits for which the coefficients have been established. No study gives an adequate analysis and good definition of the discharge characteristics of the weir over the entire range of operation. In all of them, hydraulics of the weir has been much simplified and in the experimental analysis only individual factors affecting the discharge coefficient are considered. Thus, the values of discharge obtained using these equations may deviate from the reality significantly. Today, however, a precise description of the pivoting weir hydraulics is necessary for design. Hence this study on the pivoting sharp crested rectangular weir was initiated.

### 1.4 Objectives of the Study

The objectives of the study are:

1. To adequately and precisely describe the flow over weir over the entire range of operation, when the weir is operating under free flow and submerged conditions.
2. To determine how the geometry of the weir and channel affects the discharge coefficients.
3. To determine how the angle of weir inclination affects the discharge and whether the coefficient that accounts for weir inclination also depends on geometry of the weir and channel.
4. To explain the effects of submergence on the discharge coefficient and deduce the expression for submergence coefficient .
5. To explain how the weir geometry affects the submergence coefficient.
6. To advise the applicability of Eq. 18

## Chapter 2

### LABORATORY SET-UP AND EXPERIMENTAL PROCEDURE

#### 2.1 Design Criteria

For the purpose of this study it was necessary to develop an apparatus that could physically simulate the variety of conditions of flow over weir. The specific requirements of the test apparatus were the following:

1. To allow for weir to operate under free flow and submerged conditions.
2. To allow for weir to operate in a suppressed mode or as a weir with side contractions.
3. To allow for adjustments of the weir angle from almost  $0^\circ$  to  $90^\circ$ .
4. To be capable of providing steady flow conditions at flume inlet in the desired range of flow.
5. To minimize the disturbances of the flow due to weir adjustment mechanism.
6. To provide sufficient aeration of nappe when weir operates under free flow conditions.
7. To minimize the leakage of water along the sides of the weir.
8. To allow for downstream depth control when weir operates under

submerged flow conditions.

9. To provide precise measurements of upstream and downstream head over weir.

10. To minimize the effects of the boundary layer on the velocity profiles.

## 2.2 Apparatus layout

### 2.2.1 Experimental Flume

The layout of the rectangular experimental flume used in this study is shown on Fig.12 and Fig.13. The flume was 0.6m wide and 6m long. The side walls were made of Plexiglass to allow easy viewing of the operation of the model and they could be adjusted from vertical to inclined position. The thickness of Plexiglass walls was 12.5mm.

A stilling tank was located at the upstream end of the flume. The model weir with the adjusting mechanism was located at 4m distance from the flume inlet. Another weir was installed at the downstream end of flume at 2m from the upstream weir. The flume bottom was made very smooth to prevent the development of the boundary layer, which would affect the the velocity profiles. The velocity profiles were measured at three cross-sections along the flume using Nixon Probes, and the experiment has shown that they were vertical. Hence the possible boundary layer development occurred well under the range

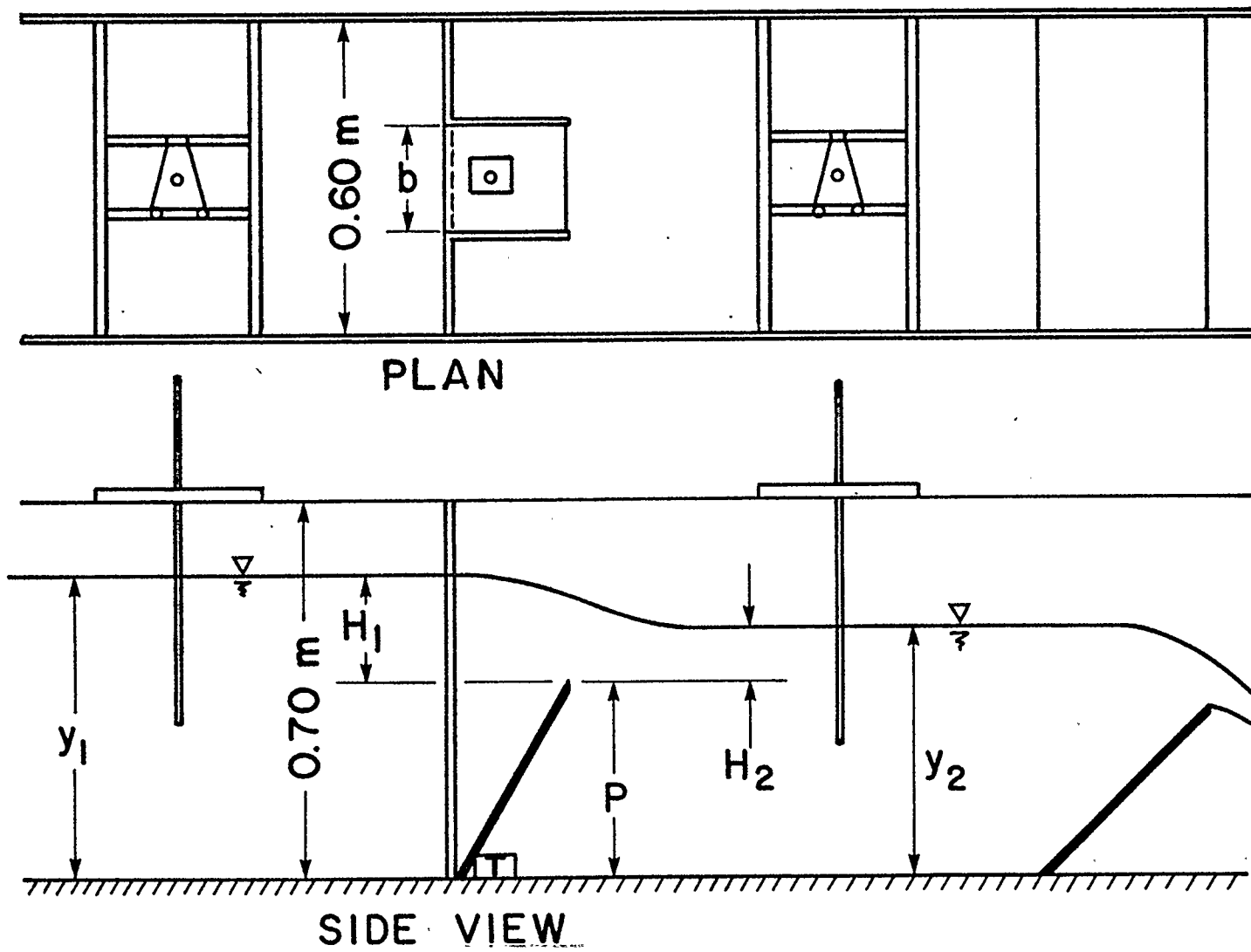


Fig.12 Experimental flume layout



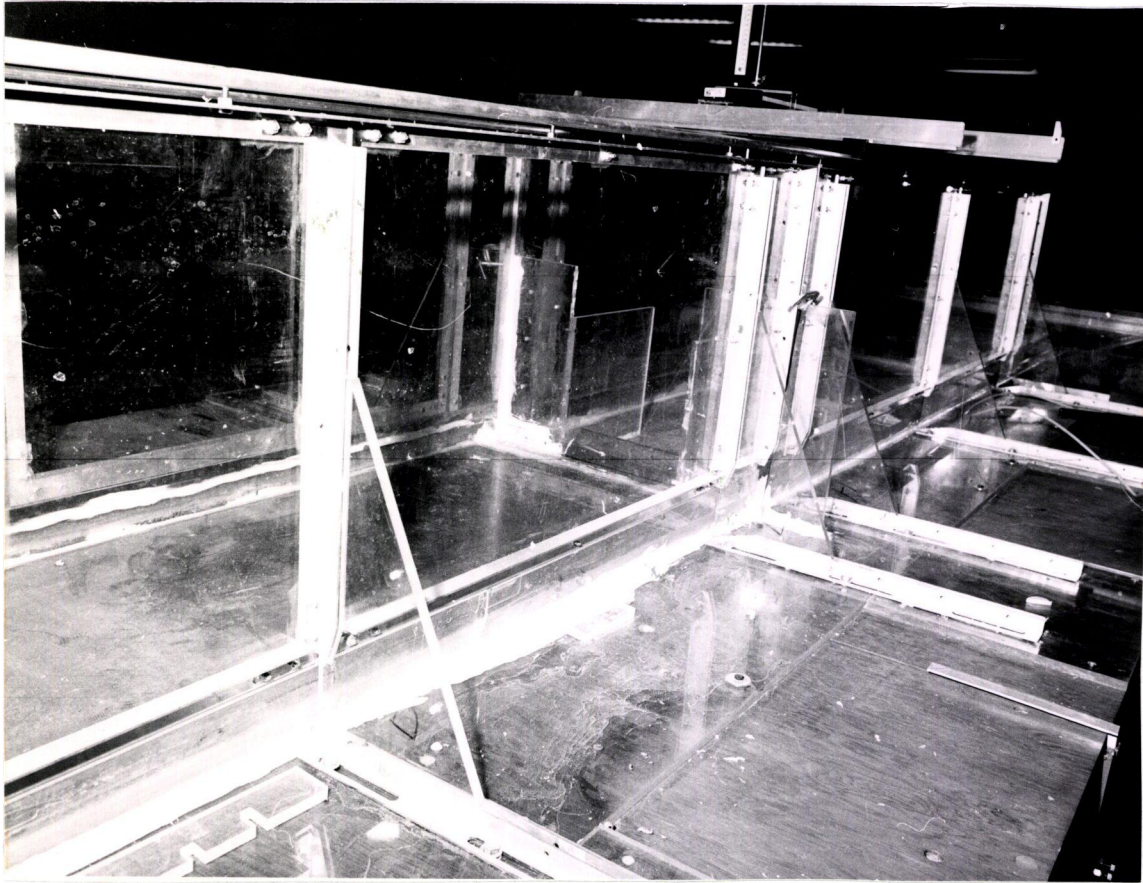


Fig.13 Experimental flume - detail with the model weir

of measurements, and did not affect the measurements.

### 2.2.2 Supply System

Water was fed into the flume from a large stilling tank which provided steady flow conditions at the flume inlet. The discharge into a stilling tank was measured by an electromagnetic flow meter. The discharge was calibrated using a weight tank and the test has shown that the error of discharge readings ranged from 0.5% for flow of 20 l/s to 2% for flow of 5 l/s, which is in the range of acceptable error. A gate valve located on the supply pipe was used to control the discharge to the stilling tank.

### 2.2.3 Model weirs

Nine different model weirs were used in the experimental program. The dimensions of weirs are tabulated in Table 2. The weirs were made of aluminium with rubber seals along the sides to prevent leakage. Plexiglass angles for width adjustment were used at the side of the weir, to keep the weir in place and to prevent the spilling of water flowing over the weir.

The weir angle was adjusted by a screw mechanism located under the weir in the downstream section of the flume. When the weir was operating under free flow conditions, the aeration of the nappe was achieved by affixing a

flexible rubber hose to the underside of the weir and running the hose outside of the channel. This proved efficient for the larger values of weir height (70 mm or more). For the lower values, however, the depth of the water beneath the weir was high enough to fill the hose with water, thus making it ineffective. As better solution could not be found, this procedure was continued.

Weir N°	Length (mm)	Width (mm)
1.	75	270
2.	155	270
3.	230	270
4.	75	420
5.	155	420
6.	230	420
7.	75	570
8.	155	570
9.	230	570

Table 2. Length and width of model weirs

#### 2.2.4 Downstream Control and Measuring Devices

Another weir was installed at the downstream end of the flume to control the downstream depth of the flow when the upstream weir operated under submerged flow conditions. A ratchet control mechanism was used to adjust the height of downstream weir.

Upstream and downstream depths of flow were measured using two point gauges suspended above the weir on a trolley. The point gauges could measure the depth of the flow with an accuracy of 0.1mm.

### 2.3 Experimental procedure

#### 2.3.1 General

The purpose of the experiments conducted on a laboratory flume was to collect the raw data necessary for the study. For every model weir the data were collected for both submerged and unsubmerged flow conditions in a series of experimental runs. The factors that were varied are:

- flow rate
- weir width
- weir length
- weir inclination angle (frontal inclination only)

The width of the flume bottom as well as the type of weir used were not changed.

### 2.3.2 Experimental Runs for Unsubmerged Flow

For weirs operating under free flow conditions, the discharge rate was varied five times for every weir angle, ranging from 1 l/s to 25 l/s. The angle of weir inclination was varied seven times, including vertical position. For each flow rate three readings of upstream depth were taken at the same cross-section and the average of three values was considered the depth of flow at that section. Since there was no need to control downstream depth of flow, the downstream weir was held in a horizontal position.

### 2.3.3 Experimental Runs for Submerged Flow

The weir operates under submerged flow conditions when the downstream depth of flow rises above weir crest. In the experimental flume this was achieved by operating the downstream weir. The height of the downstream weir was changed seven times for each flow rate and upstream weir angle to achieve seven degrees of submergence of upstream weir. The flow rate was varied five times for one upstream weir angle. It follows that thirty five experimental runs were conducted for each upstream weir angle. For each run

three readings of upstream depth and six readings of downstream depth were taken. The upstream depth was measured at three points on the same cross-section, while downstream depth was measured in two cross-sections approximately 10 cm apart. The average of three values of upstream depth and six values of downstream depth were considered the depth of flow at that section.

#### 2.3.4 Measurement Procedure

To ensure that measurements of the depth of flow were accurate and to conserve time, the following measurement procedure was adopted:

1. Rulers on the point gauges were zeroed with the channel bottom, as the flume construction was such that downstream channel was 1.25 cm lower than upstream .
2. The model weir was set to desired height by operating the adjustment mechanism and the point gauge.
3. The downstream weir was set to horizontal position.
4. The pump was switched on and the valve opened. The flow was set at the highest level to fill the stilling tank.
5. Once the stilling tank was full and the flow entered the flume, the discharge was set at the desired level for first unsubmerged flow run by operating the gate valve. Steady flow condition had to be reached before the

depth could be measured, hence the first set of readings was taken after waiting about five minutes for flow to become steady.

6. After the first set of readings was taken, the discharge was decreased to the next level and after five minutes the next set of readings was taken.

7. After all five unsubmerged flow runs were performed, the discharge was set at the highest level for submerged flow runs.

8. The downstream weir was raised and adjusted so that upstream weir crest was just slightly submerged. After five minutes six downstream and three upstream readings were taken.

9. The downstream weir was raised to achieve higher submergence and depth readings taken again.

10. After the tests were completed for full range of submergence (seven positions of the downstream weir), the flow rate was decreased and the procedure repeated.

11. When the tests were completed for five different values of discharge, the inclination of upstream weir was changed and the procedure outlined above repeated. After completing the experimental program for seven positions of the weir, the raw data for the particular weir were collected. The new model weir was then installed.

The procedure described above was repeated for all nine model weirs. The raw data were recorded on special sheets during the experimental procedure

and then transferred to the computer and analysed.

#### 2.3.5. Entrance Conditions

To ensure that the effect of entrance conditions on flow over weir are minimized during the experimental procedure, the steady flow conditions at the flume entrance were achieved prior to taking depth readings. The flume bottom was made very smooth to prevent the boundary layer development. A number of tests were conducted which showed that the boundary layer development does not affect the flow over weir.



## Chapter 3

### DATA OBSERVATIONS AND ANALYSIS

#### 3.1 Introduction

The raw data for each weir were collected using experimental procedure described in Chapter 2. The data analysis was then conducted using SMART Spreadsheet software . A number of worksheets was developed in order to summarize the data and do the necessary calculations for both submerged and unsubmerged flow. The specific worksheets that summarized the data were then used to plot graphs. The Tech-Graph-Pad software was used for graphs. As the Tech-Graph\_pad software can read the data from LOTUS Spreadsheet software only, all data files had to be imported from SMART to LOTUS prior to plotting graphs.

A description and example of worksheets and graphs and the steps in the data analysis are presented in this chapter.

#### 3.2 Unsubmerged Flow

The unsubmerged flow data for one position of the weir is summarized in a worksheet shown on Table 3. Since the experimental program was conducted

worksheets of this type were needed to present the data. Once the discharge and the upstream depth readings were entered, the worksheet calculates the average depth of flow and the upstream head over weir  $H_1$ . The upstream head over weir is defined as the height of the water above weir crest.

The upstream head  $H_1$  is plotted versus discharge  $Q$  in Fig.14 and Fig.15. There are seven plots for seven weir angles. The plots are concave-down curves of second order and they all follow the same pattern. All  $Q$ - $H_1$  plots for one weir were then summarized in one graph to show the consistency of the pattern. The  $Q$ - $H_1$  plots for nine weirs are shown in Fig.16 to Fig.20.

The basic weir equation is given in a form:

$$Q = K_1 \times C \times H_1^{1.5} \quad (20)$$

where:  $C$  - constant for one width of the weir

$g$  - acceleration due to gravity

$b$  - width of the weir

The constant  $C$  is calculated using the expression:

$$C = \frac{2}{3} \sqrt{2g} \times b \quad (21)$$

# UNSUBMERGED FLOW

INITIAL DATA      P = 95.00  
                          L = 155.00  
                          B = 600.00  
                          B = 420.00

## UPSTREAM FLOW LEVELS

Q (l/s)	U1	U2	U3	Uav	H1
1.10	105.40	105.70	106.30	105.80	10.80
4.90	126.50	126.50	126.60	126.53	31.53
8.70	142.50	142.60	142.00	142.37	47.37
12.60	154.20	154.60	155.30	154.70	59.70
16.60	166.80	166.80	167.40	167.00	72.00

## SUMMARY OF RESULTS

Q (l/s)	H1
1.10	10.80
4.90	31.53
8.70	47.37
12.60	59.70
16.60	72.00

Table 3. Example of worksheet with unsubmerged flow data

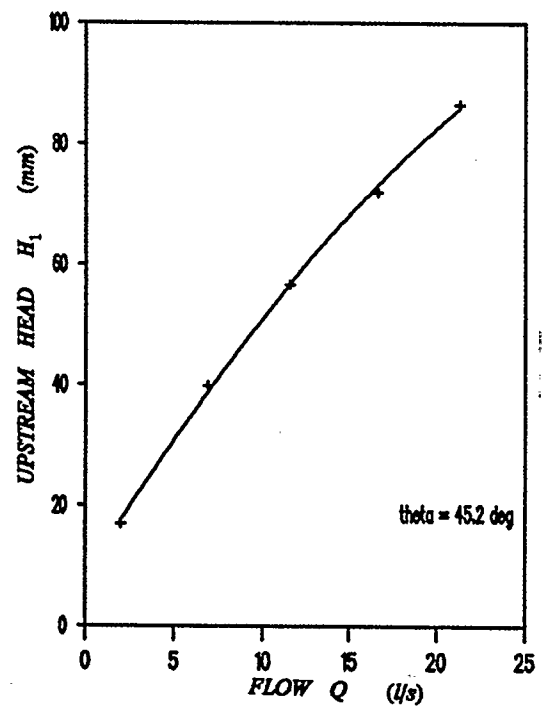
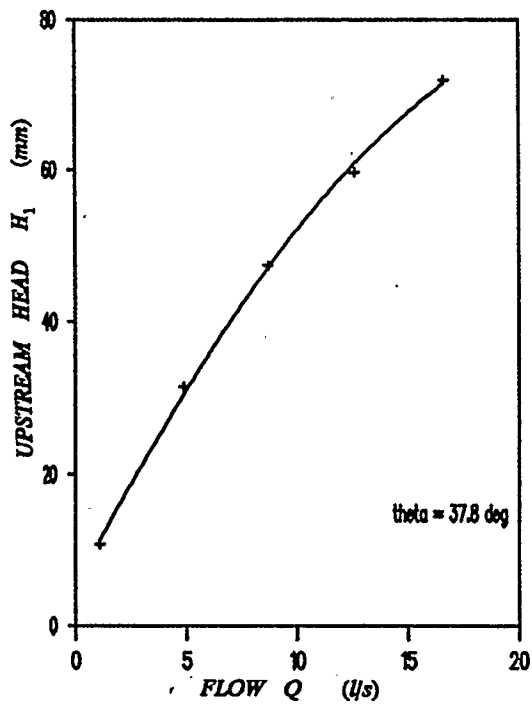
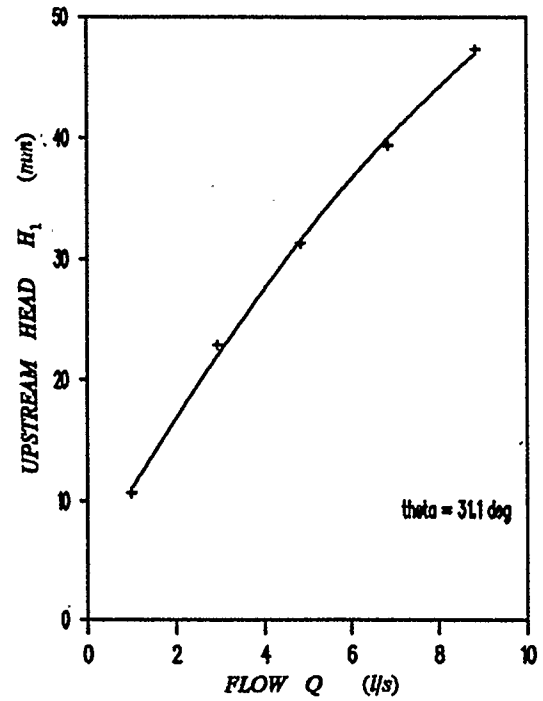
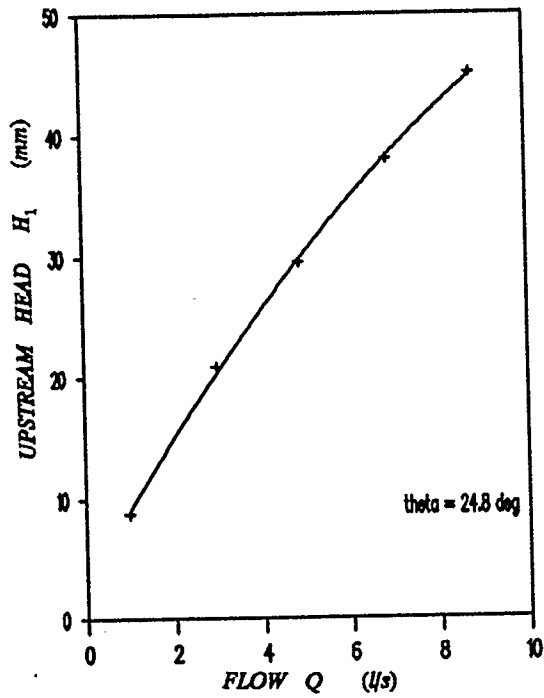


Fig.14  $Q$  vs  $H_1$  for weir length 155 mm, width 420 mm and inclination of  $\theta=24.8^\circ$ ,  $\theta=31.1^\circ$ ,  $\theta=37.8^\circ$ , and  $\theta=45.2^\circ$

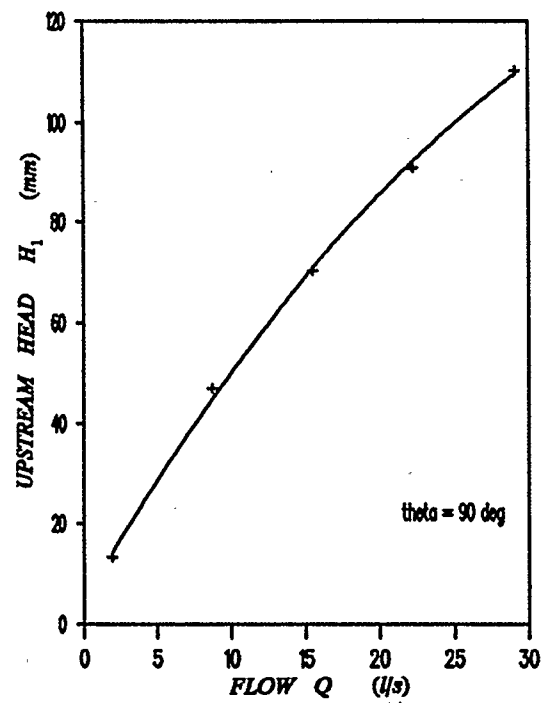
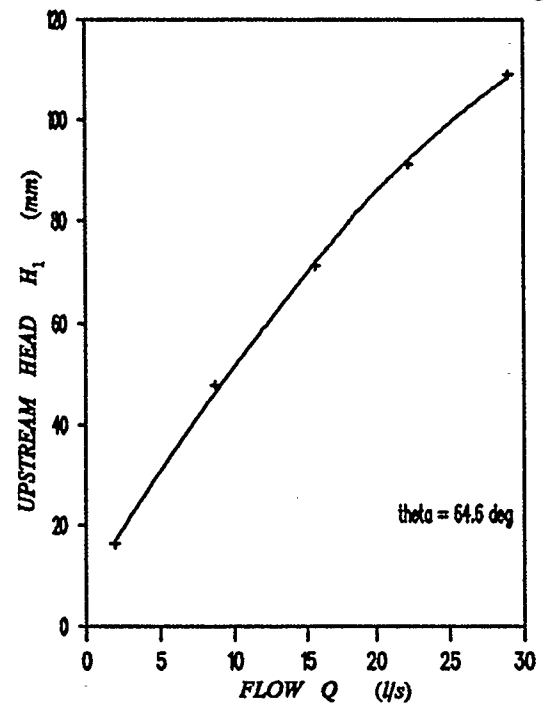
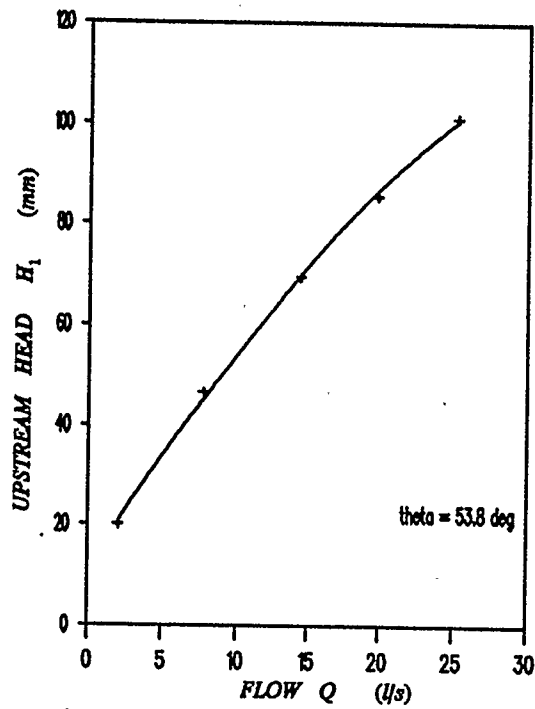


Fig.15  $Q$  vs  $H_1$  for weir length 155 mm, width 420 mm and inclination of  $\theta=53.8^\circ$ ,  $\theta=64.6^\circ$ , and  $\theta=90^\circ$

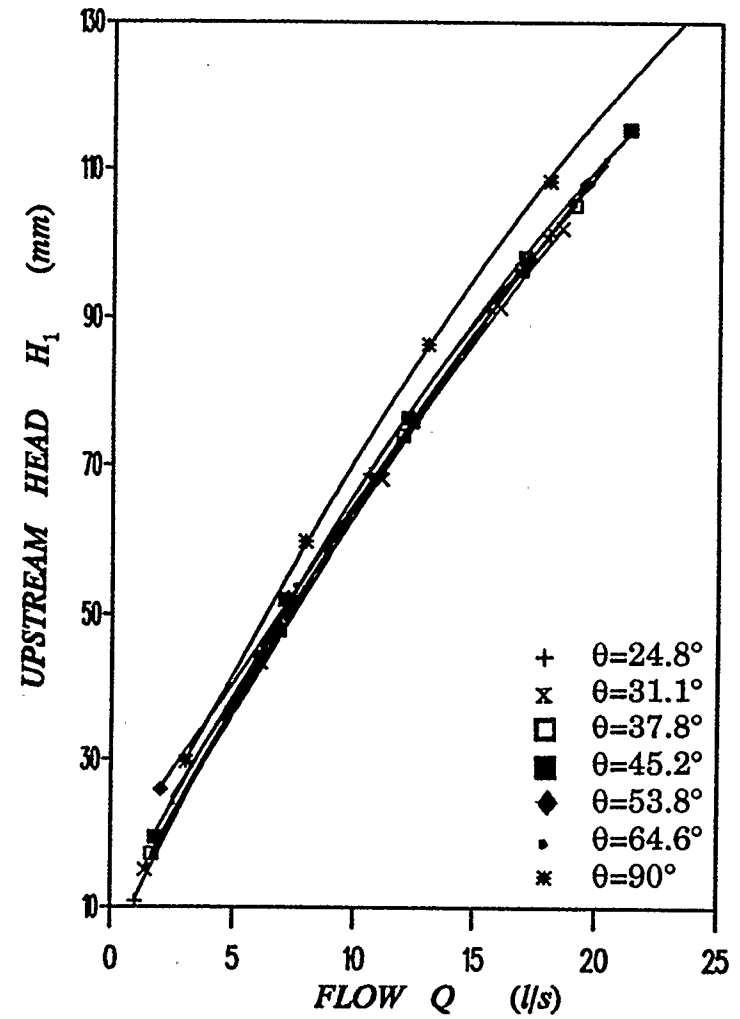
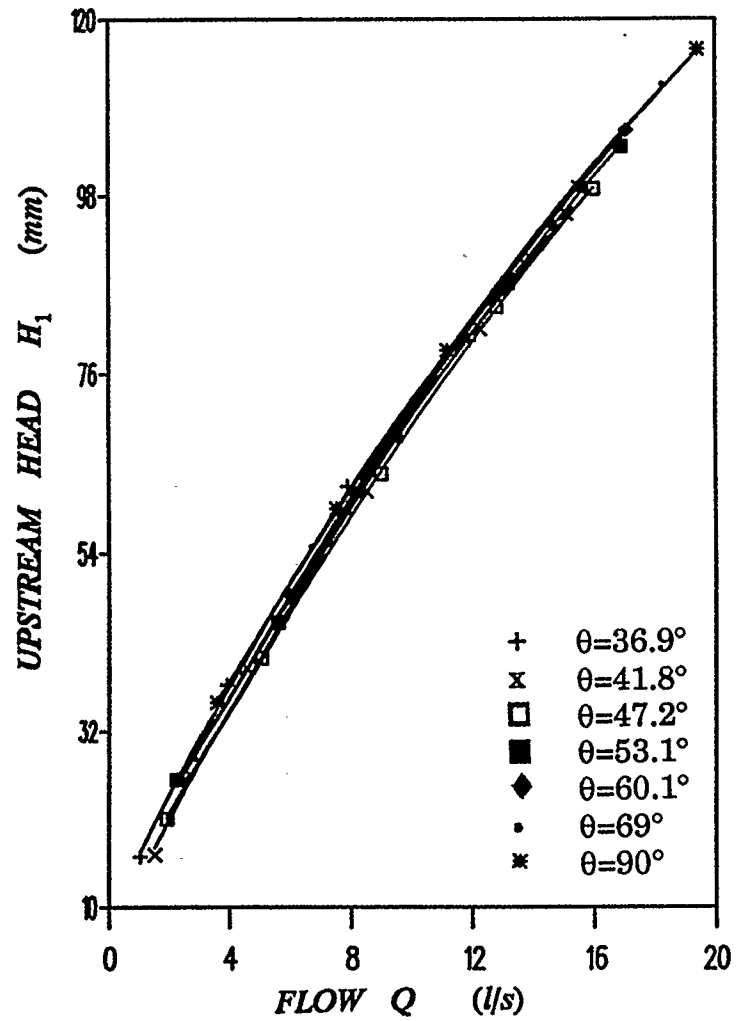


Fig.16  $Q$  vs  $H_1$  for weir length 75 mm, width 270 mm, and weir length 155 mm, width 420 mm

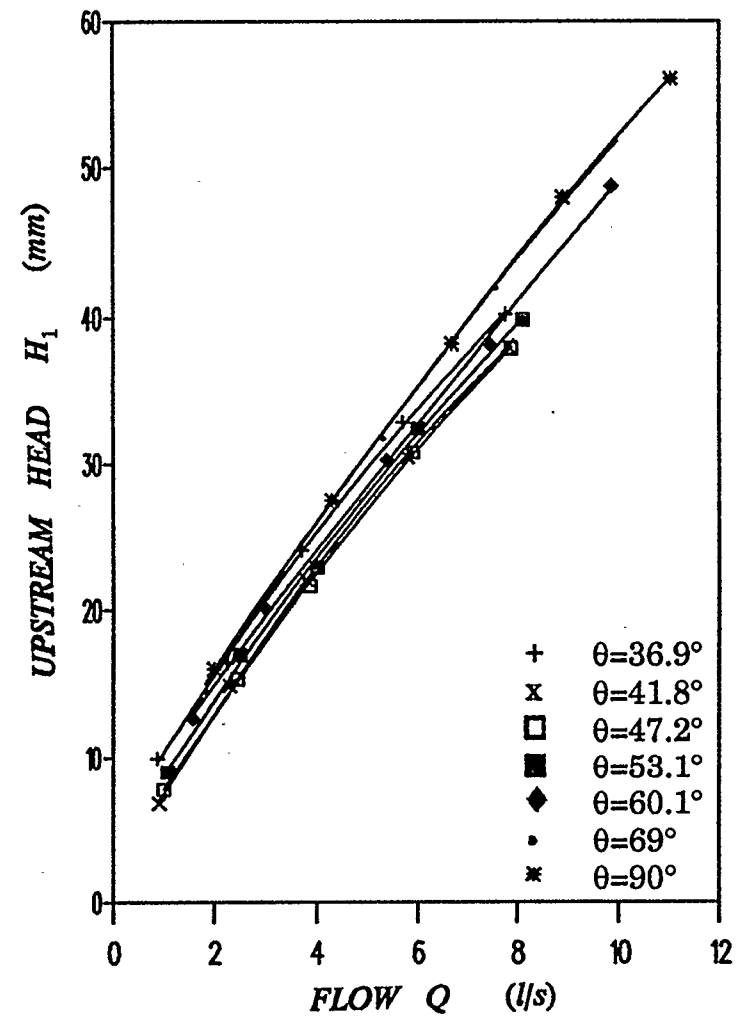
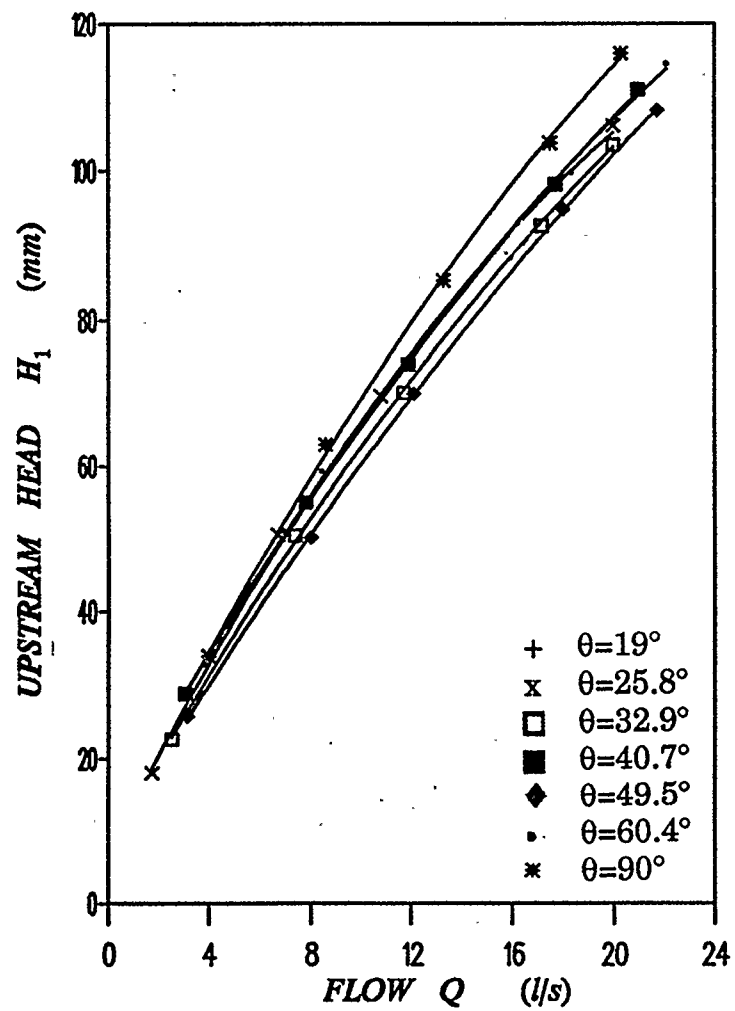


Fig.17  $Q$  vs  $H_1$  for weir length 230 mm, width 270 mm, and weir length 75 mm, width 420 mm

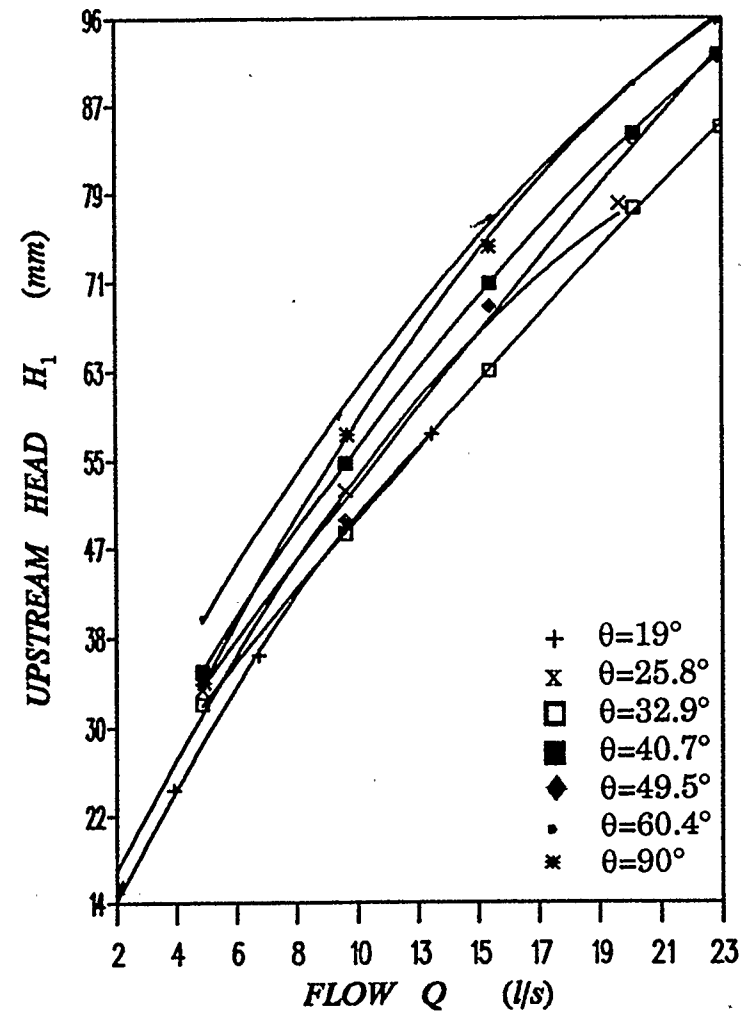
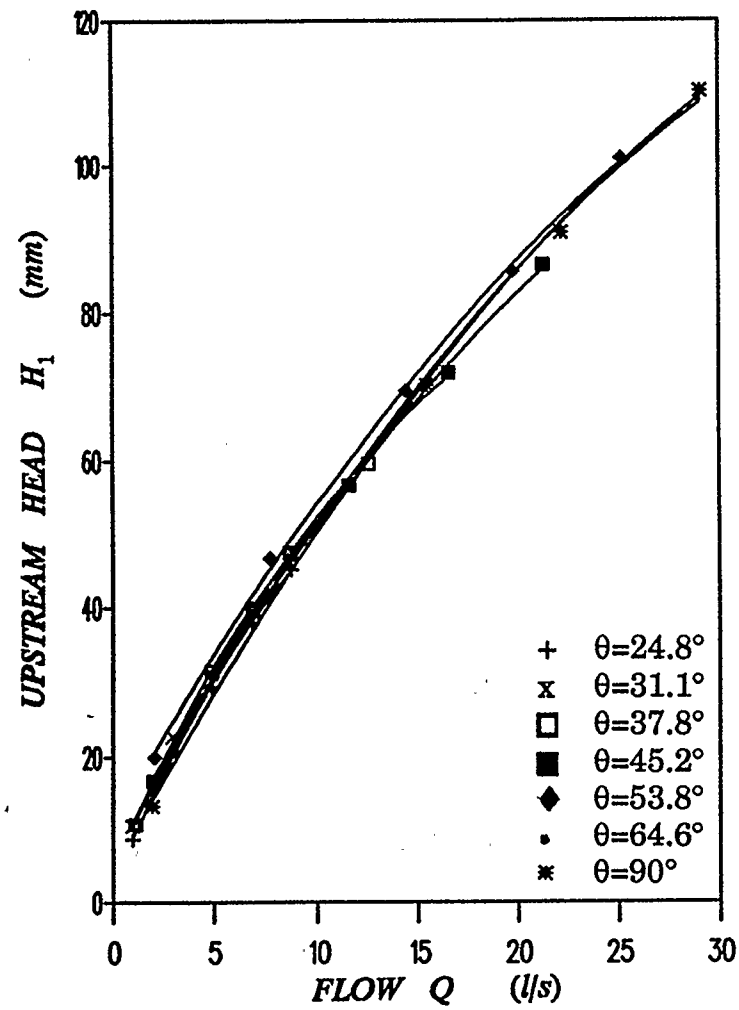


Fig.18  $Q$  vs  $H_1$  for weir length 155 mm, width 420 mm, and weir length 230 mm, width 420 mm



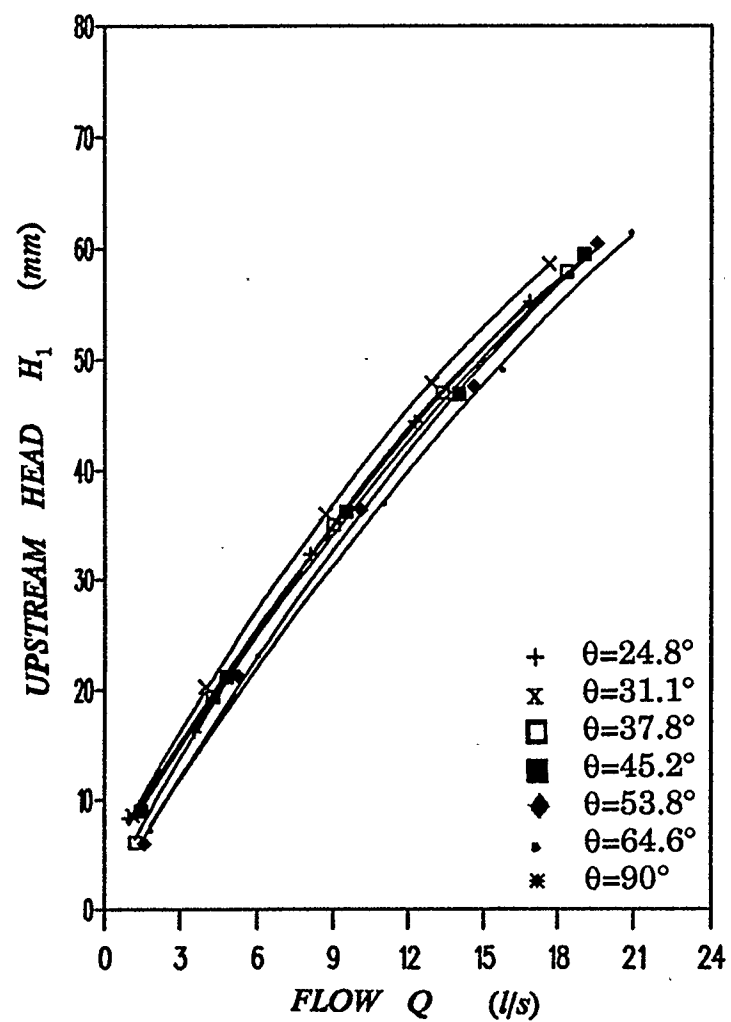
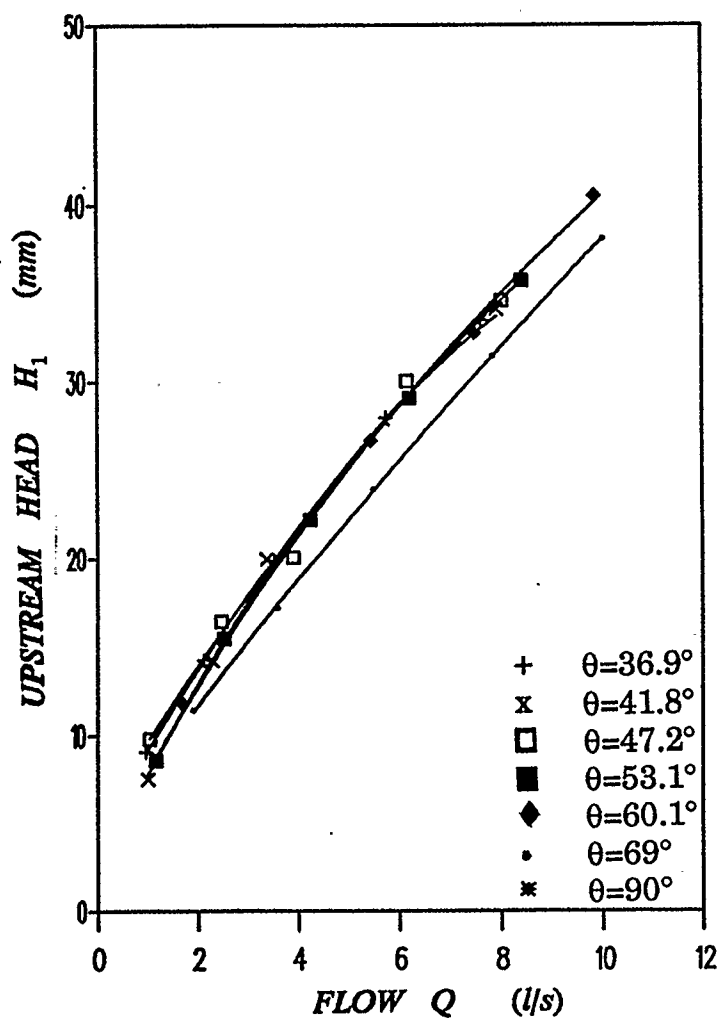


Fig.19  $Q$  vs  $H_1$  for weir length 75 mm, width 570 mm, and weir length 155 mm, width 570 mm

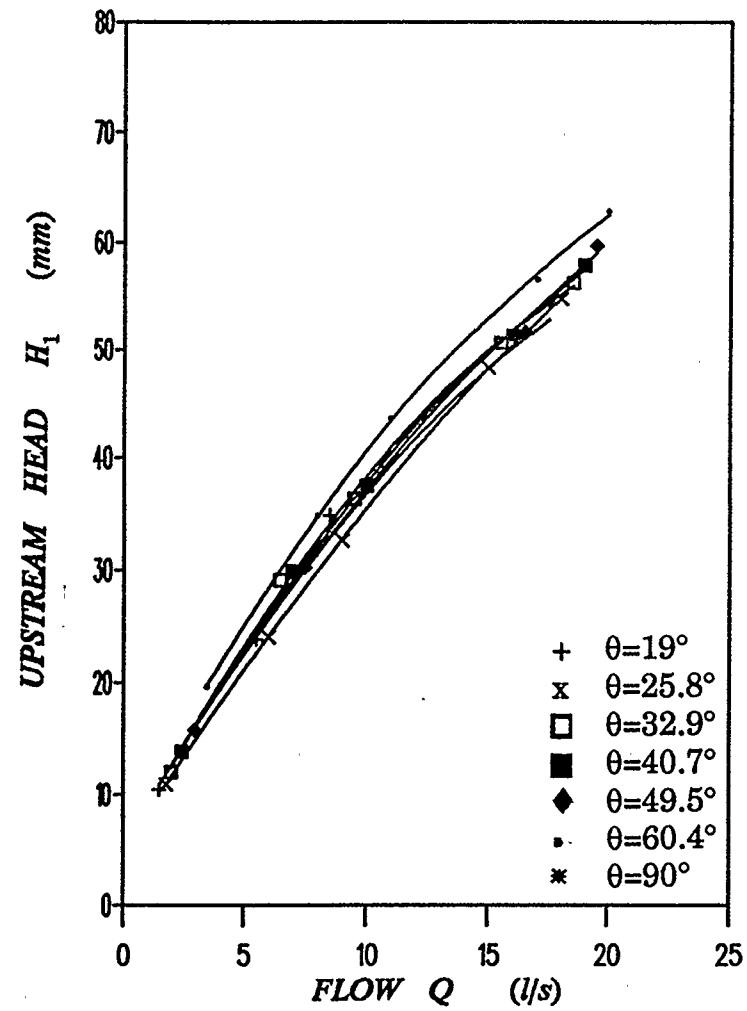


Fig.20  $Q$  vs  $H_1$  for weir length 230 mm, width 570 mm

The constant calculated this way has units of  $[\text{mm}^{1.5}/\text{s}]$ , and the values of  $C$  are as shown in the Table 4. The upstream head over weir  $H_1$  has units of  $[\text{mm}]$ . The discharge is given in  $[\text{l/s}]$ . The coefficient  $K_1$  is unitless, and in order to obtain the values of  $K_1$  the term  $CxH_1^{1.5}$  needs to be given in  $[\text{l/s}]$  as well. For that purpose the term  $CxH_1^{1.5}$  was multiplied by  $10^{-6}$ , as  $1\text{l} = 10^6 \text{ mm}^3$ .

The worksheet presented in Table 4 summarizes the unsubmerged flow data for all seven positions of the weir. This worksheet also calculates the right hand side of the weir equation, which is used to determine the values of the unsubmerged flow coefficient  $K_1$ .

Given the form of Equation (20), it is obvious that when the product  $CxH_1^{1.5}$  is plotted versus  $Q$ , the straight line results and the slope of the line is actually the unsubmerged flow coefficient  $K_1$ . The values of  $CxH_1^{1.5}$  were calculated as shown in Table 4.

In Fig.21 and Fig.22 the product  $CxH_1^{1.5}$  is plotted versus  $Q$ . The slope of resulting straight line is the unsubmerged coefficient  $K_1$  as discussed above. The regression coefficient  $R$  for all plots equals unity and all data points fall exactly on line. In Fig.23 to Fig. 27 the  $Q$ - $CxH_1^{1.5}$  plots for one weir are summarized.

## UNSUBMERGED FLOW DATA

CONSTANT (C) = 25212.60  
 WEIR LENGTH (L) = 75.00  
 WEIR WIDTH (B) = 270.00

FOR WEIR HEIGHT (P) = 45.00

Q(l/s)	$H_1$	$H_1^{1.5}$	$CH_1^{1.5}$
1.03	16.30	65.81	1.66
3.93	37.93	233.60	5.89
7.89	62.13	489.72	12.35
11.90	80.13	717.29	18.08
14.70	94.30	915.73	23.09

FOR WEIR HEIGHT (P) = 50.00

Q(l/s)	$H_1$	$H_1^{1.5}$	$CH_1^{1.5}$
1.52	16.53	67.21	1.69
4.55	40.03	253.27	6.39
8.50	61.60	483.43	12.19
12.27	81.53	736.17	18.56
15.13	95.73	936.64	23.62

FOR WEIR HEIGHT (P) = 55.00

Q(l/s)	$H_1$	$H_1^{1.5}$	$CH_1^{1.5}$
1.92	20.97	96.03	2.42
5.05	41.27	256.13	6.68
8.98	63.67	508.05	12.81
12.82	84.27	773.59	19.50
15.99	98.80	982.05	24.76

Table 4. Example of worksheet with unsubmerged flow data summary

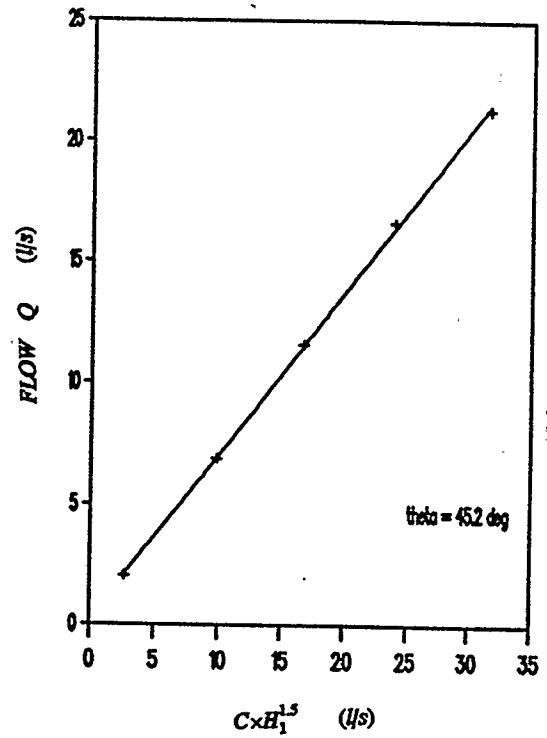
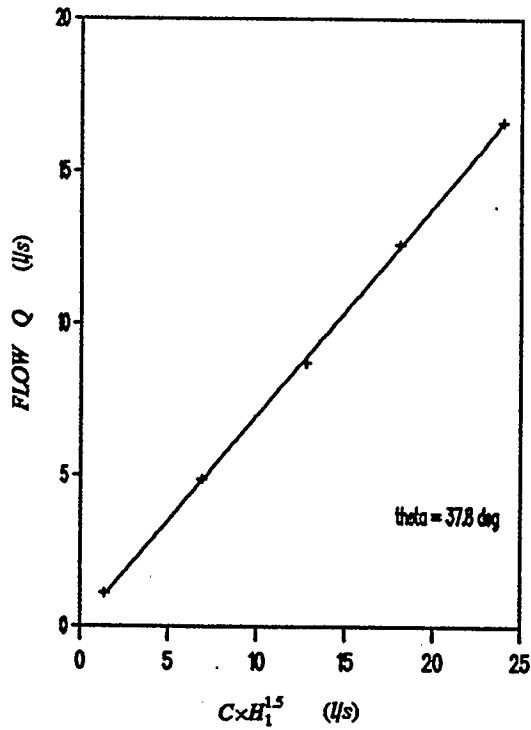
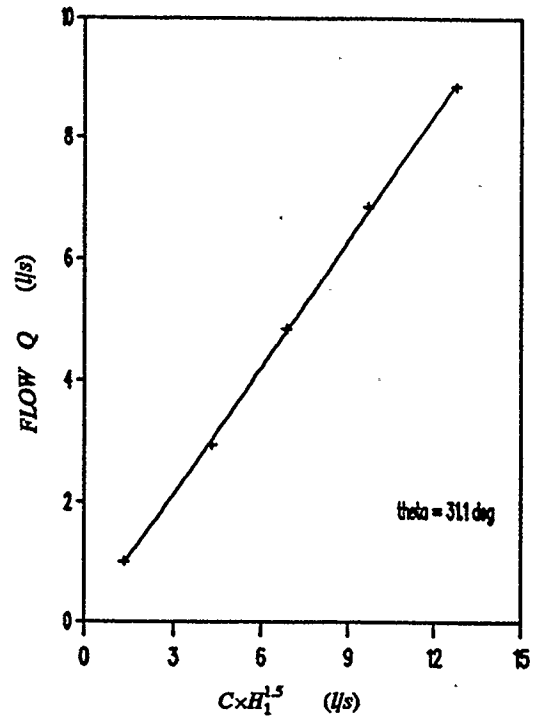
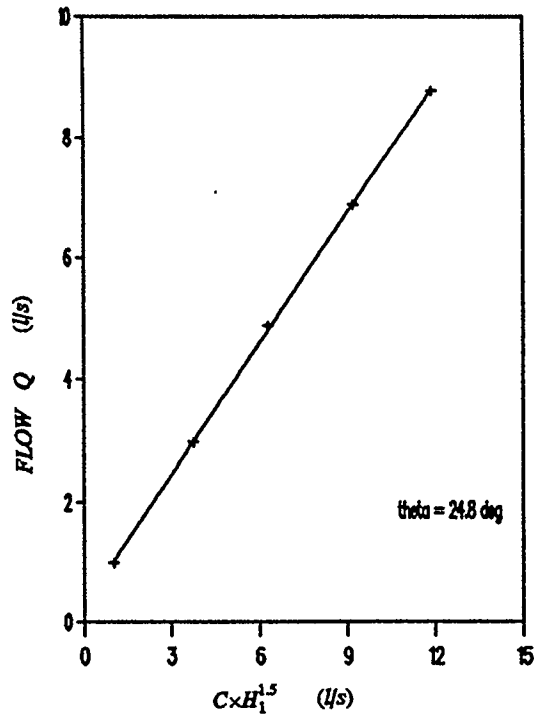


Fig.21  $Q$  vs  $C \times H_1^{1.5}$  for weir length 155 mm, width 420 mm, and inclination of  $\theta = 24.8^\circ$ ,  $\theta = 31.1^\circ$ ,  $\theta = 37.8^\circ$ , and  $\theta = 45.2^\circ$

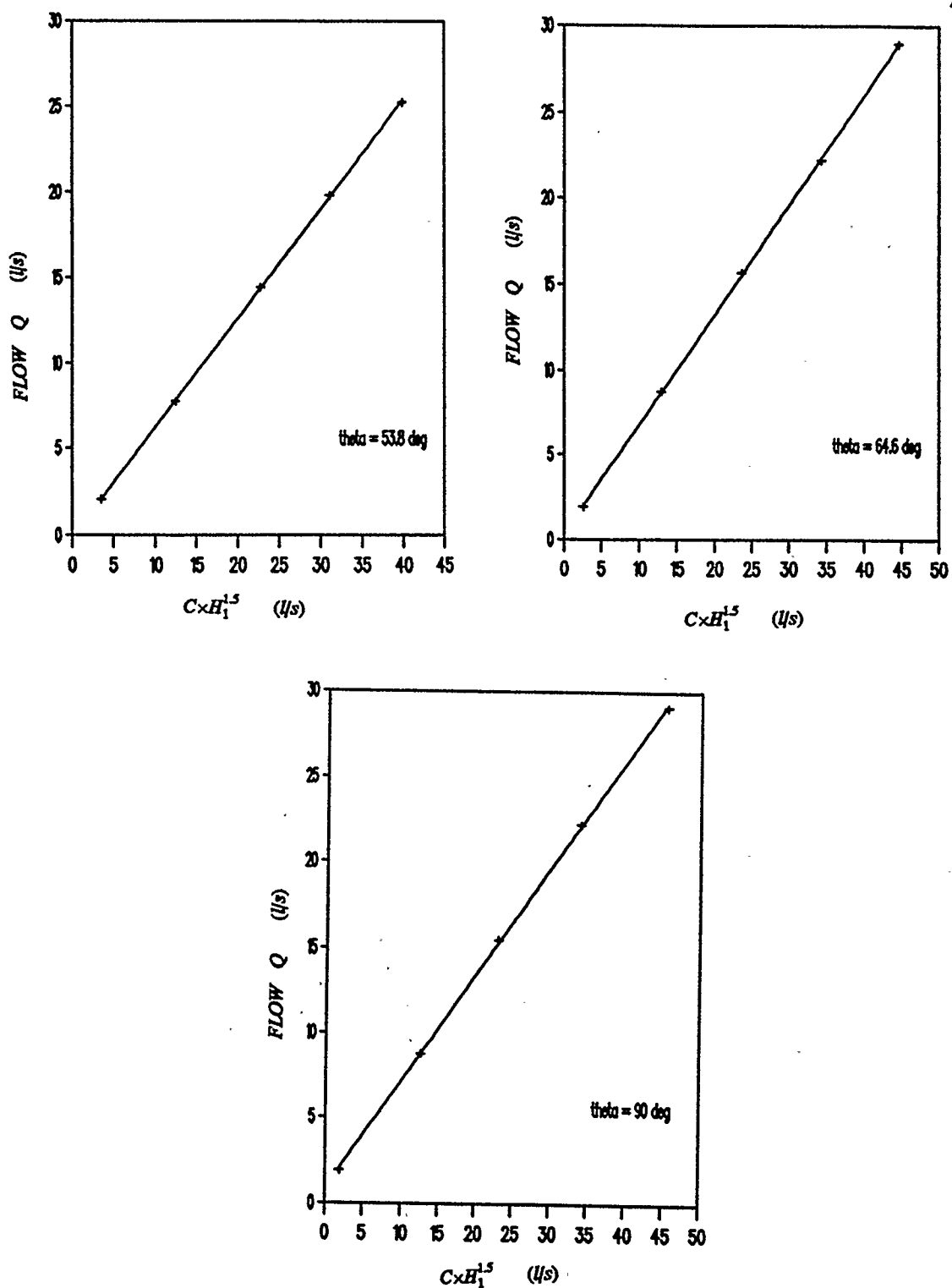


Fig.22  $Q$  vs  $C \times H_1^{1.5}$  for weir length 155 mm, width 420 mm, and inclination of  $\theta = 53.8^\circ$ ,  $\theta = 64.6^\circ$ , and  $\theta = 90^\circ$

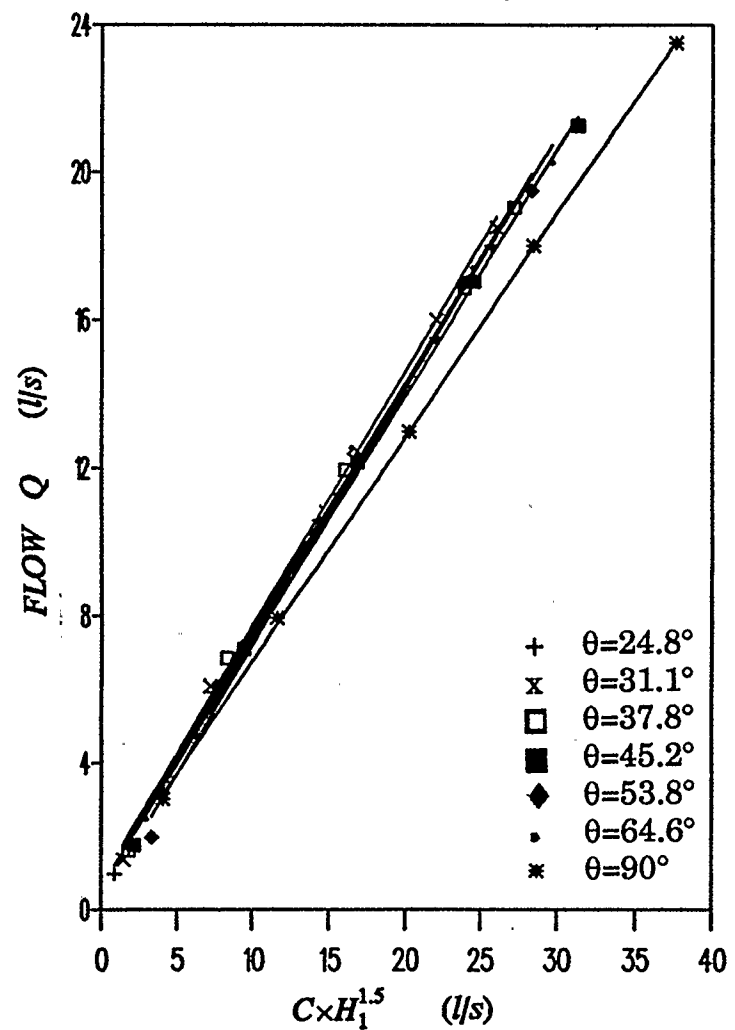
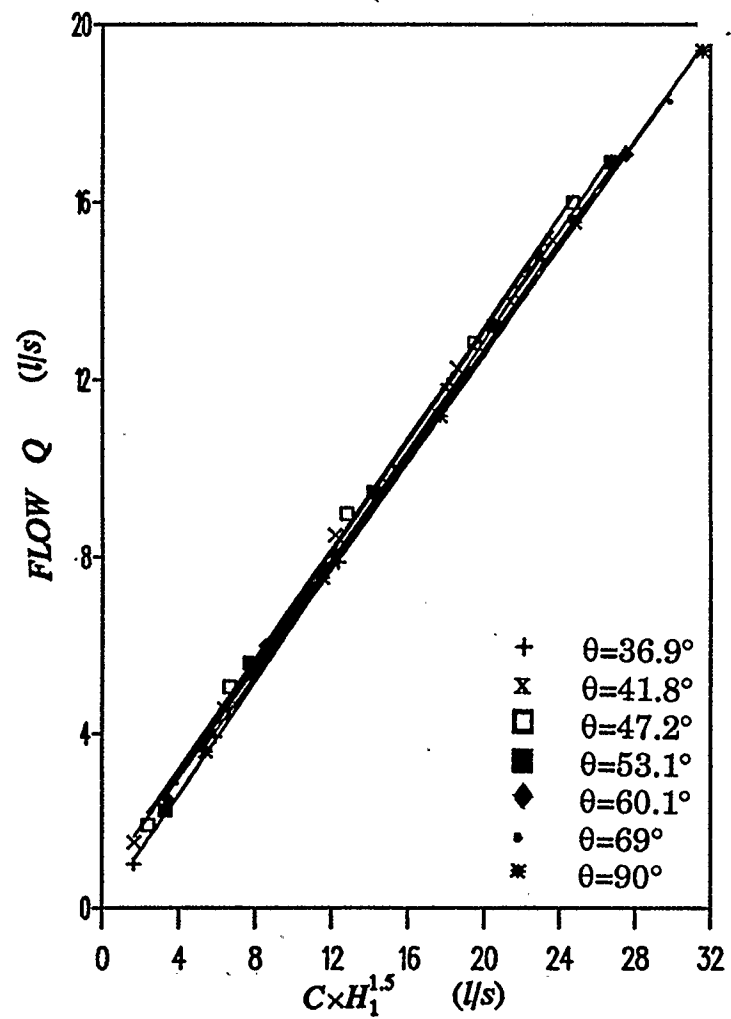


Fig.23  $Q$  vs  $C \times H_1^{1.5}$  for weir length 75 mm, width 270 mm, and weir length 155 mm, width 270 mm

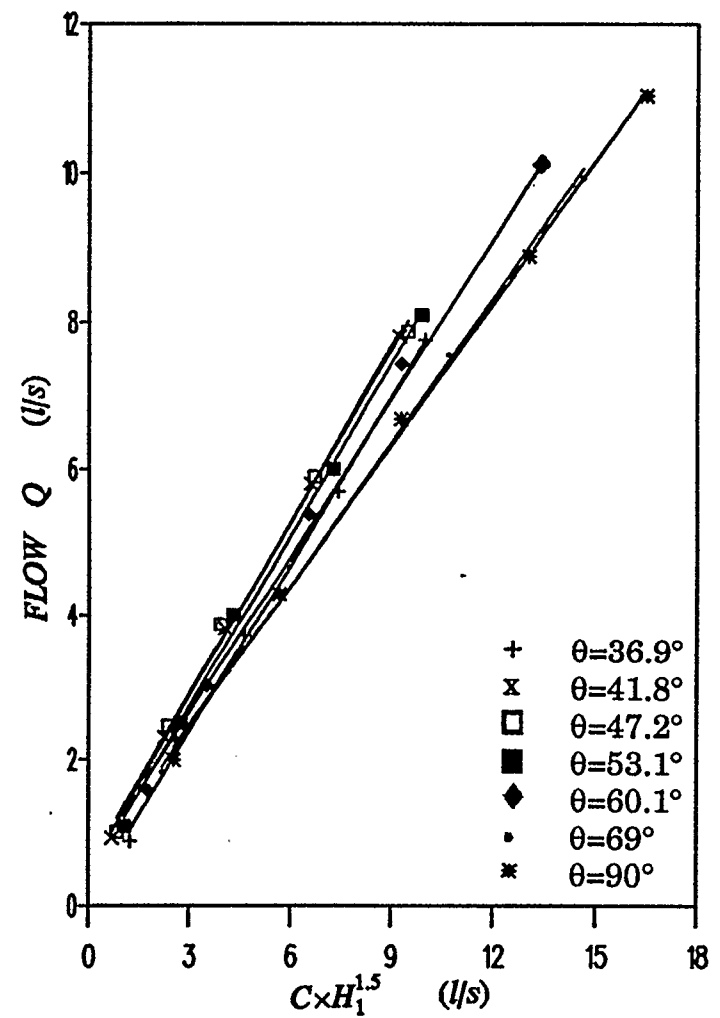
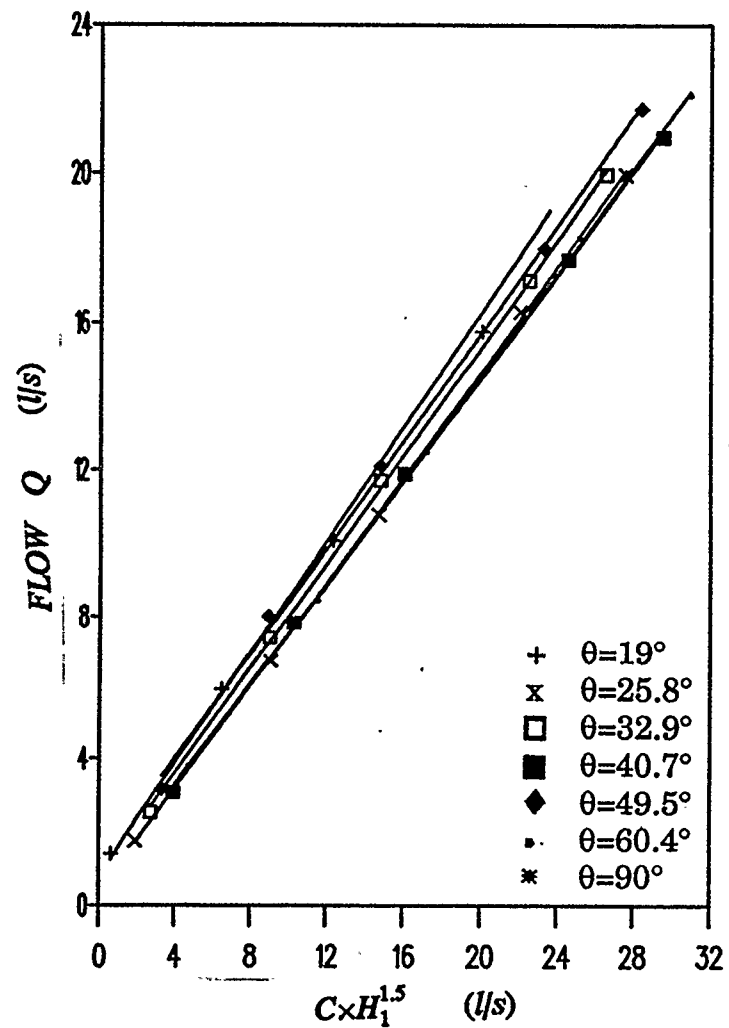


Fig.24  $Q$  vs  $C \times H_1^{1.5}$  for weir length 230 mm, width 270 mm, and weir length 75 mm, width 420 mm



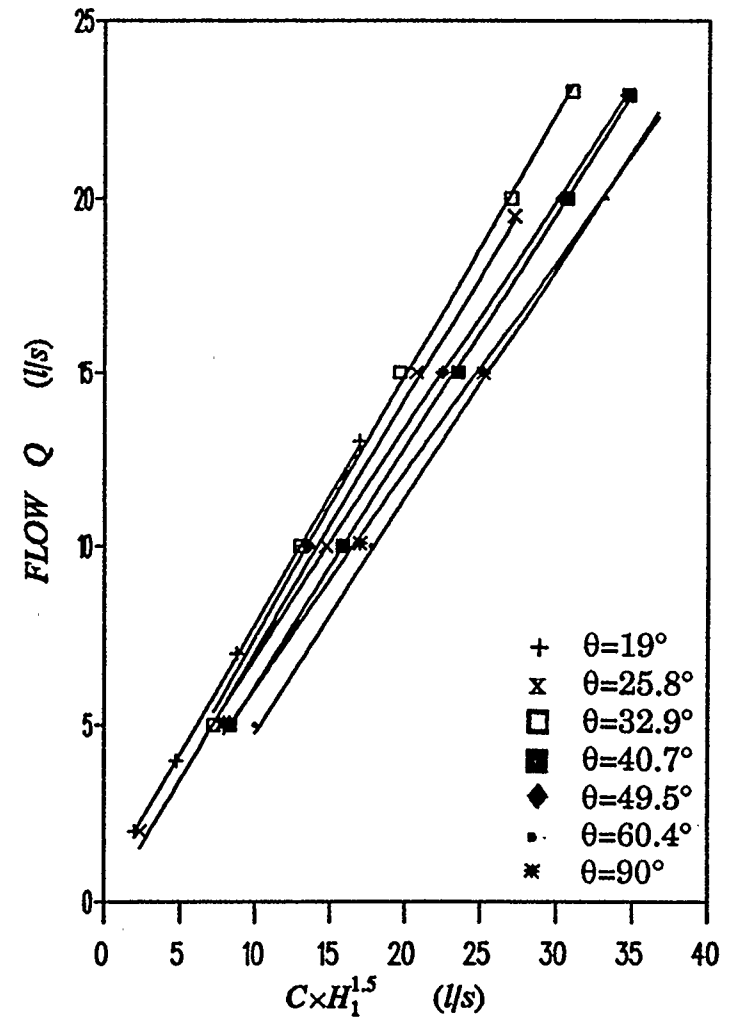
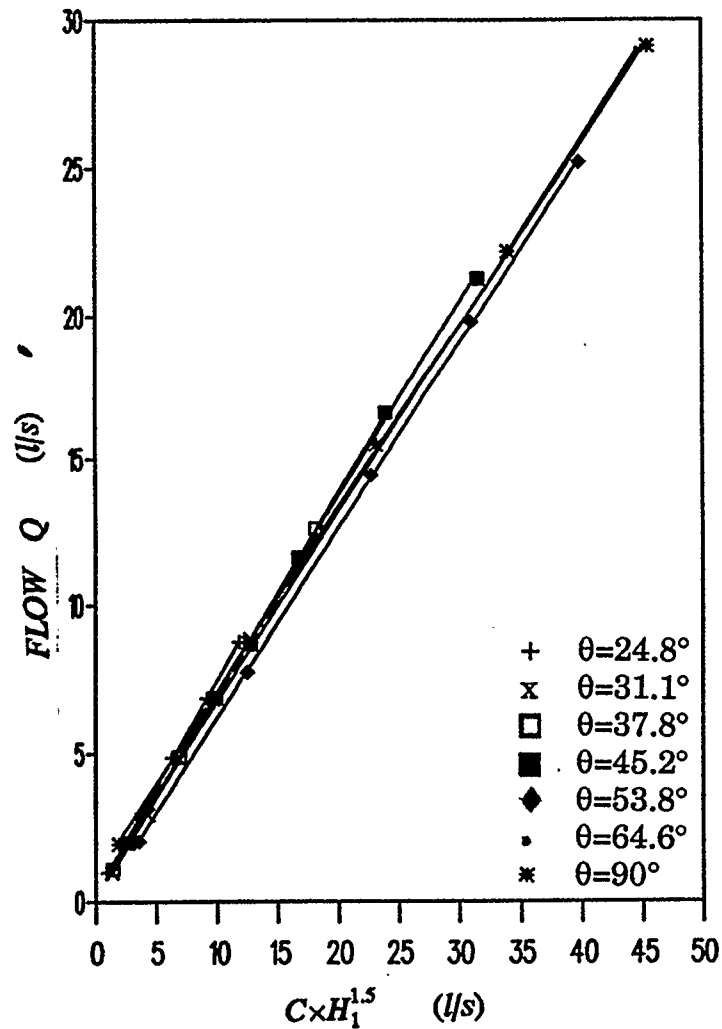


Fig.25  $Q$  vs  $C \times H_{11.5}$  for weir length 155 mm, width 420 mm, and weir length 230 mm, width 420 mm

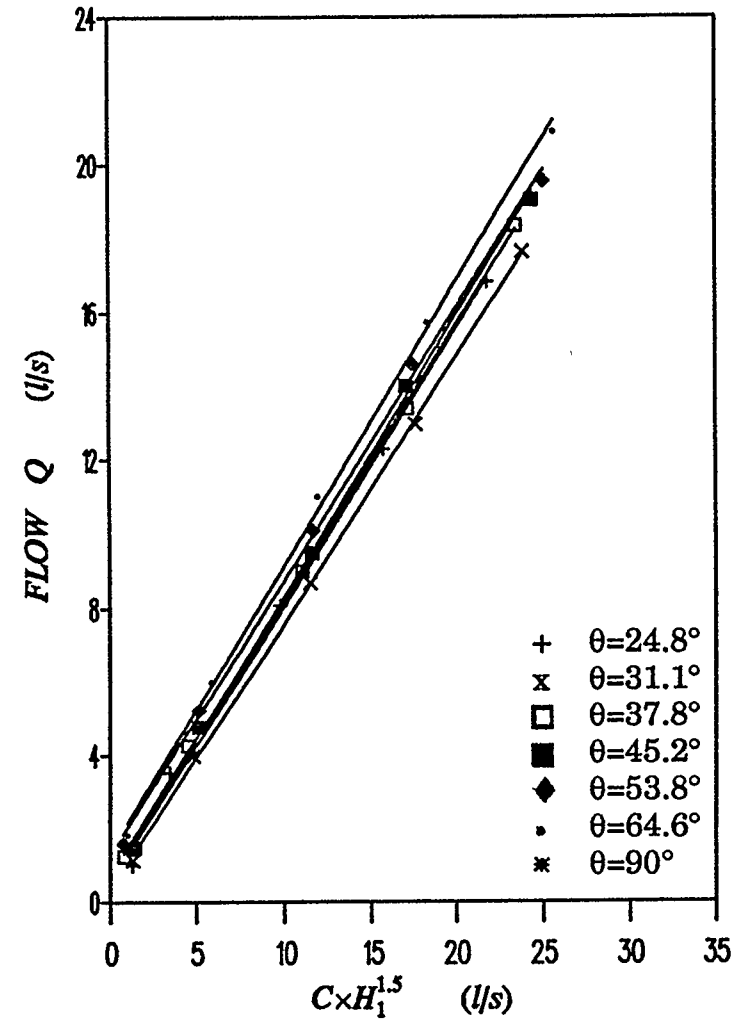
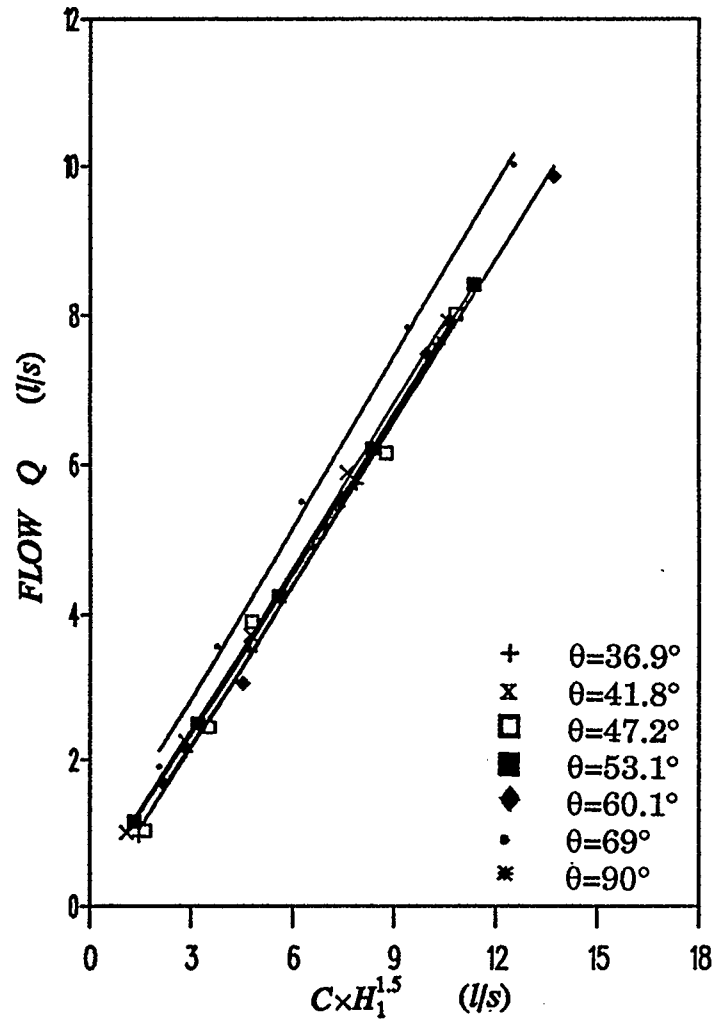


Fig.26  $Q$  vs  $C \times H_1^{1.5}$  for weir length 75 mm, width 570 mm, and weir length 155 mm, width 570 mm

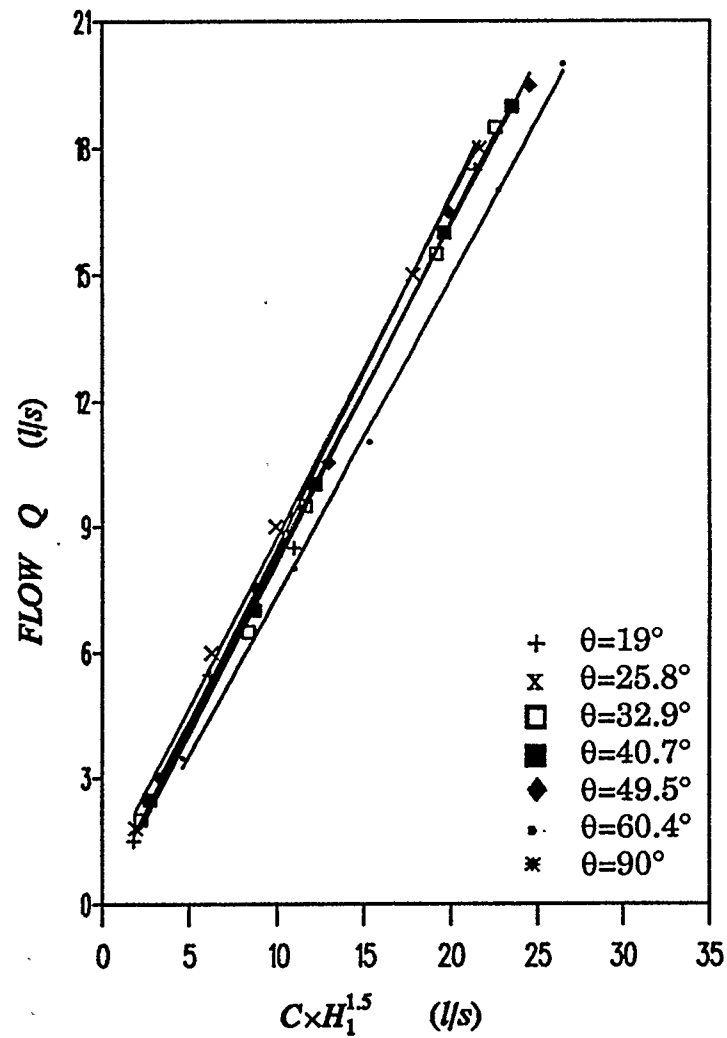


Fig.27  $Q$  vs  $C \times H_1^{1.5}$  for weir length 230 mm, width 570 mm

The values of unsubmerged flow coefficient  $K_1$  for one weir angle were calculated using the regression analysis method. The values of  $CxH_1^{1.5}$  and  $Q$  calculated in Table 4 were used and the regression analysis performed. For that purpose the linear probabilistic regression model was used. This model makes an assumption that the mean value of dependent variable for a given value of independent variable is a straight line and data points deviate about this line by a random error, i.e.

$$y = \beta_0 + \beta_1 x + \varepsilon \quad (22)$$

where:  $y$  - dependent variable

$x$  - independent variable

$\varepsilon$  - random error

$(\beta_0 + \beta_1 x)$  - mean value of  $y$  for a given  $x$

$\beta_0$  - point at which the line intercepts through the  $y$  axis

$\beta_1$  - amount of increase in the deterministic component of  $y$  for every one unit of increase in  $x$ , i.e. the slope of the line

$\beta_0$  and  $\beta_1$  are unknown parameters of the deterministic portion of the model.

The Eq.(20) can be written in a form:

$$Q = K_1 \times C \times H_1^{1.5} + y_{intercept} \quad (23)$$

and then the unknown parameters are  $y_{\text{intercept}}$  and  $K_1$ . In order to fit a linear regression model to a set of data the estimators for the parameters  $y_{\text{intercept}}$  and  $K_1$  must be determined. For that purpose the least squares method is used. The straight line that best fits the set of data is then defined as the line that satisfies the least squares criterion, that is, the sum of squared errors will be smaller than for any other straight line model. This line is called the least squares line.

Using the method outlined above, the slope may be estimated as:

$$\beta_1 = \frac{SS_{xy}}{SS_{xx}} \quad (24)$$

and the point at which the line intercepts the y-axis as:

$$y_{\text{intercept}} = \bar{y} - \beta_1 \bar{x} \quad (25)$$

where:

$$SS_{xy} = \sum (x_i - \bar{x})(y_i - \bar{y}) = \sum x_i y_i - \frac{(\sum x_i)(\sum y_i)}{n} \quad (26)$$

$$SS_{xx} = \sum (x_i - \bar{x})^2 = \sum x_i^2 - \frac{(\sum x_i)^2}{n} \quad (27)$$

$n$  = sample size

The standard deviation of the random error must be estimated from the data. The standard deviation measures the variation of the  $y$  values about the least squares line.

Using the procedure described above, the values of  $K_1$  were estimated for every angle of the weir. The correlation coefficient  $R$  which is actually a quantitative measure of the strength of the linear relationship between two variables was computed as:

$$R = \frac{SS_{xy}}{\sqrt{SS_{xx} + SS_{yy}}} \quad (28)$$

The correlation coefficient provides information about the utility of the model. Values of the correlation coefficient closer to unity indicate strong relationship between  $y$  and  $x$ . When  $R$  equals unity, the data points fall exactly on the least squares line. For all calculated values of  $K_1$  in this study, the correlation coefficients equal unity.

The calculated values of  $K_1$  for seven angles of inclination of the weir, along with the corresponding values of the  $R$  are shown in Tab. 5 to Tab.13.

angle	$K_1$	R
36.9°	0.64	1.00
41.8°	0.63	1.00
47.2°	0.63	1.00
53.1°	0.62	1.00
60.1°	0.60	1.00
69°	0.59	1.00
90°	0.60	1.00

Table 5. Values of  $K_1$  for weir length 75 mm, and width 270 mm

angle	$K_1$	R
24.8°	0.68	1.00
31.1°	0.69	1.00
37.8°	0.68	1.00
45.2°	0.67	1.00
53.8°	0.70	1.00
64.6°	0.67	1.00
90°	0.61	1.00

Table 6. Values of  $K_1$  for weir length 155 mm, and width 270 mm

angle	$K_1$	R
19°	0.78	1.00
25.8°	0.72	1.00
32.9°	0.73	1.00
40.7°	0.70	1.00
49.5°	0.73	1.00
60.4°	0.70	1.00
90°	0.62	1.00

Table 7. Values of  $K_1$  for weir length 230 mm, and width 270 mm

angle	$K_1$	R
36.9°	0.77	1.00
41.8°	0.81	1.00
47.2°	0.79	1.00
53.1°	0.79	1.00
60.1°	0.72	1.00
69°	0.64	1.00
90°	0.62	1.00

Table 8. Values of  $K_1$  for weir length 75 mm, and width 420 mm



angle	$K_1$	R
24.8°	0.72	1.00
31.1°	0.69	1.00
37.8°	0.69	1.00
45.2°	0.67	1.00
53.8°	0.64	1.00
64.6°	0.64	1.00
90°	0.63	1.00

Table 9. Values of  $K_1$  for weir length 155 mm, and width 420 mm

angle	$K_1$	R
19°	0.73	1.00
25.8°	0.70	1.00
32.9°	0.75	1.00
40.7°	0.68	1.00
49.5°	0.65	1.00
60.4°	0.66	1.00
90°	0.61	1.00

Table 10. Values of  $K_1$  for weir length 230 mm, and width 420 mm

angle	$K_1$	R
36.9°	0.74	1.00
41.8°	0.74	1.00
47.2°	0.74	1.00
53.1°	0.72	1.00
60.1°	0.73	1.00
69°	0.77	1.00
90°	0.65	1.00

Table 11. Values of  $K_1$  for weir length 75 mm, and width 570 mm

angle	$K_1$	R
24.8°	0.75	1.00
31.1°	0.72	1.00
37.8°	0.75	1.00
45.2°	0.76	1.00
53.8°	0.74	1.00
64.6°	0.77	1.00
90°	0.63	1.00

Table 12. Values w  $K_1$  for weir length 155 mm, and width 570 mm

angle	$K_1$	R
19°	0.84	1.00
25.8°	0.81	1.00
32.9°	0.81	1.00
40.7°	0.80	1.00
49.5°	0.79	1.00
60.4°	0.76	1.00
90°	0.65	1.00

Table 13. Values of  $K_1$  for weir length 230 mm, and width 570 mm

It is apparent from the tables that there are different values of  $K_1$  for different weir angles, therefore there could exist some relationship between  $K_1$  and  $\theta$ . In order to find the relationship, the values of  $K_1$  were plotted versus  $\theta$ , and the data points connected with lines, as shown on Fig.28 to Fig.36.

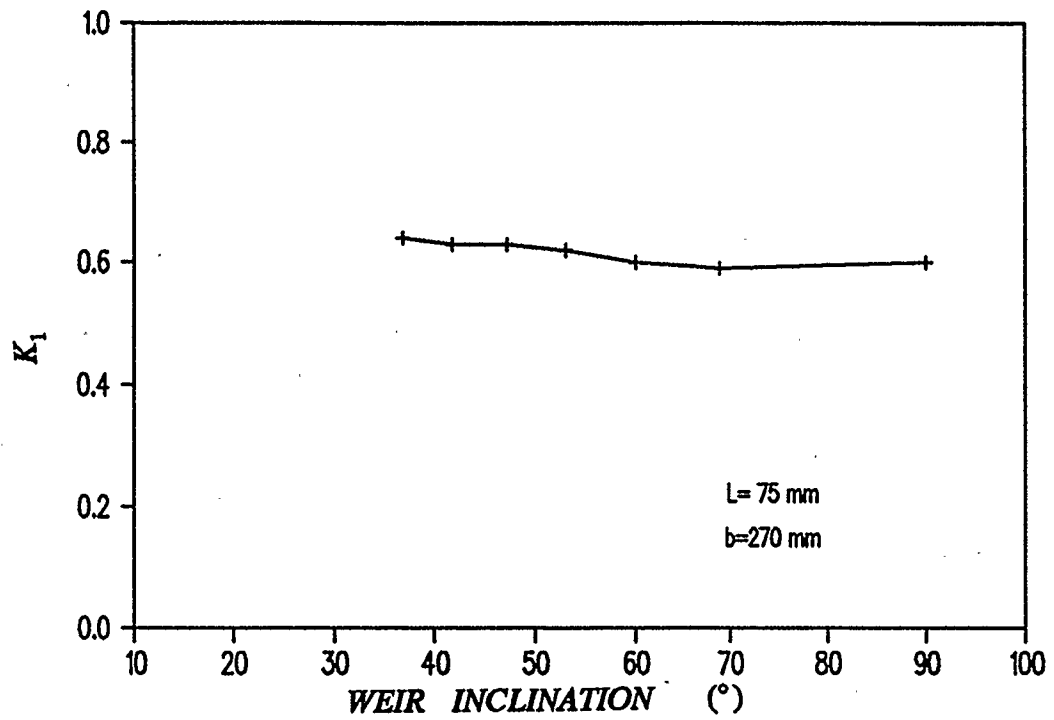


Fig.28  $K_1$  vs  $\theta$  for weir length 75 mm, width 270 mm

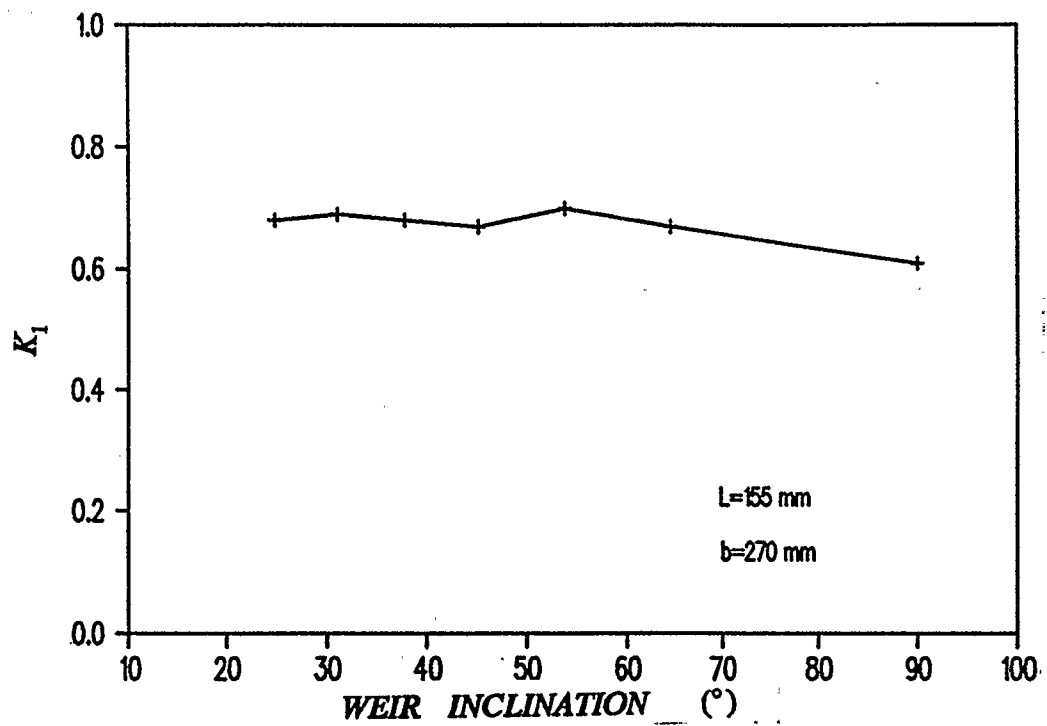


Fig.29  $K_1$  vs  $\theta$  for weir length 155 mm, width 270 mm

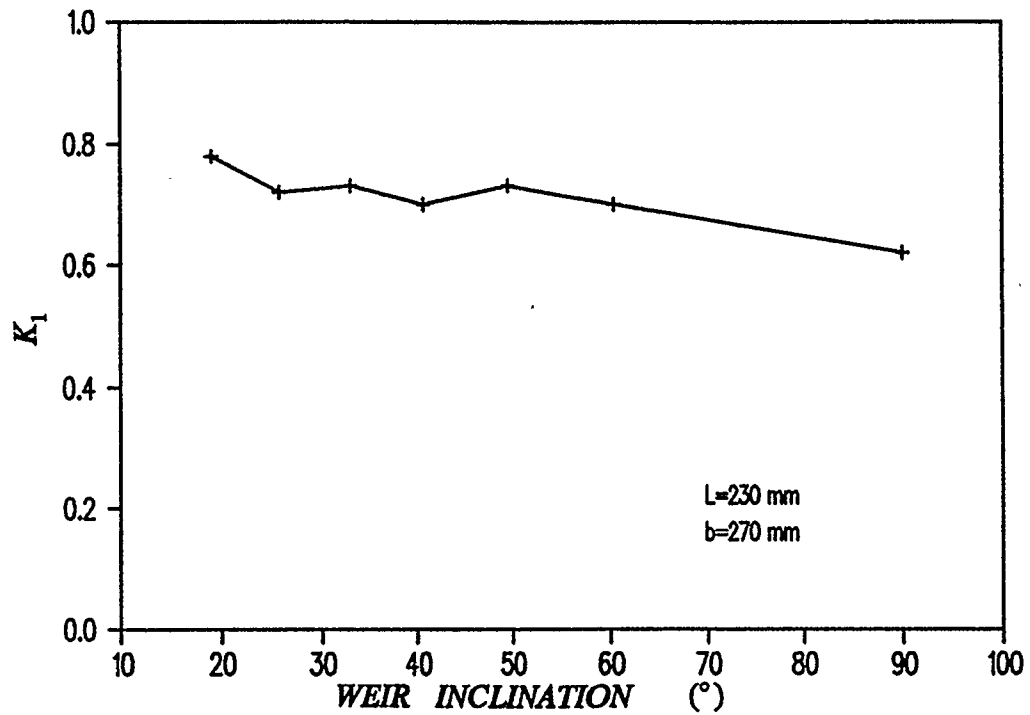


Fig.30  $K_1$  vs  $\theta$  for weir length 230 mm, width 270 mm

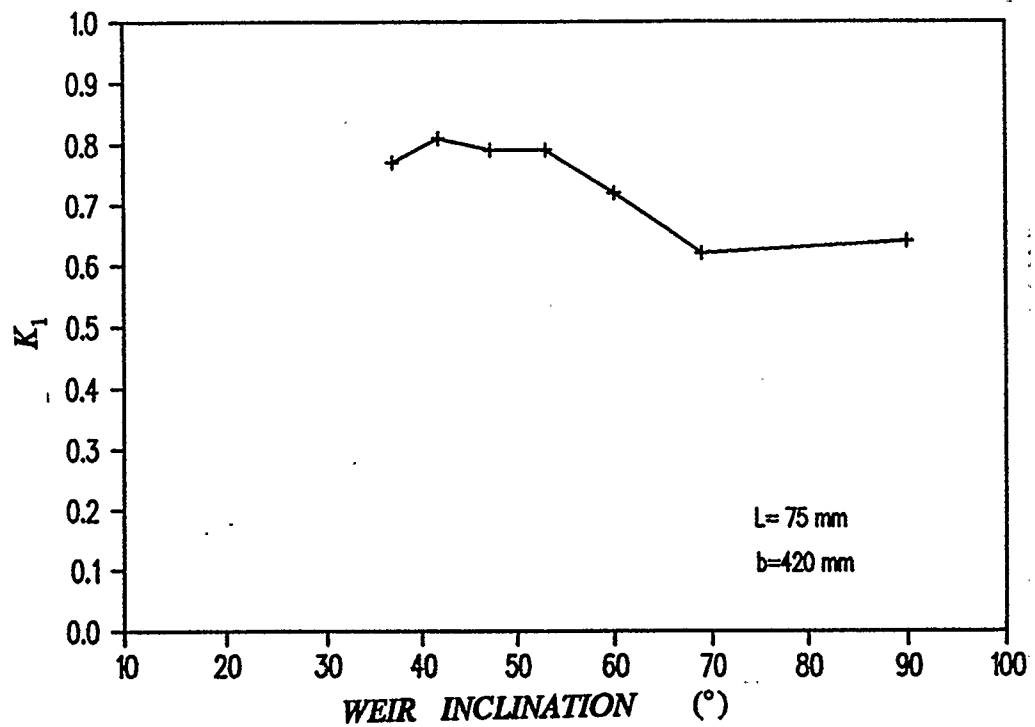


Fig.31  $K_1$  vs  $\theta$  for weir length 75 mm, width 420 mm

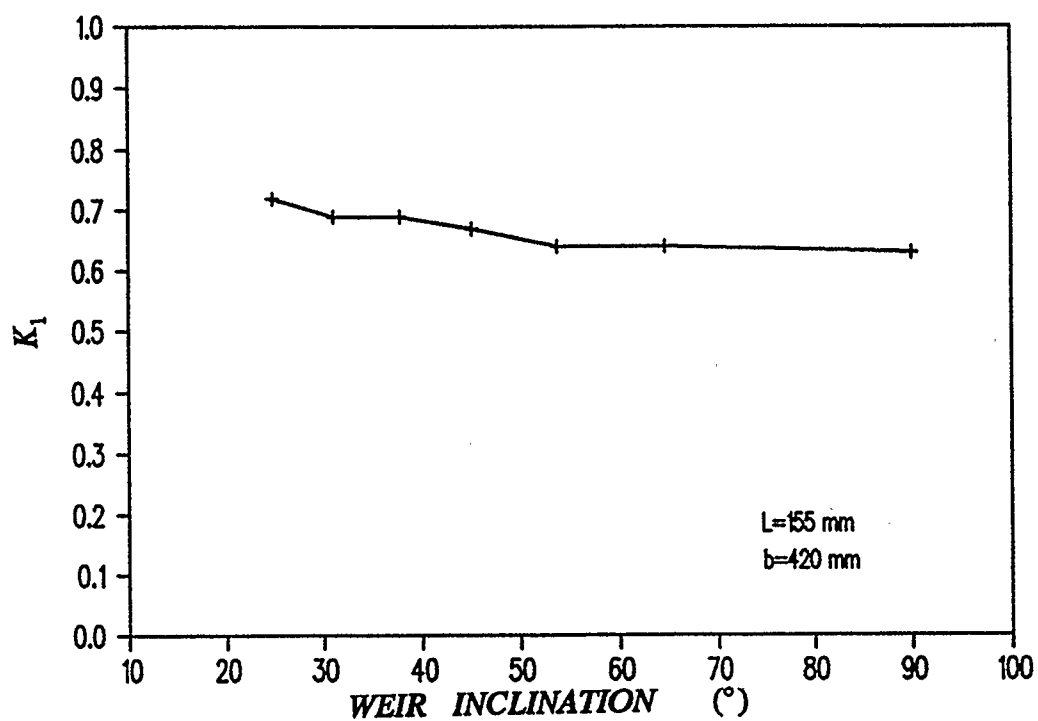


Fig.32  $K_1$  vs  $\theta$  for weir length 155 mm, width 420 mm

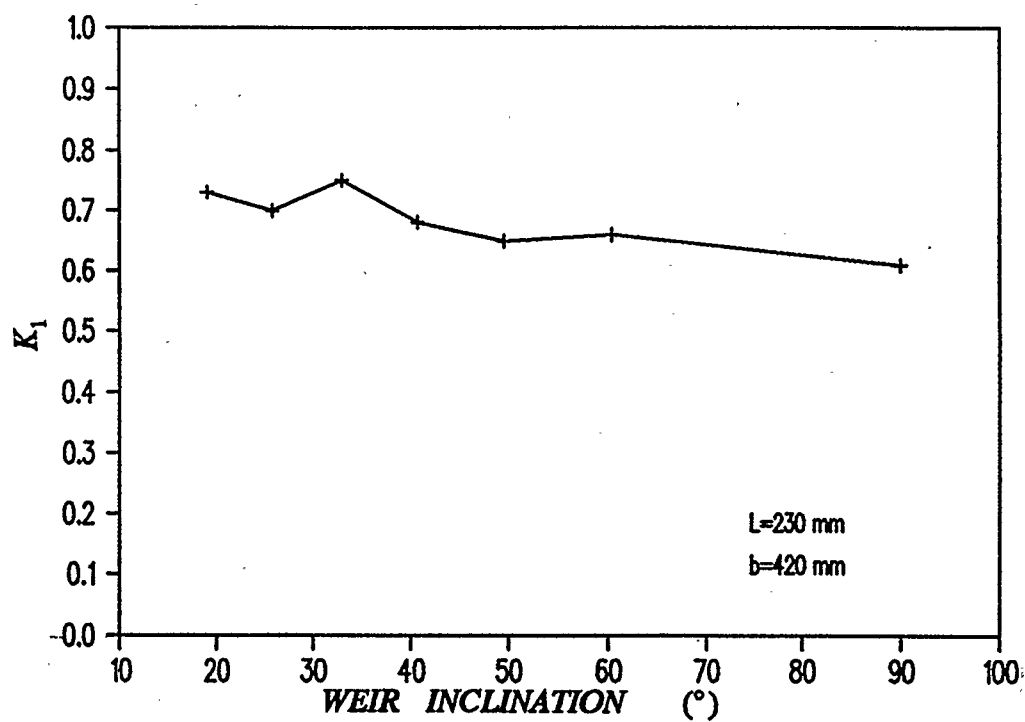


Fig.33  $K_1$  vs  $\theta$  for weir length 230 mm, width 420 mm

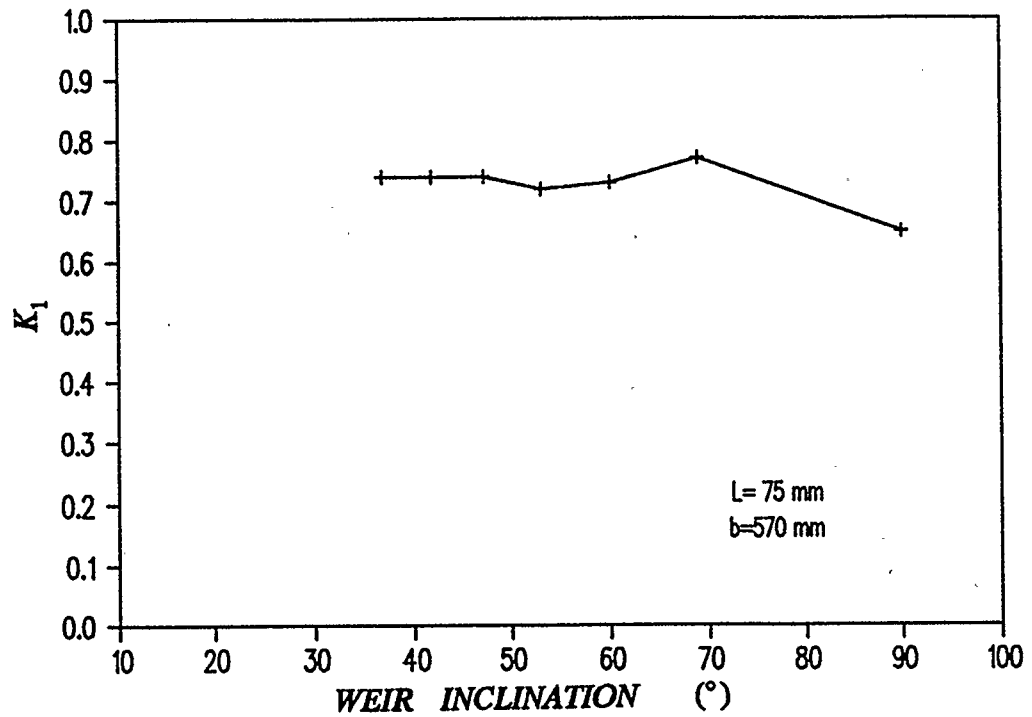


Fig.34  $K_1$  vs  $\theta$  for weir length 75 mm, width 570 mm

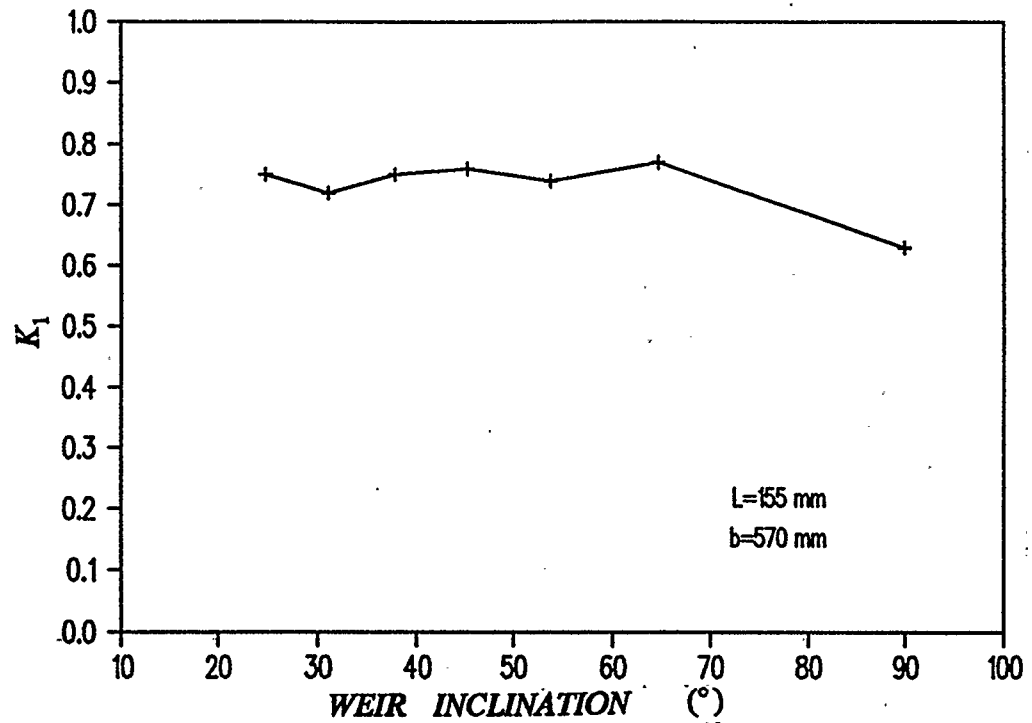


Fig.35  $K_1$  vs  $\theta$  for weir length 155 mm, width 570 mm

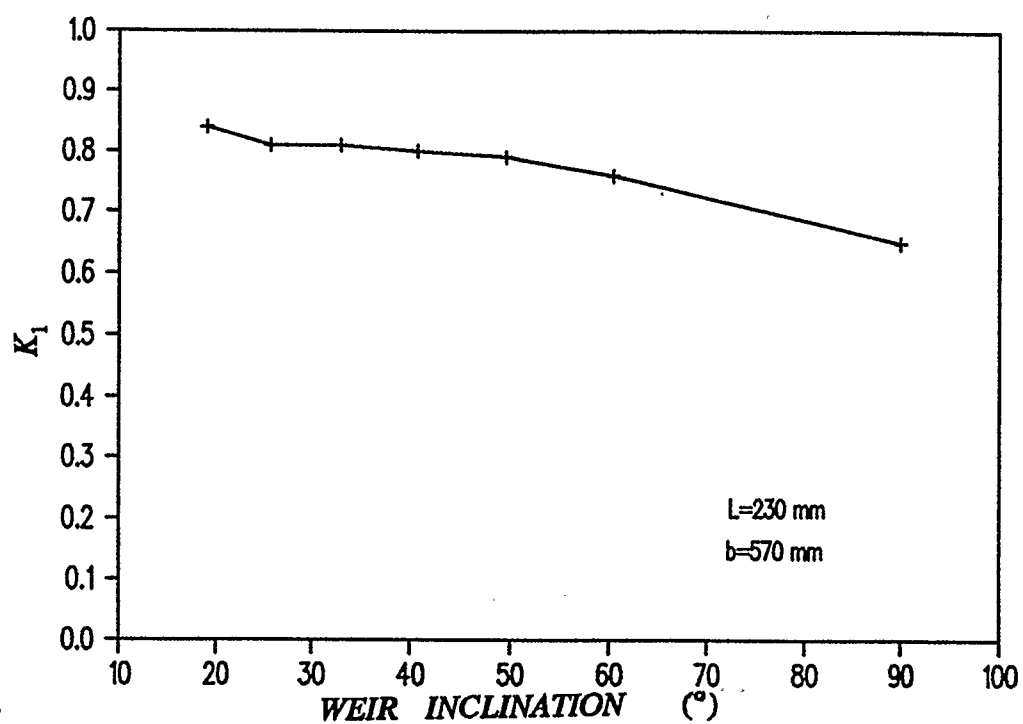


Fig.36  $K_1$  vs  $\theta$  for weir length 230 mm, width 570 mm



The unsubmerged coefficient  $K_1$  as given by Eq. (20) is actually a combined coefficient which includes the effects of the geometry of approach channel, the ratio of upstream head over weir to weir height, and effects of weir inclination. In order to separate the effects of geometry from effects of weir inclination, equation of the following type was used:

$$K_1 = K_0 \times K_e \quad (29)$$

The coefficient  $K_e$  in Eq.29 is the effective discharge coefficient which is a function of the ratio of weir width to the width of upstream channel and head over weir to weir height. The effective discharge coefficient is defined by equation<sup>(1)</sup> as:

$$K_e = a + b \times \frac{H_1}{P} \quad (30)$$

where a and b are empirically determined as functions of the ratio  $b/B$ <sup>(1)</sup>:

$$0.587 < a < 0.602$$

$$-0.0023 < b < 0.075$$

For different widths of the weir,  $K_e$  was calculated using following expressions:

1. For  $b = 270$  mm and  $b/B = 0.45$ ,

$$K_e = 0.5915 + 0.0085 \frac{H_1}{P} \quad (31)$$

2. For  $b = 420$  mm and  $b/B = 0.70$ ,

$$K_e = 0.5950 + 0.0300 \frac{H_1}{P} \quad (32)$$

3. For  $b = 570$  mm and  $b/B = 0.95$ ,

$$K_e = 0.6010 + 0.0695 \frac{H_1}{P} \quad (33)$$

where  $P$  is the height of the weir crest of the inclined weir above the channel bottom.

The Eqs. 31, 32 and 33 are taken from the study on weir hydraulics conducted by Georgia Institute of Technology (1978) <sup>(5)</sup>

The coefficient  $K_\theta$  in the Eq.29 is the inclination coefficient which accounts for the effect of the angle of inclination of the weir.

The Eq.20 may now be written in a form:

$$Q = K_\theta K_e C H_1^{1.5}$$

Values of  $K_e$  and of the product  $K_e C x H_1^{1.5}$  for different weir angles, flow rates and upstream head over weir were calculated using worksheet shown in Table 14. Then the linear regression was performed on the data and the values of  $K_e$  were obtained, in the same manner as the values of  $K_1$ .

The Fig.37 and Fig.38 are plots of  $Q$  versus  $K_e C x H_1^{1.5}$  for different weir angles. Regression coefficients for these lines equal unity. Figures 39 to 43 summarize all  $Q$ - $K_e C x H_1^{1.5}$  plots for one weir.

Once all  $K_e$  values for one weir were calculated, they were summarized as shown in Tables 15 to 23.

UNSUBMERGED COEFFICIENT  $K_0$ 

CONSTANT (C) = 25212.60  
 WEIR LENGTH (L) = 75.00  
 WEIR WIDTH (B) = 270.00

FOR WEIR HEIGHT (P) = 45.00

Q(l/s)	$H_1$	$H_1^{1.5}$	$CH_1^{1.5}$	$K_e$	$K_e CH_1^{1.5}$
1.03	16.30	65.81	1.66	0.59	0.99
3.93	37.93	233.60	5.89	0.60	3.53
7.89	62.13	489.72	12.35	0.60	7.45
11.90	80.13	717.29	18.08	0.61	10.67
14.70	94.30	915.73	23.09	0.61	14.06

FOR WEIR HEIGHT (P) = 50.00

Q(l/s)	$H_1$	$H_1^{1.5}$	$CH_1^{1.5}$	$K_e$	$K_e CH_1^{1.5}$
1.52	16.53	67.21	1.69	0.59	1.01
4.55	40.03	253.27	6.39	0.60	3.82
8.50	61.60	483.43	12.19	0.60	7.34
12.27	81.53	736.17	18.56	0.61	11.23
15.13	95.73	936.64	23.62	0.61	14.35

FOR WEIR HEIGHT (P) = 55.00

Q(l/s)	$H_1$	$H_1^{1.5}$	$CH_1^{1.5}$	$K_e$	$K_e CH_1^{1.5}$
6					
1.92	20.97	96.03	2.42	0.59	1.44
5.05	41.27	256.13	6.68	0.60	4.00
8.98	63.67	508.05	12.81	0.60	7.70
12.82	84.27	773.59	19.50	0.60	11.79
15.99	98.80	982.05	24.76	0.61	15.02

Table 14. Example of worksheet with data summary and  $K_e$

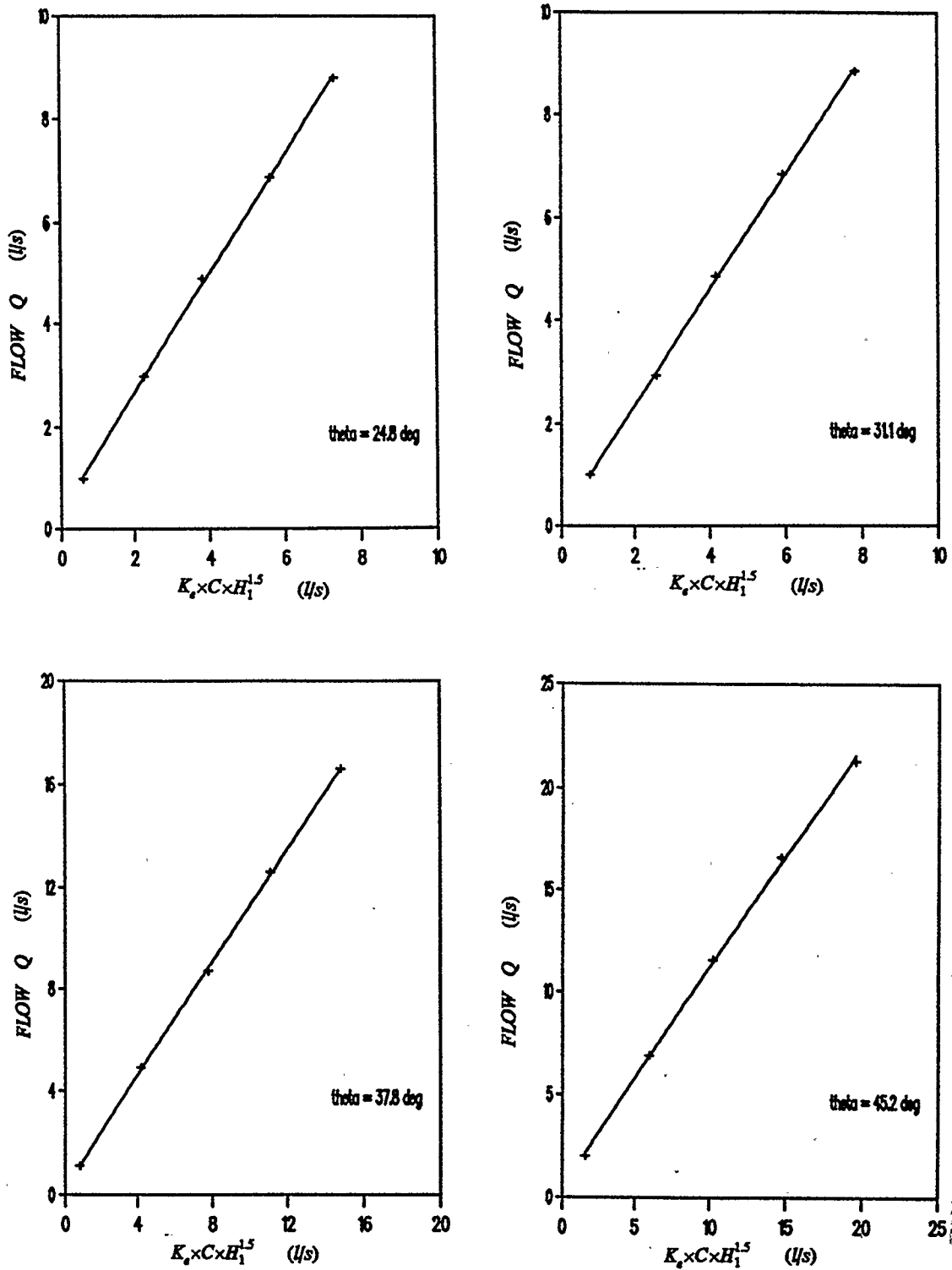


Fig.37  $Q$  vs  $K_e \times C \times H_1^{1.5}$  for weir length 155 mm, width 420 mm, and inclination of  $\theta=24.6^\circ, \theta=31.1^\circ, \theta=37.8^\circ, \theta=45.2^\circ$

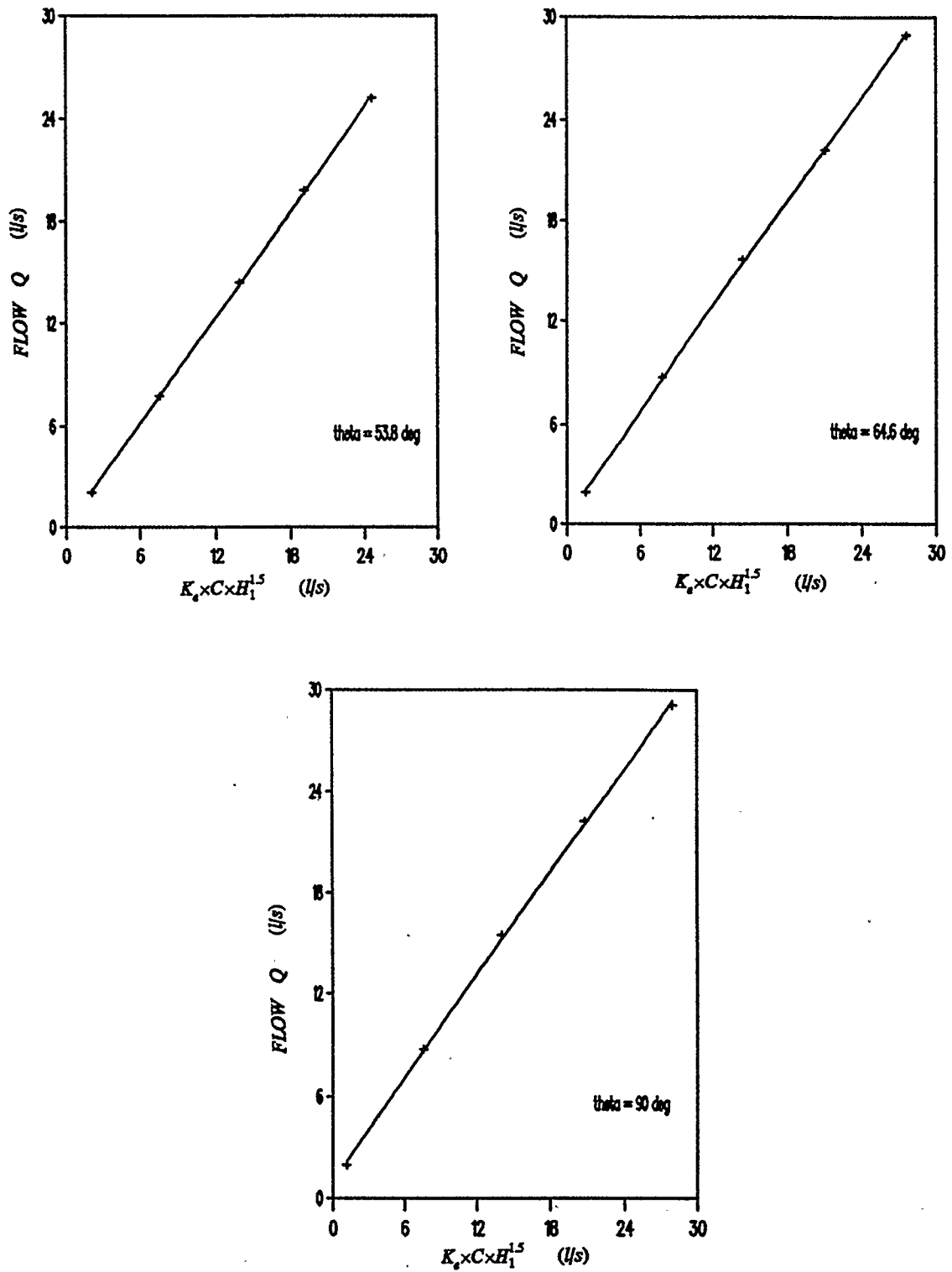


Fig.38  $Q$  vs  $K_e \times C \times H_1^{1.5}$  for weir length 155 mm, width 420 mm, and inclination of  $\theta = 53.8^\circ$ ,  $\theta = 64.6^\circ$ , and  $\theta = 90^\circ$

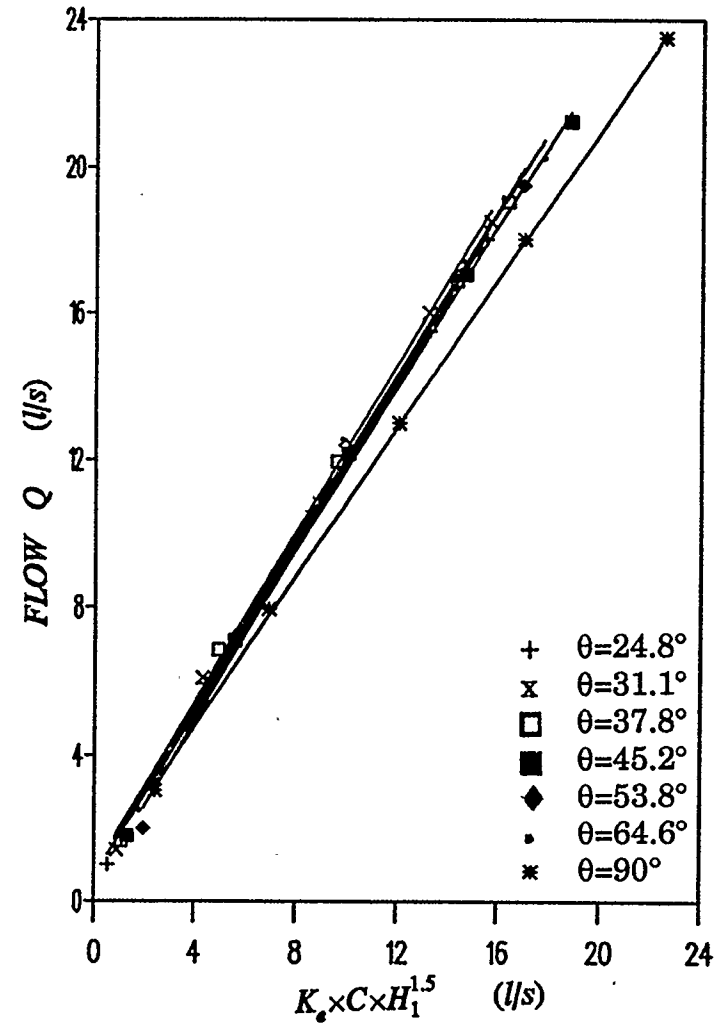
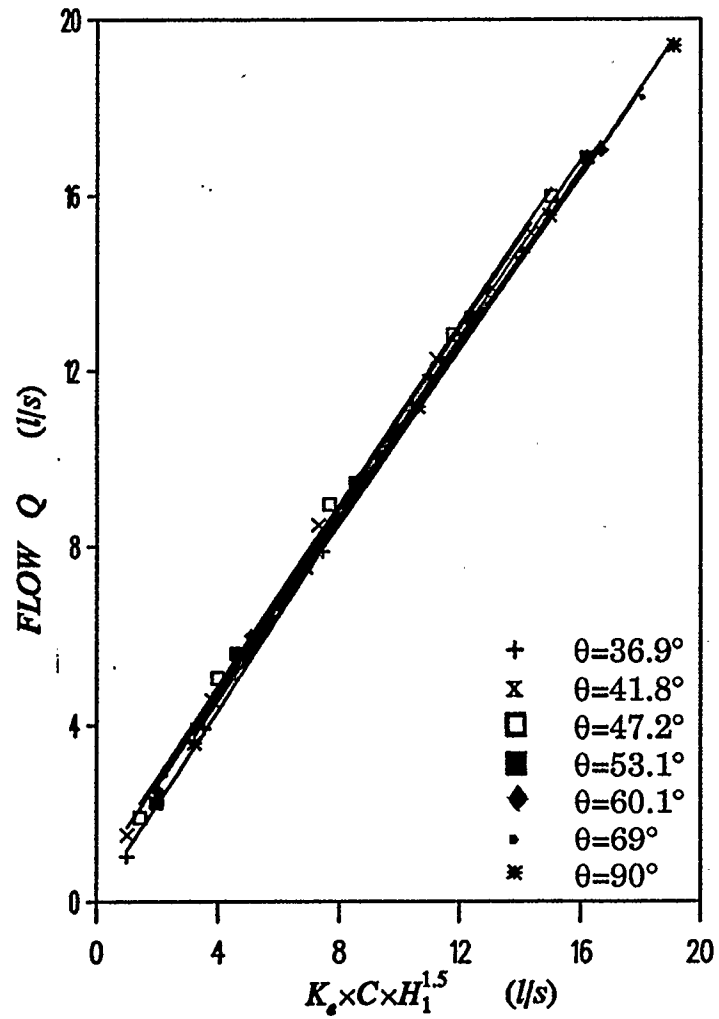


Fig.39  $Q$  vs  $K_e \times C \times H_1^{1.5}$  for weir length 75 mm, width 270 mm,  
and weir length 155 mm, width 270 mm

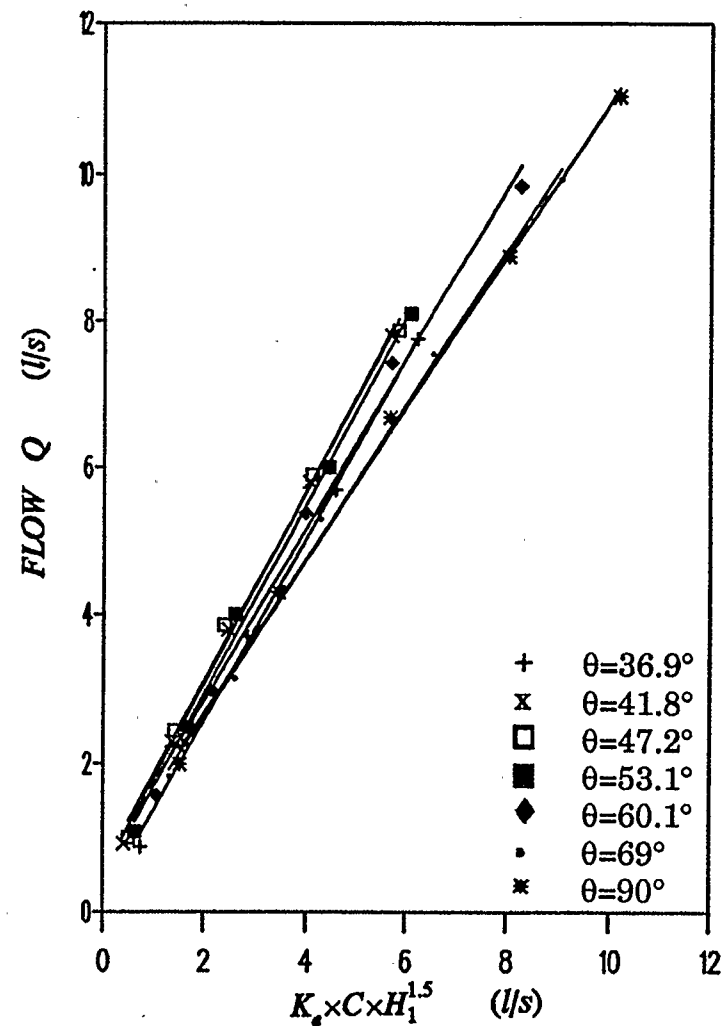
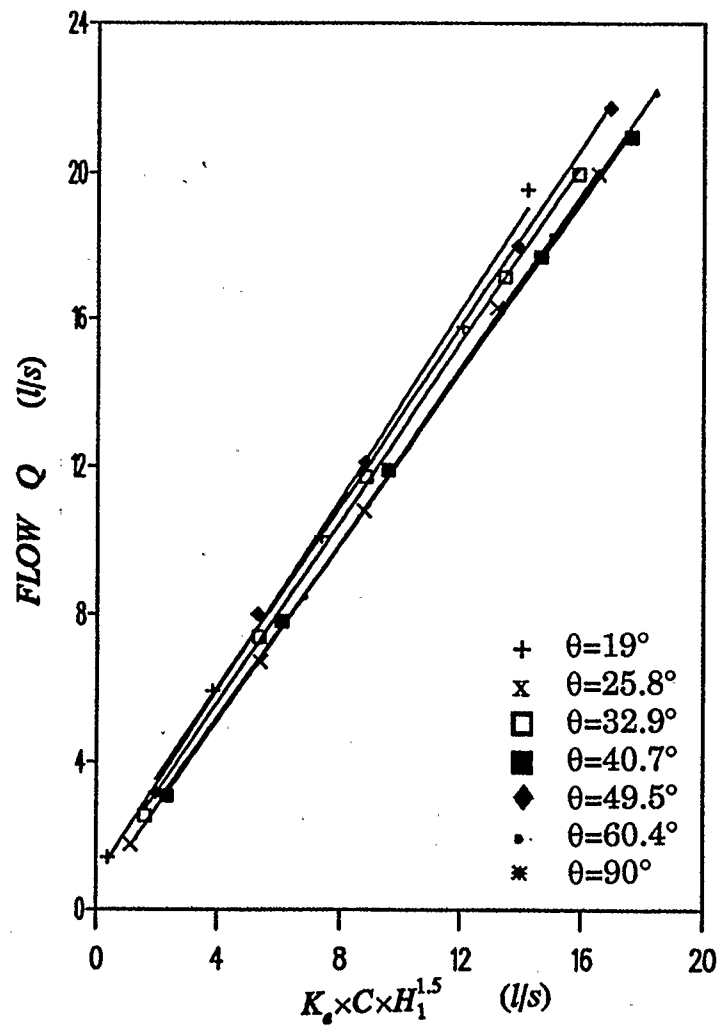


Fig.40  $Q$  vs  $K_e \times C \times H_1^{1.5}$  for weir length 230 mm, width 270 mm,  
and weir length 75 mm, width 420 mm



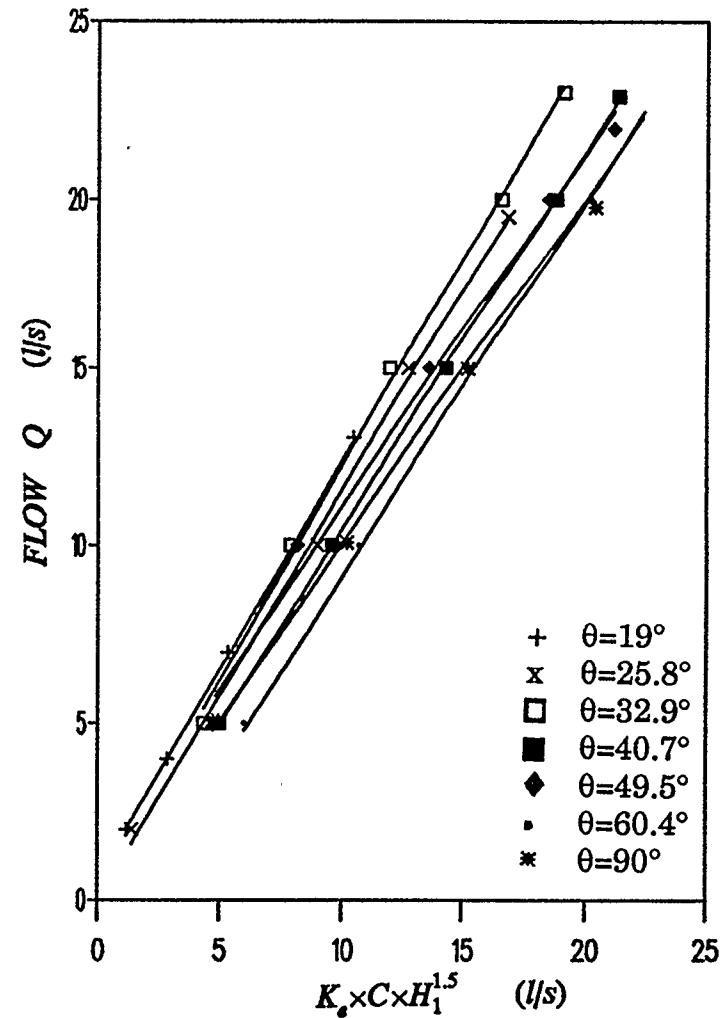
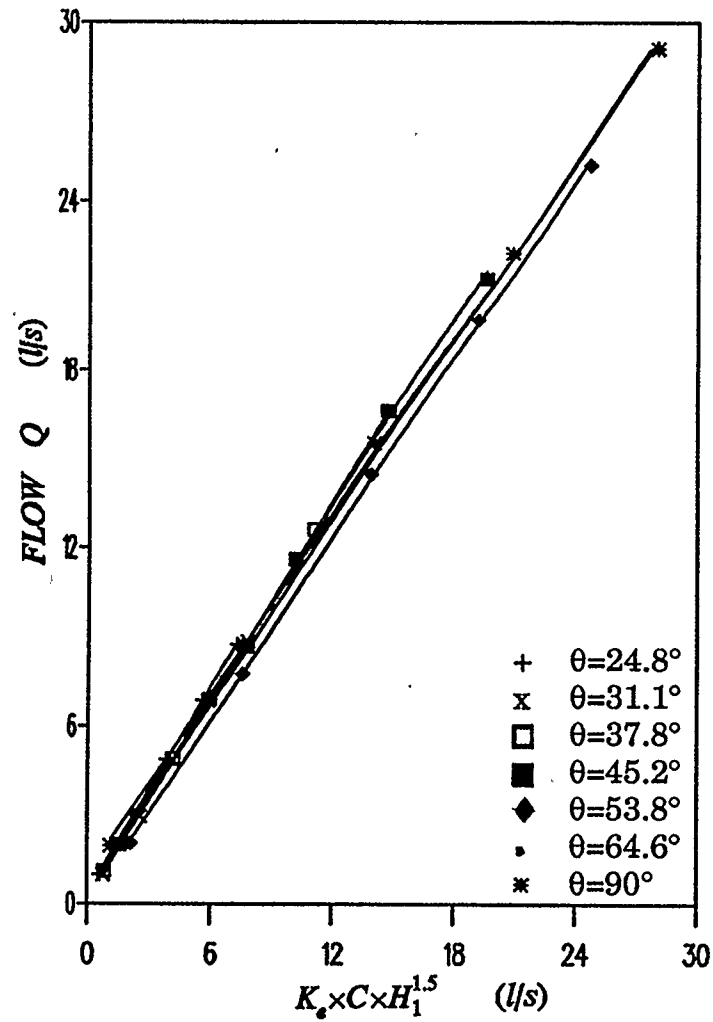


Fig.41  $Q$  vs  $K_e \times C \times H_1^{1.5}$  for weir length 155 mm, width 420 mm,  
and weir length 230 mm, width 420 mm

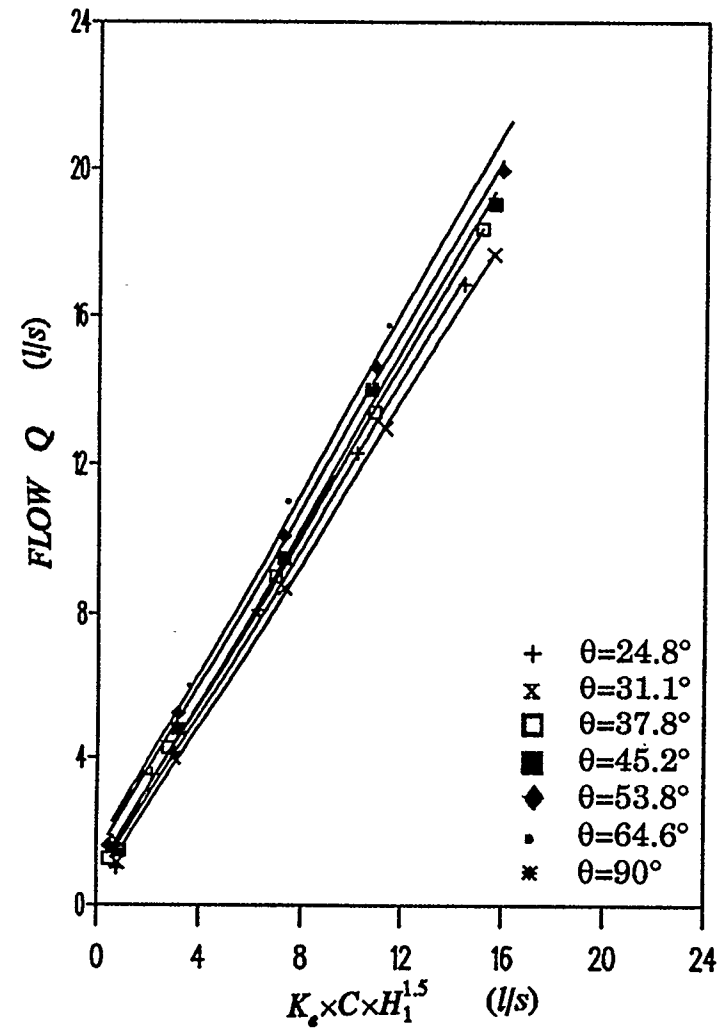
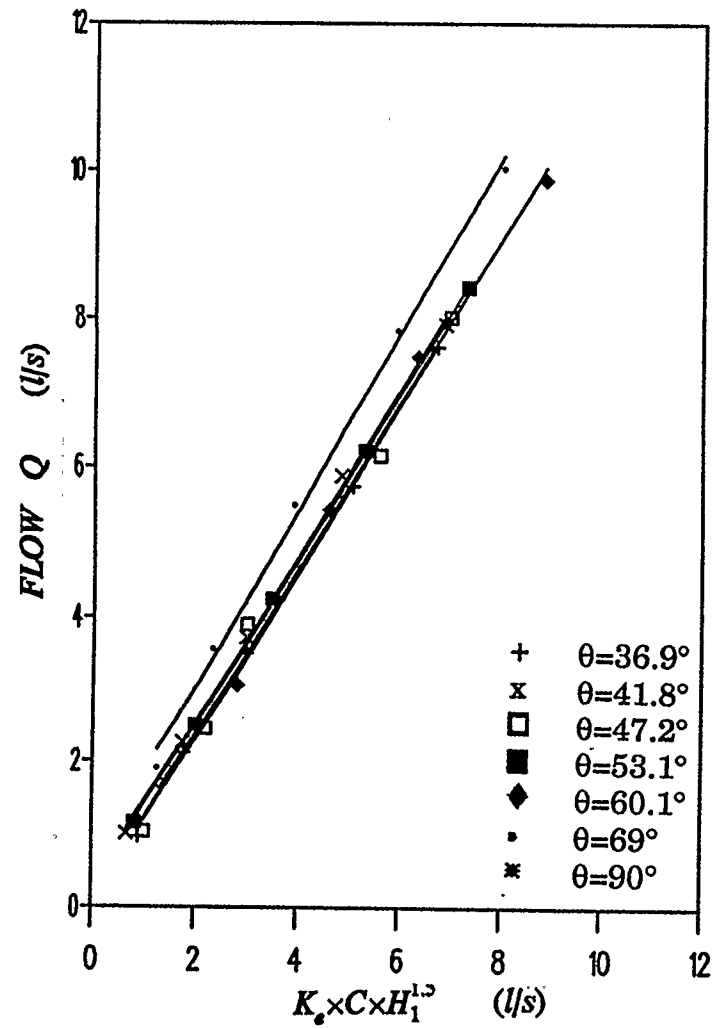


Fig.42  $Q$  vs  $K_e \times C \times H_1^{1.5}$  for weir length 75 mm, width 570 mm,  
and weir length 155 mm, width 570 mm

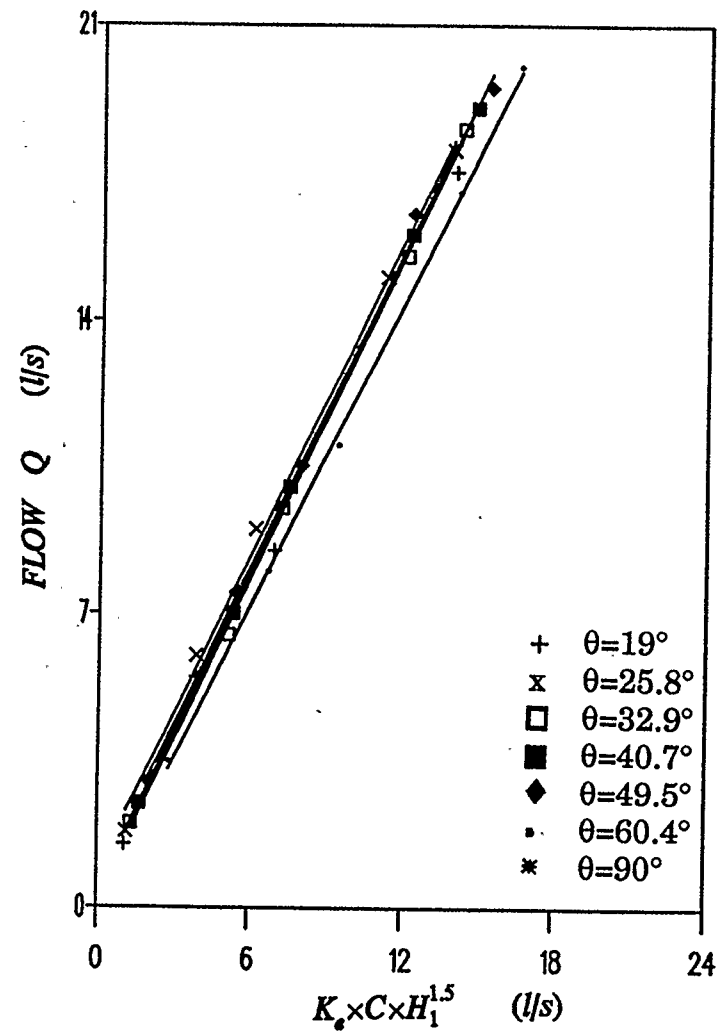


Fig.43  $Q$  vs  $K_e \times C \times H_1^{1.5}$  for weir length 230 mm, width 570 mm

angle	$K_\theta$	R
36.9°	1.05	1.00
41.8°	1.02	1.00
47.2°	1.02	1.00
53.1°	1.01	1.00
60.1°	0.99	1.00
69°	0.99	1.00
90°	1.00	1.00

Table 15. Values of  $K_\theta$  for weir length 75 mm, and width 270 mm

angle	$K_\theta$	R
24.8°	1.13	1.00
31.1°	1.15	1.00
37.8°	1.12	1.00
45.2°	1.11	1.00
53.8°	1.16	1.00
64.6°	1.12	1.00
90°	1.00	1.00

Table 16. Values of  $K_\theta$  for weir length 155 mm, and width 270 mm

angle	$K_\theta$	R
19°	1.28	1.00
25.8°	1.19	1.00
32.9°	1.22	1.00
40.7°	1.17	1.00
49.5°	1.22	1.00
60.4°	1.18	1.00
90°	1.02	1.00

Table 17. Values of  $K_\theta$  for weir length 230 mm, and width 270 mm

angle	$K_\theta$	R
36.9°	1.23	1.00
41.8°	1.30	1.00
47.2°	1.25	1.00
53.1°	1.27	1.00
60.1°	1.16	1.00
69°	1.06	1.00
90°	1.01	1.00

Table 18. Values of  $K_\theta$  for weir length 75 mm, width 420 mm

angle	$K_\theta$	R
24.8°	1.16	1.00
31.1°	1.13	1.00
37.8°	1.11	1.00
45.2°	1.08	1.00
53.8°	1.03	1.00
64.6°	1.03	1.00
90°	1.00	1.00

Table 19. Values of  $K_\theta$  for weir length 155 mm, and width 420 mm

angle	$K_\theta$	R
19°	1.18	1.00
25.8°	1.16	1.00
32.9°	1.21	1.00
40.7°	1.10	1.00
49.5°	1.06	1.00
60.4°	1.08	1.00
90°	1.00	1.00

Table 20. Values of  $K_\theta$  for weir length 230 mm, and width 420 mm

angle	$K_\theta$	R
36.9°	1.19	1.00
41.8°	1.12	1.00
47.2°	1.13	1.00
53.1°	1.12	1.00
60.1°	1.12	1.00
69°	1.19	1.00
90°	1.01	1.00

Table 21. Values of  $K_\theta$  for weir length 75 mm, and width 570 mm

angle	$K_\theta$	R
24.8°	1.13	1.00
31.1°	1.11	1.00
37.8°	1.16	1.00
45.2°	1.19	1.00
53.8°	1.17	1.00
64.6°	1.20	1.00
90°	1.00	1.00

Table 22. Values of  $K_\theta$  for weir length 155 mm, and width 570 mm

angle	$K_\theta$	R
19°	1.28	1.00
25.8°	1.26	1.00
32.9°	1.28	1.00
40.7°	1.27	1.00
49.5°	1.25	1.00
60.4°	1.21	1.00
90°	1.03	1.00

Table 23. Values of  $K_\theta$  for weir length 230 mm, width 570 mm

To determine the relationship between  $K_\theta$  and weir angle,  $K_\theta$  values were plotted versus angle  $\theta$ , as shown on Fig 44 to Fig 52, and the data points were connected with a line .



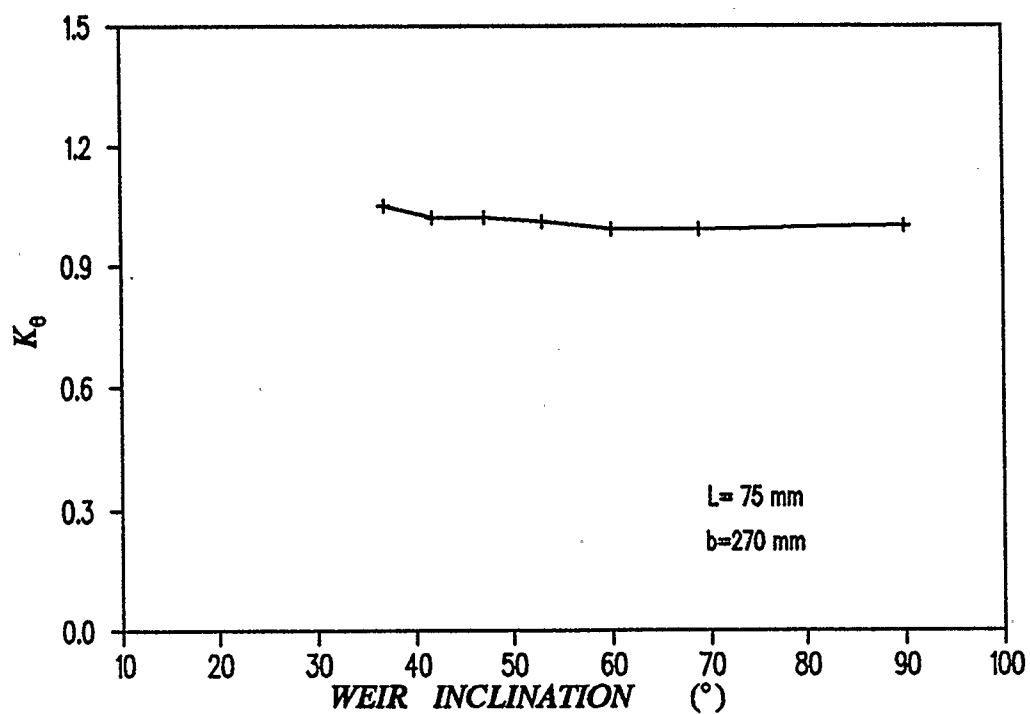


Fig.44  $K_\theta$  vs  $\theta$  for weir length 75 mm, width 270 mm

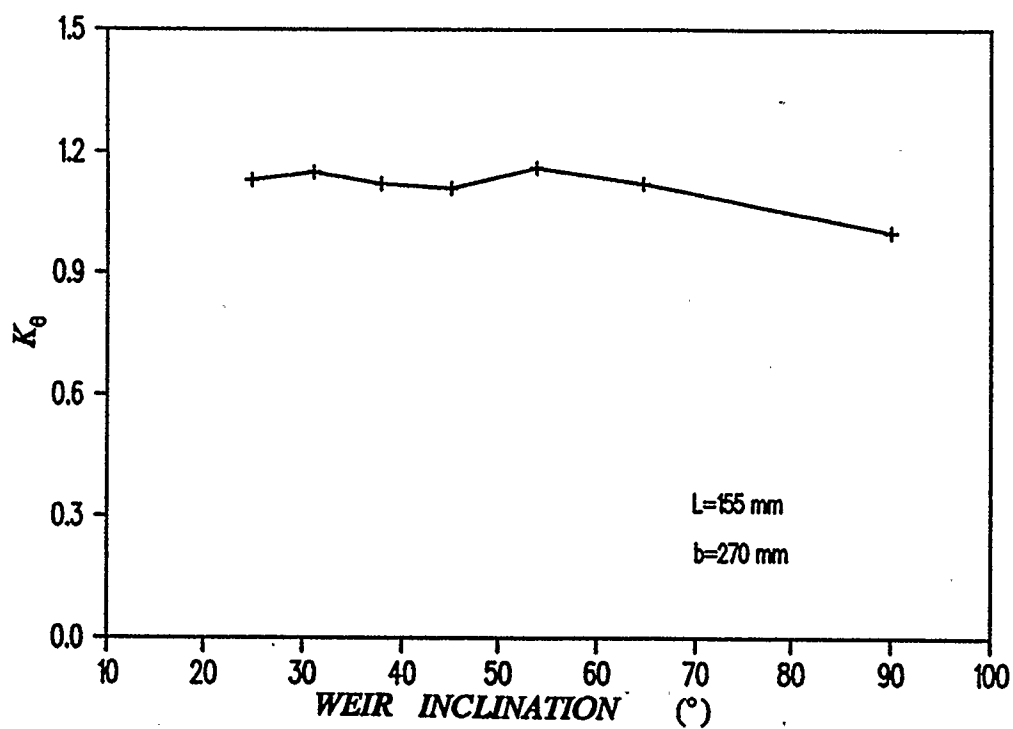


Fig.45  $K_\theta$  vs  $\theta$  for weir length 155 mm, width 270 mm

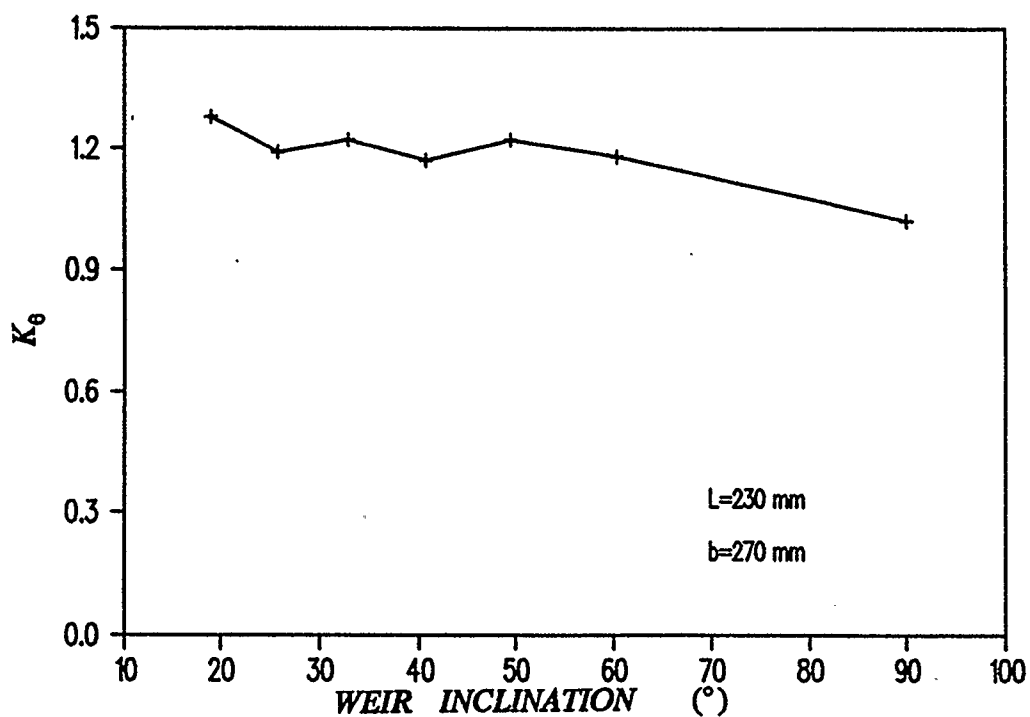


Fig.46  $K_\theta$  vs  $\theta$  for weir length 230 mm, width 270 mm

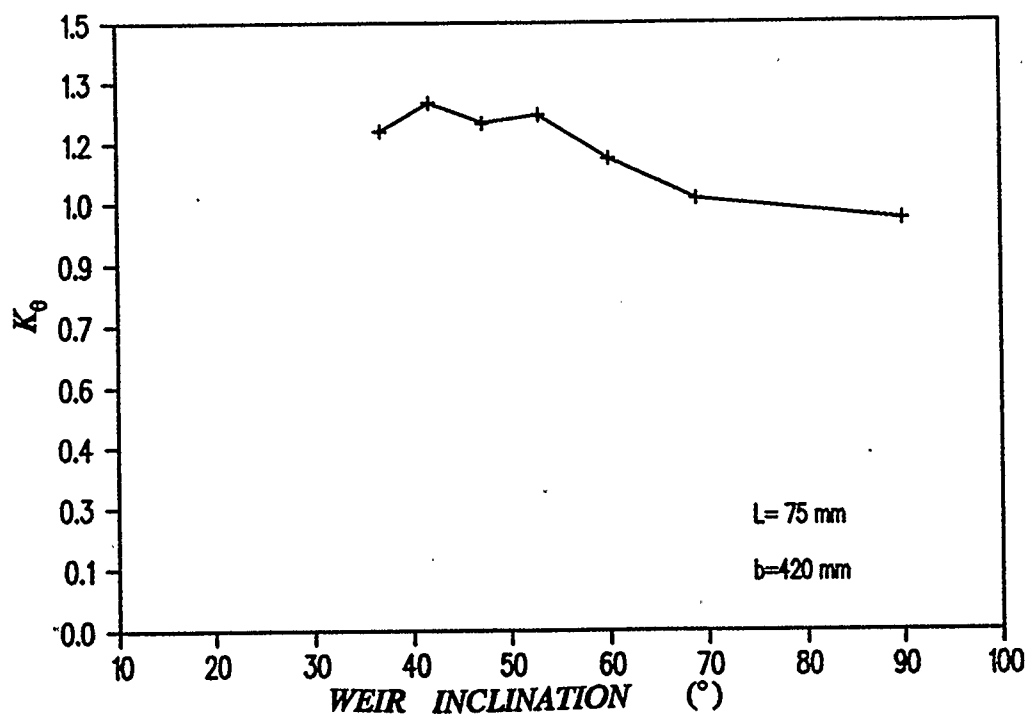


Fig.47  $K_\theta$  vs  $\theta$  for weir length 75 mm, width 420 mm

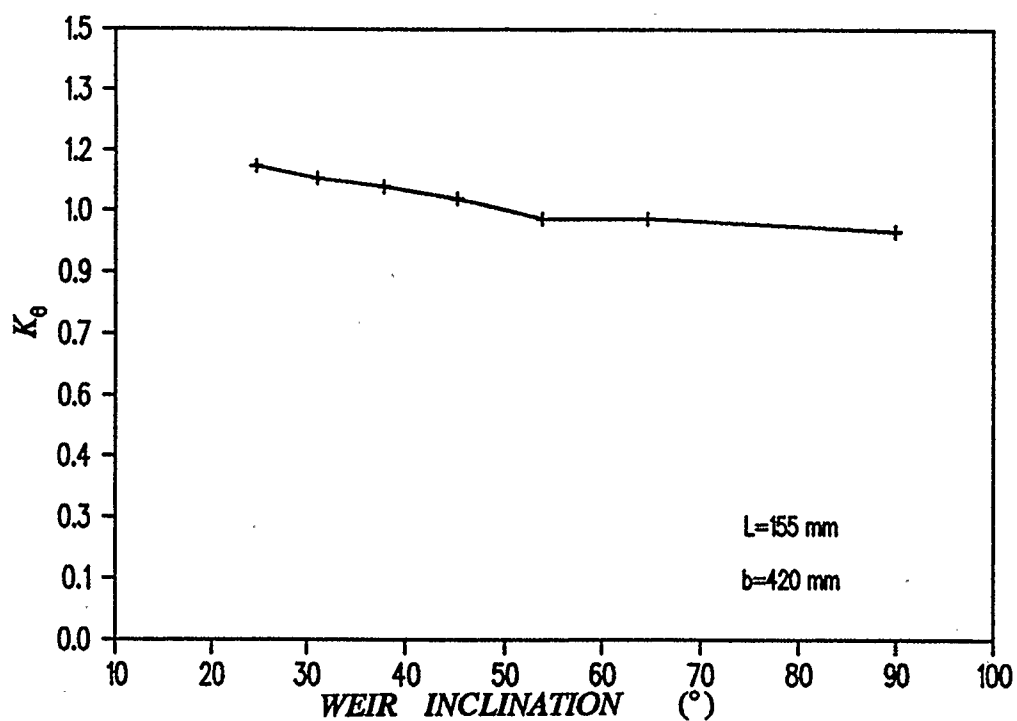


Fig.48  $K_\theta$  vs  $\theta$  for weir length 155 mm, width 420 mm

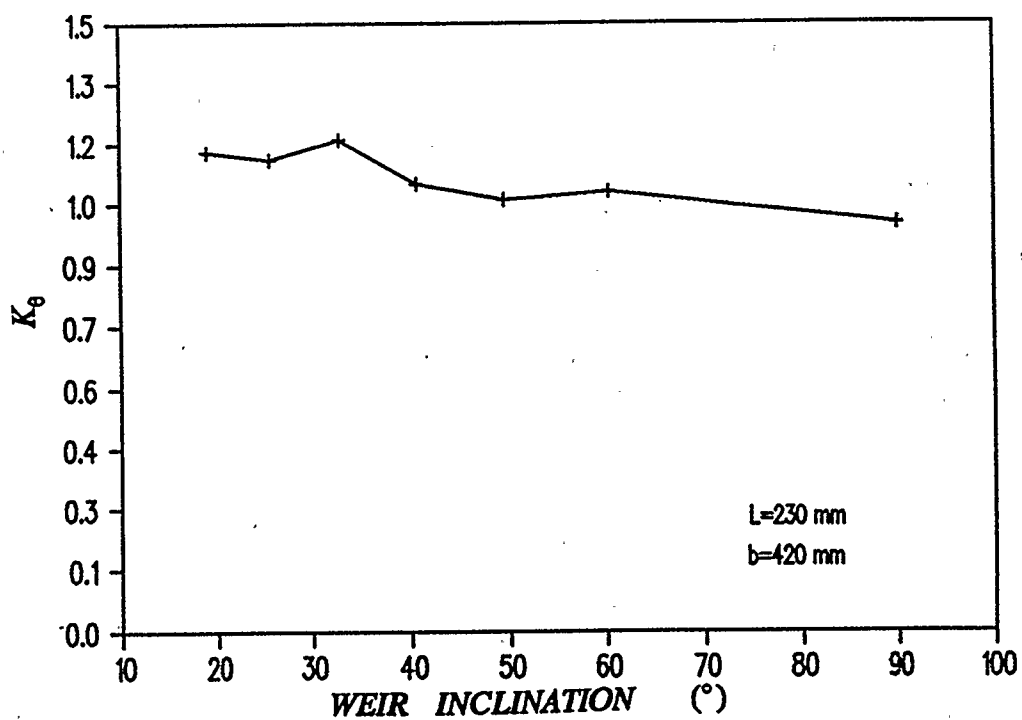


Fig.49  $K_\theta$  vs  $\theta$  for weir length 230 mm, width 420 mm

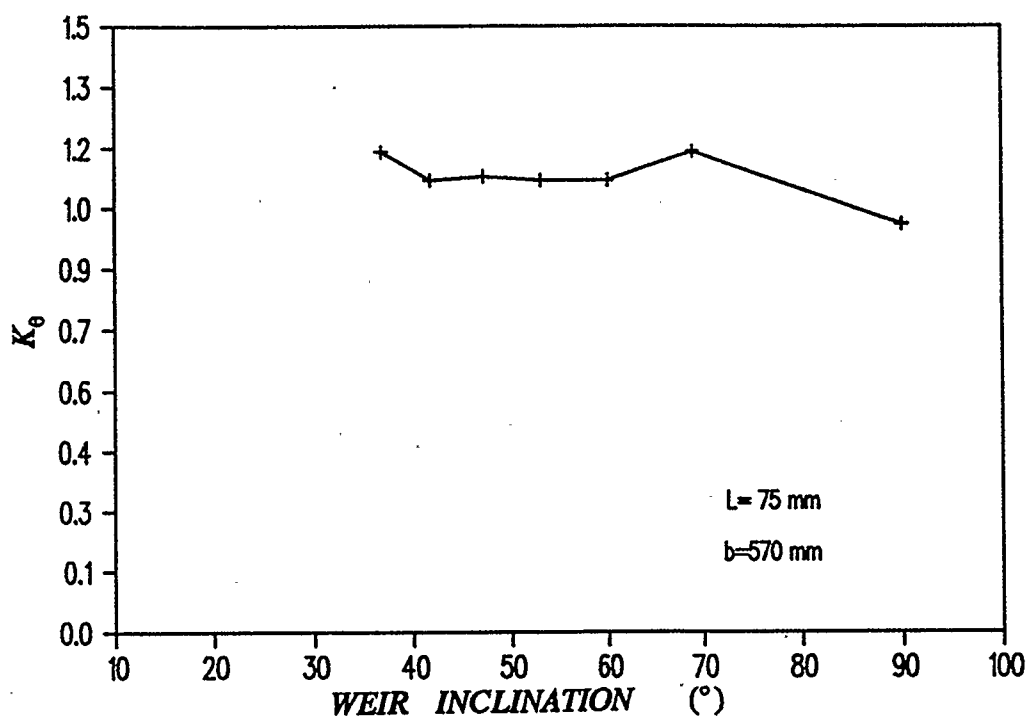


Fig.50  $K_\theta$  vs  $\theta$  for weir length 75 mm, width 570 mm

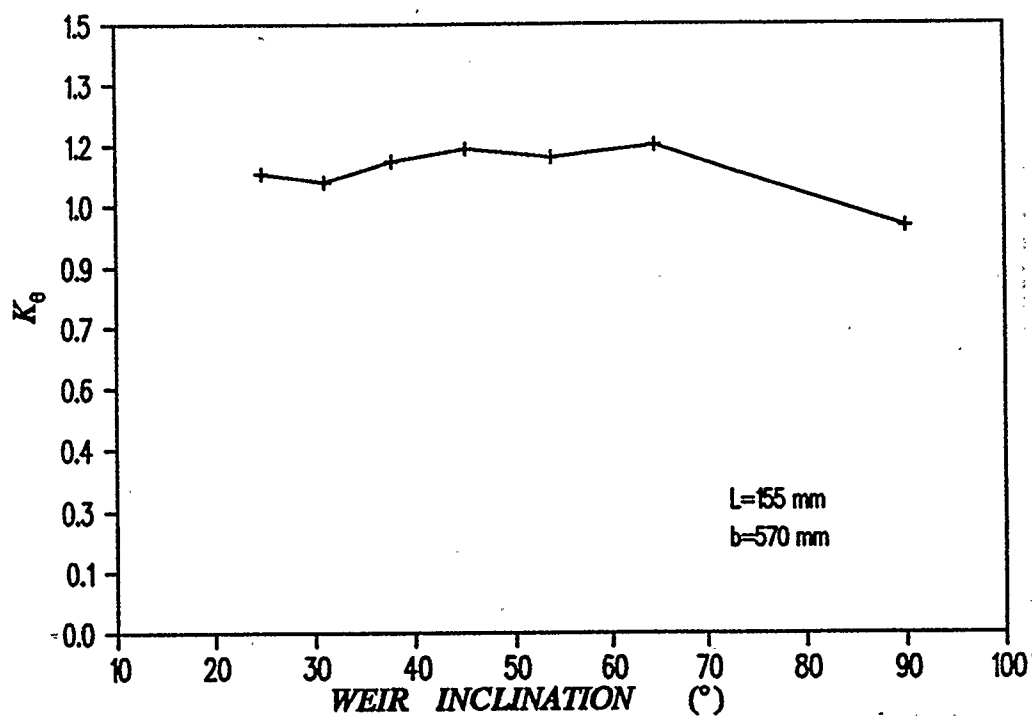


Fig.51  $K_\theta$  vs  $\theta$  for weir length 155 mm, width 570 mm

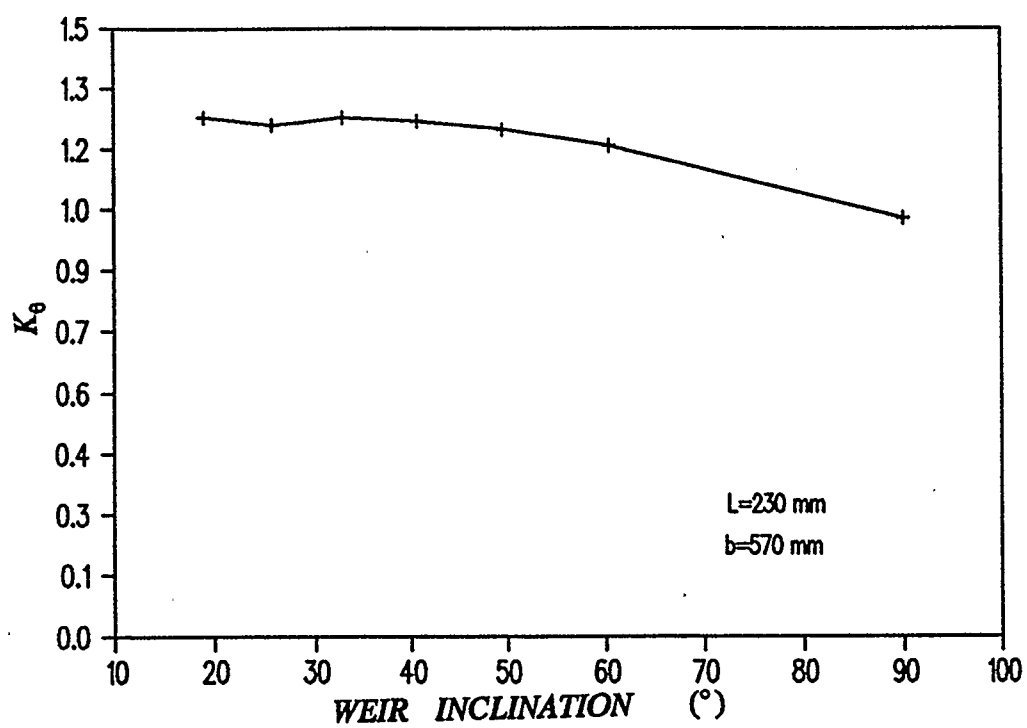


Fig.52  $K_\theta$  vs  $\theta$  for weir length 230 mm, width 570 mm

### 3.3 Submerged Flow

The raw data for submerged flow over weir were summarized in a similar manner as unsubmerged flow data. When the weir operated under submerged flow conditions, the position of the downstream weir was changed seven times for each flow rate and upstream weir angle, to achieve seven degrees of submergence. The flow rate was varied seven times for each upstream weir angle. It follows that 35 worksheets were needed to present the submerged flow data for one weir. Example of such worksheet, which also calculates the upstream and downstream head over weir, is shown on Table 24.

## SUBMERGED FLOW

## INITIAL DATA

$P = 95.00 \text{ mm}$   
 $L = 155.00 \text{ mm}$   
 $b = 420.00 \text{ mm}$   
 $B = 600.00 \text{ mm}$

for flow  $Q = 3.90 \text{ l/s}$

## DOWNSTREAM FLOW LEVELS

D1	D2	D3	D4	D5	D6	Dav
109.6	108.1	109.3	110.5	109.0	109.5	109.33
122.1	122.2	123.0	123.2	122.5	123.9	122.82
134.3	134.9	134.7	135.5	135.6	136.0	135.17
145.1	145.0	145.3	145.7	145.7	146.3	145.52
153.0	153.0	153.2	153.5	153.7	154.2	153.43
162.4	162.5	162.5	162.5	162.7	163.4	162.67
170.0	171.0	171.0	171.0	171.1	171.3	170.90

## UPSTREAM FLOW LEVELS

U1	U2	U3	Uav
124.1	124.8	125.5	124.80
129.4	130.0	130.7	130.03
138.1	138.8	139.1	138.67
146.8	147.3	148.1	147.40
154.7	155.0	154.6	154.77
162.7	163.1	164.2	163.33
170.4	171.1	172.0	171.17

## SUMMARY OF RESULTS

$H_2$	$H_1$
14.33	29.80
27.82	35.03
40.17	43.67
50.52	52.40
58.43	59.77
67.67	68.33
75.90	76.17

Table 24. Example of worksheet with submerged flow data

The equation used to describe submerged flow over weir is given in a form:

$$Q = K_2 \times K_1 \times C H_1^{1.5} \quad (35)$$

where:  $K_2$  - submergence coefficient, accounts for effects of submergence

$K_1$  - unsubmerged coefficient, obtained using the procedure explained above.

The submergence coefficient is defined by equation:

$$K_2 = 10^b \left[ 1 - \left( \frac{H_2}{H_1} \right)^{1.5} \right]^m \quad (36)$$

where  $m$  is an empirically determined exponent.

It is apparent from the form of Eq.35 that it can be written as:

$$Q = K_2 \times Q_1 \quad (37)$$

where  $Q_1$  is flow over weir without submergence.

Thus it can be stated that:

$$\frac{Q}{Q_1} = 10^b \left[ 1 - \left( \frac{H_2}{H_1} \right)^{1.5} \right]^m \quad (38)$$



In order to find the exponents  $m$  and  $b$ , the Eq. 36 was transformed to a logarithmic form as:

$$\log\left(\frac{Q}{Q_1}\right) = b + m \log\left[1 - \left(\frac{H_2}{H_1}\right)^{1.5}\right] \quad (39)$$

From the form of Eq.39 it is obvious that the plot of  $\log(Q/Q_1)$  versus  $\log[1-(H_2/H_1)^{1.5}]$  will be a straight line of slope  $m$  and it will intercept the y-axis at point  $b$ . The values of  $\log(Q/Q_1)$  and  $\log[1-(H_2/H_1)^{1.5}]$  were calculated as shown in Table 25. The linear regression was performed and values of  $m$  and  $b$  calculated for every position of the weir. The submerged coefficient is then calculated using Eq. 36.

Fig. 53 to 56 are plots of  $\log(Q/Q_1)$  versus  $\log[1-(H_2/H_1)^{1.5}]$  for seven angles of weir inclination. In the first case, for weir angle of 24.6 deg, the data points are scattered and the regression coefficient for this case is only 0.90. The data scatter occurred due to the surface jet phenomenon which was observed when weir angles were smaller than 30 deg. Surface jet phenomenon will be discussed in Appendix A.

Figure 57 represents plots of  $\log(Q/Q_1)$  versus  $\log[1-(H_2/H_1)^{1.5}]$  for seven positions of the weir plotted on the same graph in order to observe the pattern.

SUBMERGED FLOW DATA FOR LENGTH 155 mm, WIDTH 270 mm,  
AND HEIGHT 65 mm  $K_1 = 0.68$

LOG(Q/Q <sub>1</sub> )	LOG[1-(H <sub>2</sub> /H <sub>1</sub> ) <sup>1.5</sup> ]	REGRESSION	K <sub>2</sub>	
-0.03	-0.02	-0.04	0.92	b = -0.03
-0.03	-0.03	-0.04	0.91	
-0.01	-0.05	-0.04	0.90	m = 0.30
-0.01	-0.06	-0.03	0.89	
-0.03	-0.06	-0.04	0.89	R = 0.95
-0.04	-0.15	-0.04	0.84	
-0.07	-0.15	-0.05	0.84	
-0.11	-0.16	-0.06	0.83	
-0.08	-0.17	-0.05	0.83	
-0.05	-0.18	-0.05	0.82	
-0.14	-0.24	-0.07	0.79	
-0.11	-0.28	-0.06	0.77	
-0.13	-0.31	-0.07	0.75	
-0.09	-0.32	-0.06	0.75	
-0.14	-0.43	-0.07	0.69	
-0.20	-0.46	-0.09	0.68	
-0.17	-0.46	-0.08	0.68	
-0.15	-0.47	-0.07	0.64	
-0.23	-0.56	-0.10	0.62	
-0.20	-0.60	-0.09	0.60	
-0.23	-0.65	-0.08	0.57	
-0.27	-0.72	-0.11	0.55	
-0.27	-0.76	-0.11	0.52	
-0.28	-0.86	-0.11	0.51	
-0.31	-0.89	-0.11	0.49	
-0.31	-0.94	-0.11	0.47	
-0.36	-1.00	-0.12	0.46	
-0.36	-1.03	-0.13	0.43	
-0.41	-1.12	-0.12	0.42	
-0.37	-1.15	-0.09	0.42	
-0.40	-1.15	-0.13	0.38	
-0.46	-1.31	-0.15	0.33	
-0.47	-1.52	-0.16	0.31	
-0.51	-1.59	-0.17	0.20	
-0.60	-2.26	-0.21	0.19	

Table 24. Example of worksheet with submerged flow data summary and calculated exponents m, b and coefficients K<sub>2</sub>

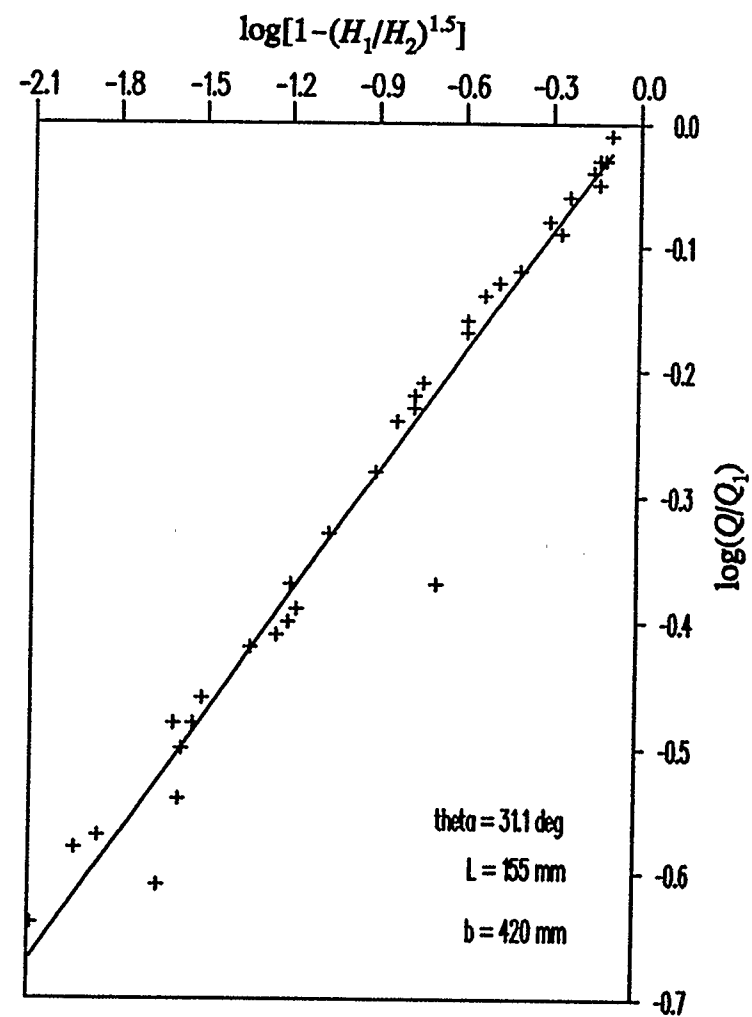
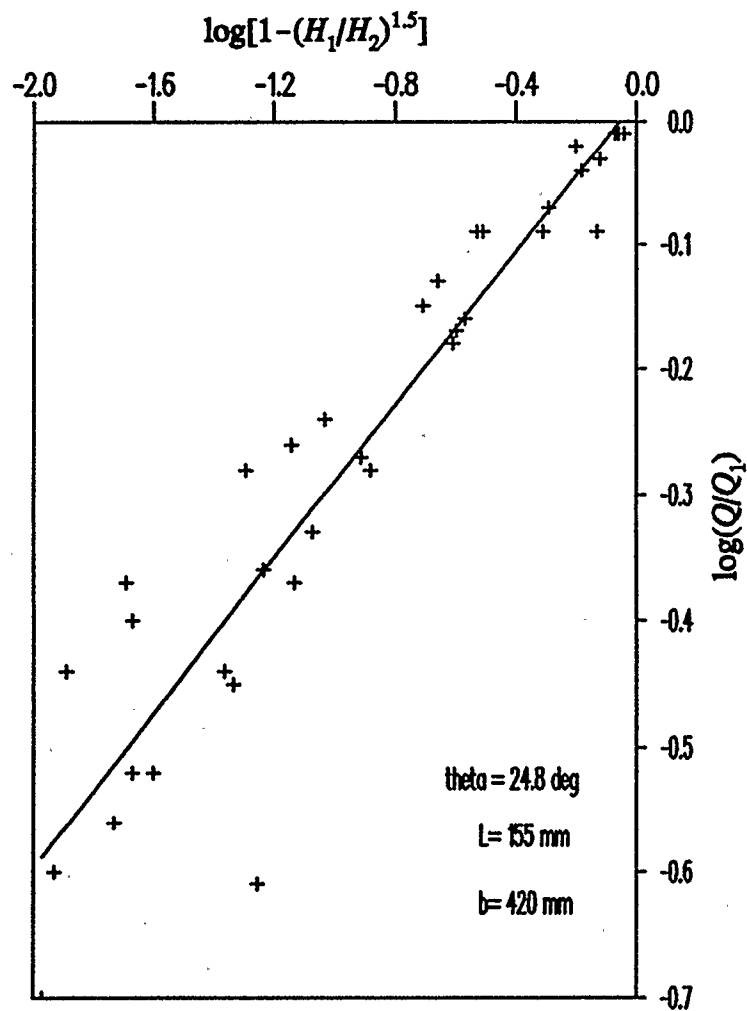


Fig.53 Slope (m) and intercept (b) for weir length 155mm, width 420 mm

and inclination  $\theta=24.6^\circ$  and  $\theta=31.1^\circ$

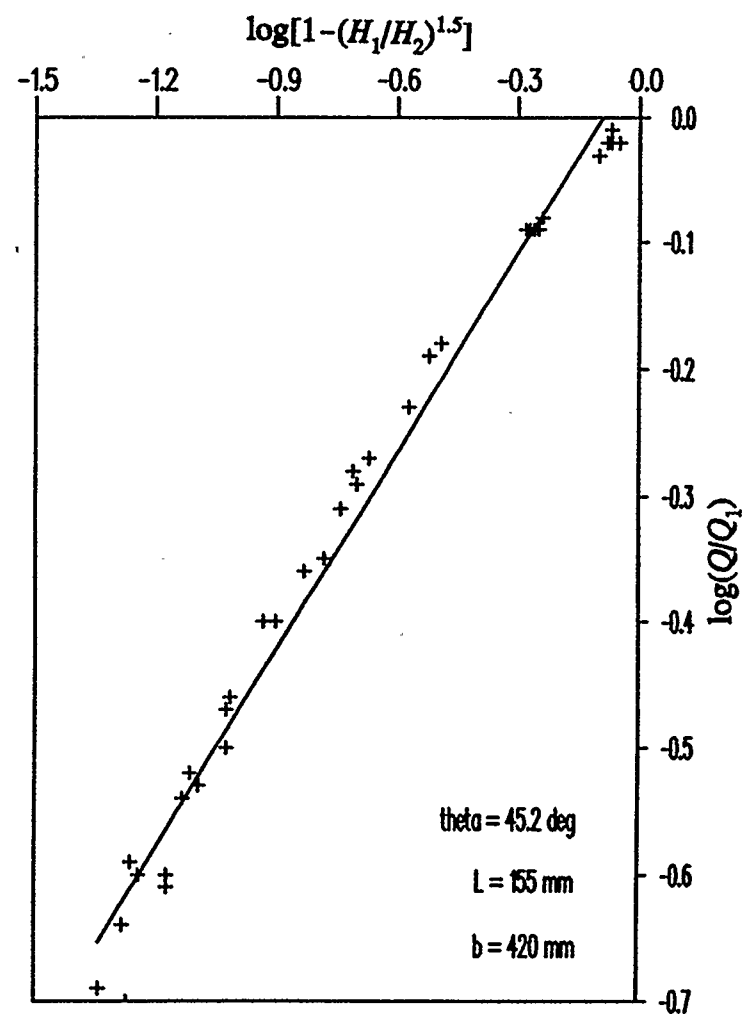
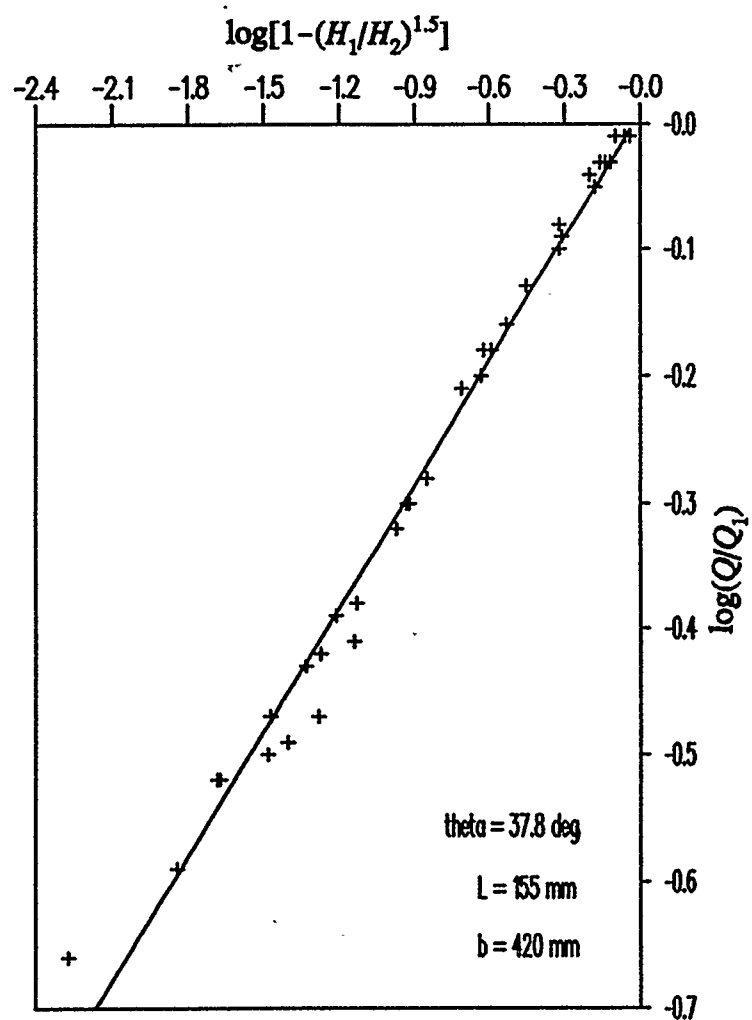


Fig.54 Slope (m) and intercept (b) for weir length 155 mm, width 420 mm  
and inclination  $\theta=37.8^\circ$  and  $\theta=45.2^\circ$

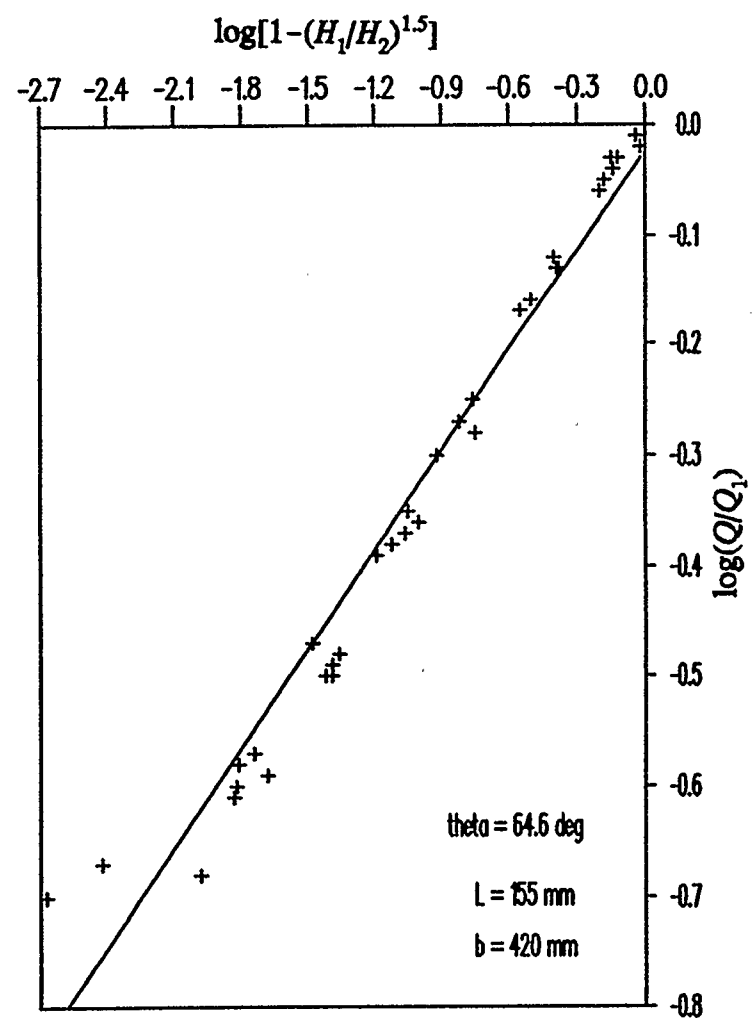
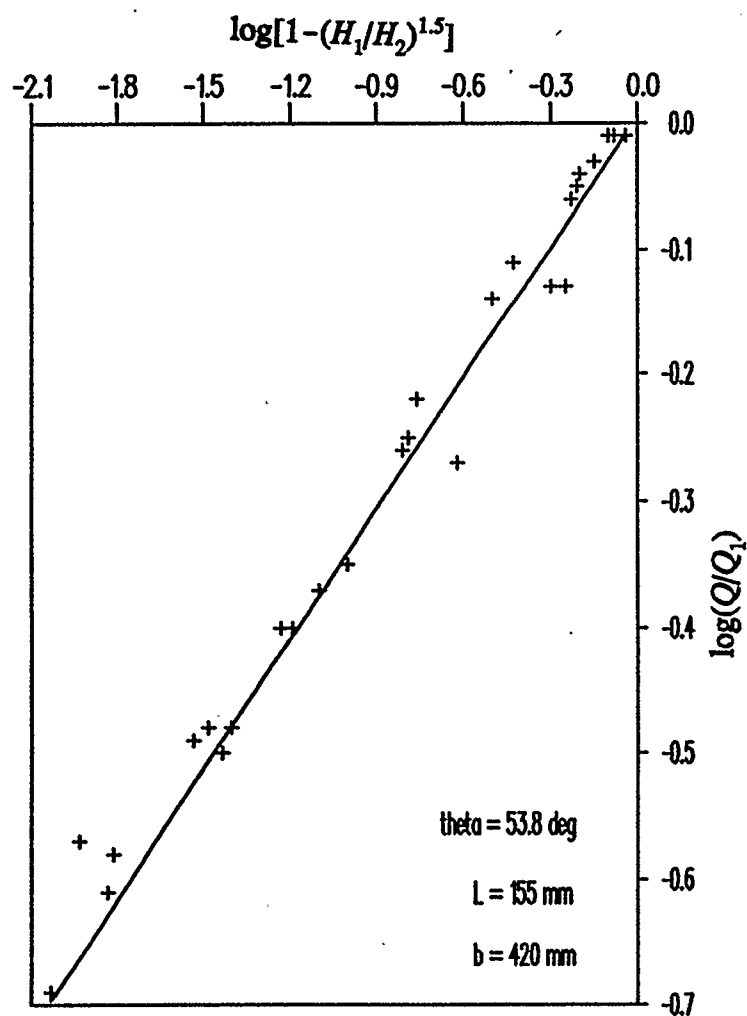


Fig.55 Slope (m) and intercept (b) for weir length 155 mm, width 420 mm

and inclination  $\theta=53.8^\circ$  and  $\theta=64.6^\circ$

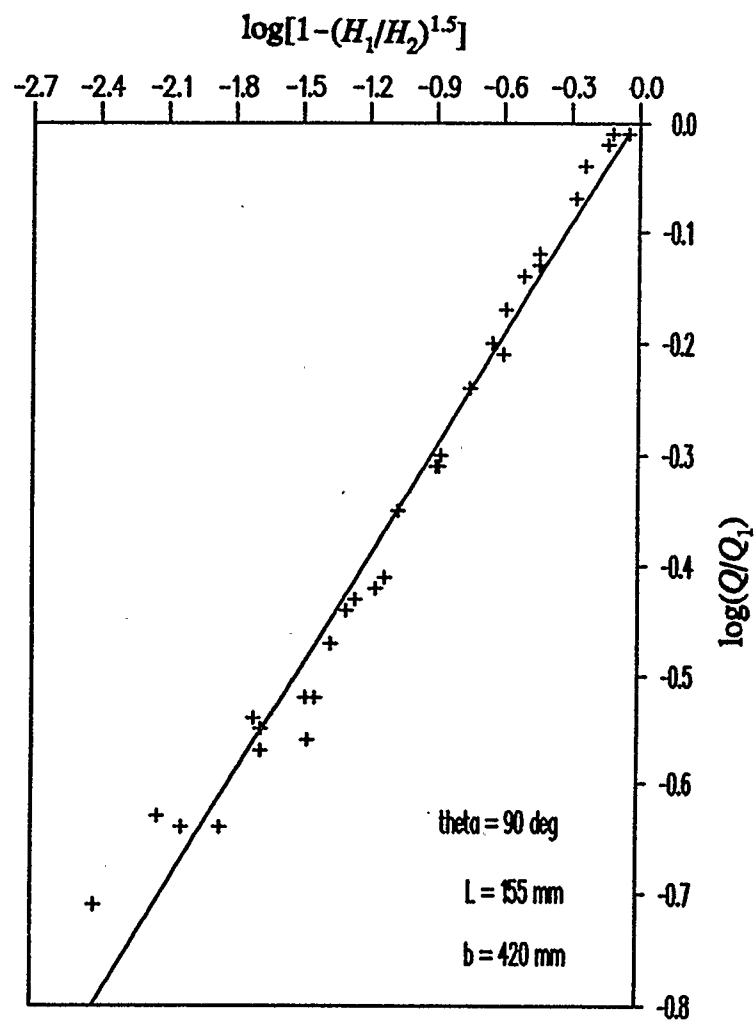


Fig.56 Slope (m) and intercept (b) for weir length 155 mm, width 420 mm and inclination  $\theta=90^\circ$

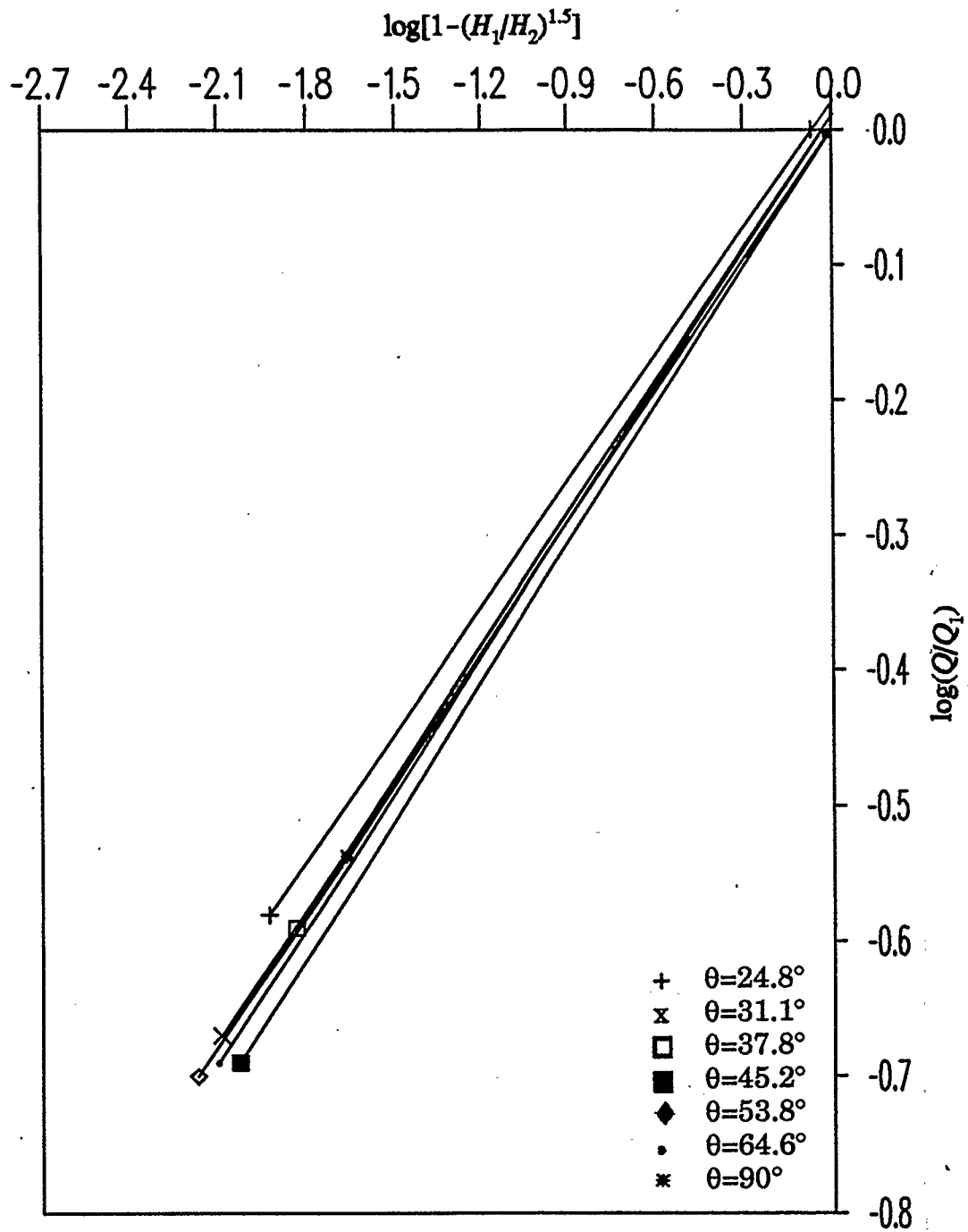


Fig.57 Slope (m) and intercept (b) for weir length 155 mm, width 420 mm and all angles of inclination

It is apparent from the graphs that the least squares line intercepts the y-axis at the points very close to zero. The values of b vary between -0.03 to 0.05.

This implies that the Eq.36 may be written in a form:

$$K = [1 - (\frac{H_2}{H_1})^{1.5}]^m \quad (40)$$

Values of m and b determined using the procedure discussed above for different weir angles are summarized in Tables 26 to 32.

angle	36.9°	41.8°	47.2°	53.1°	60.1°	69°	90°
m	0.49	0.47	0.41	0.45	0.40	0.42	0.40
b	0.02	-0.01	-0.01	-0.01	0.00	0.02	0.00
R	0.96	0.93	0.93	0.96	0.94	0.94	0.97

Table 26. Values of m, b and R for weir of length 75 mm and width 420 mm



angle	24.8°	31.1°	37.8°	45.2°	53.8°	64.6°	90°
m	0.31	0.32	0.33	0.32	0.36	0.30	0.33
b	0.02	0.01	0.01	0.05	0.00	-0.02	0.01
R	0.96	0.97	0.98	0.98	0.95	0.97	0.98

Table 27. Values of m, b and R for weir of length 155 mm and width 420 mm

angle	36.9°	41.8°	47.2°	53.1°	60.1°	69°	90°
m	0.48	0.51	0.44	0.45	0.45	0.40	0.40
b	-0.05	-0.02	-0.02	0.02	-0.01	-0.03	0.00
R	0.89	0.91	0.91	0.95	0.97	0.97	0.96

Table 28. Values of m, b and R for weir of length 75 mm, width 570 mm

angle	24.8°	31.1°	37.8°	45.2°	53.8°	64.6°	90°
m	0.36	0.40	0.38	0.36	0.34	0.36	0.38
b	-0.03	0.01	-0.04	-0.02	-0.01	-0.02	0.00
R	0.92	0.91	0.97	0.94	0.95	0.97	0.90

Table 29. Values of m, b and R for weir of length 155 mm, width 570 mm

angle	36.9°	41.8°	47.2°	53.1°	60.1°	69°	90°
m	0.45	0.43	0.38	0.42	0.37	0.41	0.37
b	0.01	0.00	0.01	0.02	-0.01	-0.01	0.00
R	0.94	0.95	0.97	0.97	0.98	0.99	0.98

Table 30. Values of m, b and R for weir of length 75 mm, width 270 mm

angle	24.8°	31.1°	37.8°	45.2°	53.8°	64.6°	90°
m	0.30	0.32	0.30	0.29	0.33	0.34	0.35
b	-0.03	0.03	0.00	0.00	-0.02	0.01	0.04
R	0.95	0.89	0.93	0.94	0.98	0.97	0.97

Table 31. Values of m, b and R for weir of length 155 mm, width 270 mm

angle	19°	25.8°	32.9°	40.7°	49.5°	60.4°	90°
m	0.27	0.31	0.30	0.33	0.30	0.35	0.31
b	-0.04	0.01	0.04	-0.01	-0.01	0.00	0.01
R	0.88	0.98	0.90	0.98	0.92	0.99	0.93

Table 32. Values of m, b and R for weir of length 230 mm, width 270 mm

The submerged studies for weirs of length 230 mm, width 420 mm; and length 230 mm, width 570 mm could not be performed. The surface jet phenomenon was very prominent when the weirs were submerged, hence it was impossible to complete experimental program and take depth readings with satisfactory accuracy. The photographs of the surface jets observed when these two weirs were in operation are shown on Fig.58 and Fig.59.



Fig. 58 Surface jet observed on submerged weir  
of length 230 mm, and width 420 mm



Fig. 59 Surface jet observed on submerged weir  
of length 230 mm, and width 570 mm

### 3.4 Error Analysis

The error analysis was conducted for the smallest and largest structures (weir of length 75 mm, width 270 mm, and weir of length 230 mm, width 570 mm). Two values of discharge were considered for the analysis, one in upper and one in the lower range of operation. The values of discharge were then changed by  $\pm 5\%$  and the coefficients  $K_1$  and  $K_0$  recalculated, as shown in Table 33. The procedure showed that the values of  $K_1$  and  $K_0$  for both structures changed by 4% for both low and high flow rates. The maximum error of the flow rate readings, as determined by the discharge calibration, does not exceed 2% for low flow rates and 0.5% for high flow rates. It follows that there might be a 2% error in  $K_1$  and  $K_0$  values, for very low flow rates, while the coefficients should be correctly determined for higher flow rates.

The analysis also demonstrated that the error of  $\pm 0.1$  mm in the depth readings does not change the values of coefficients, and the  $\pm 0.1$  mm is the accuracy of the point gauges used in the experimental procedure. The regression coefficients  $R$  that correspond to  $K_0$  and  $K_1$  all equal unity which also indicates the quality of the data.

Q	H <sub>1</sub>	K <sub>1</sub>	K <sub>0</sub>
1.03	16.30	0.62	1.04
1.08	16.30	0.59	1.00
0.98	16.30	0.64	1.08
1.03	16.20	0.62	1.04
1.03	16.40	0.62	1.04
19.40	116.23	0.61	1.01
18.43	116.23	0.58	0.97
20.37	116.23	0.63	1.05
19.40	116.13	0.61	1.04
19.40	116.33	0.61	1.04
3.50	19.63	0.76	1.24
3.33	19.63	0.72	1.18
3.67	19.63	0.79	1.30
3.50	19.53	0.76	1.24
3.50	19.73	0.76	1.24
20.00	62.80	0.75	1.21
19.00	62.80	0.72	1.15
21.00	62.80	0.79	1.27
20.00	62.70	0.75	1.21
20.00	62.90	0.75	1.21

Table 33. Error analysis for unsubmerged flow over weir

The possible error in the submerged flow data might be more significant, due to the occurrence of the surface jet downstream of the submerged weir. The error shows in the data scatter (Fig. 53 to Fig. 56) and lower values of the regression coefficients. However, the regression analysis was performed on the submerged flow data, so the error was "regressed out" and it was not likely to have influenced the calculated values of  $m$  and  $b$  too much.

## Chapter 4

### DISCUSSION OF RESULTS

The extensive experimental program required for this study was carried out successfully. The data collected for unsubmerged and submerged flow over weir are within an expected range of error as evident from the error analysis. During the experimental procedure several problems were encountered.

The first problem was that the space beneath the weir nappe may not have been at atmospheric pressure for low weir heights, as the rubber hose installed for the aeration was filled with water and thus ineffective. But since the demand for air beneath the nappe for low weir heights is very small, the error due to insufficient aeration was not significant.

A factor limiting the amount of data that could be collected was encountered when the discharge was so high that the water began to overflow the flume. For this reason, the data for the larger weirs could be obtained only for lower flow rates, which implies certain limitations on the data in this range.

As mentioned earlier, the surface jet phenomenon was prominent when the weir operated under submerged flow conditions, and it made measurements



partially solved by taking depth readings very close to the channel walls, where the water surface was less disturbed. For weir of width 570 mm , however, this procedure could not be applied. Special care had to be taken to position the point gauge where the turbulence and the water surface distortion were at the minimum. Even though all precautions were taken to obtain as accurate readings as possible and to lessen the effects of the jet, certain error did occur, which shows in the data scatter and lower values of regression coefficients in the case of submerged weirs.

Equation 18 was used in the analysis, as it regards the combined effects of weir and channel geometry (coefficient  $K_e$  in Eq. 18), inclination (coefficient  $K_\theta$ ) and submergence (coefficient  $K_2$ ) on weir hydraulics.

The values of  $K_\theta$  determined in the study are not close to the values published elsewhere. There is no reason, however, to disbelieve these values, as the data do not show significant error and the analysis was successfully completed. It seems that the actual hydraulics of inclined weirs are more complex than it appears, and even the Equation 18 can not be used to fully describe the phenomena that are pronounced when the weir is inclined.

One explanation of quite unexpected pattern of  $K_\theta$  could be the fact that inclined weir operates somewhere between suppressed and contracted mode, and Eq.18 does not recognize this phenomenon.

The values of unsubmerged coefficient  $K_1$ , which is a combination of  $K_e$  and

$K_0$ , were obtained as discussed in Chapter 3, and these values were used in submerged flow analysis to determine the exponent  $m$ , intercept  $b$ , and consequently the submergence coefficient  $K_2$ . It should be noted that unsubmerged flow readings, used to obtain  $K_1$  values, were independent of submerged flow readings. Still, the values of submergence coefficient  $K_2$  are correctly determined, as could be seen from the fact that they are equal to unity at the beginning of weir submergence and then decrease in relation to the increasing degree of submergence. There might be a 3% - 5% error in the cases where the surface jet phenomenon was pronounced, as some  $K_2$  values are slightly above unity and which is theoretically incorrect and has to be a result of error in the data.

The exponent  $m$  does change with the weir inclination, but the pattern of change is not obvious. The reason for this is most likely the same as for the pattern of  $K_0$  coefficients.

It should be pointed out that that the development of a surface jet during the experiments with submerged weirs was unexpected. In the published literature dealing with the physical modeling of flow over submerged sharp crested weirs that was used as reference for this study, this phenomenon was not mentioned. The surface jet development occurred either due to some effect of inlet conditions, or because of the critical value of the Froud number of the flow downstream of the submerged weir.

## Chapter 5

### CONCLUSIONS AND RECOMMENDATIONS

#### 5.1 Conclusions

In this study the flow over a pivoting overshoot sharp crested weir was observed for weir operating under both submerged and unsubmerged conditions.

The effect of the geometry of weir and channel and  $H_1/P$  ratio on the discharge over weir is represented in the effective discharge coefficient  $K_e$ . The coefficient  $K_e$ , was calculated for every flow rate and corresponding head  $H_1$  using Eqs. 31, 32 and 33. The obtained values of  $K_e$  range from 0.59 to 0.64. It is apparent from the data that the values of  $K_e$  of 0.59 and 0.60 correspond to the small structures, i.e. weirs of width 270 mm, values of  $K_e$  between 0.60 and 0.62 correspond to the weirs of width of 420 mm and values of  $K_e$  in the upper range (0.62 to 0.64) correspond to the weirs of width 570 mm. For weirs of same width, the values of  $K_e$  are smaller for smaller  $H_1/P$  ratios.

The inclination coefficient  $K_\theta$  was determined as explained in Chapter 3, and the values are presented in Tables 15 - 23, and Fig. 44 - 45. Clearly, the

and the values are presented in Tables 15 - 23, and Fig. 44 - 45. Clearly, the values of  $K_0$  vary substantially, and there does not seem to be an observable pattern of the variations. In order to find the range of  $K_0$  variations, all values were tabulated as shown in Table 34 and plotted in Figs 60 - 65. Figures demonstrate that the pattern of  $K_0$  changes for either weir width or length and can not be determined. The Table 34 indicates that the coefficients range from 1.00 to 1.30 for all weir widths. The values of  $K_0$  for a weir in a vertical position equal unity or are very close to unity for all cases, which means that this study tends to support the existing theory for vertical weirs. However, it is extremely difficult to explain the pattern of  $K_0$  for inclined weirs. The  $K_0$  values determined in this study do not comply with the published values, except in the case of the smallest structure ( weir of length 75 mm and width 270 mm). The data used for the study, however, was collected using appropriate experimental procedures and the error is within the acceptable range. The fact that  $K_0$  ranges from 1.00 to 1.30 is significant, as it shows that the effect of weir inclination must be given an appropriate consideration in design, otherwise an error of up to 30% can occur in flow rate prediction.

$\theta$ (°)	270 mm	420 mm	570 mm
19	1.28	1.18	1.28
24.8	1.13	1.16	1.13
25.8	1.19	1.16	1.26
31.1	1.15	1.13	1.11
32.9	1.22	1.21	1.28
36.9	1.05	1.23	1.19
37.8	1.12	1.11	1.16
40.7	1.17	1.10	1.27
41.8	1.02	1.30	1.12
45.2	1.11	1.08	1.19
47.2	1.02	1.25	1.13
49.5	1.22	1.06	1.25
53.1	1.01	1.27	1.12
53.8	1.16	1.03	1.17
60.1	0.99	1.16	1.12
60.4	1.18	1.08	1.21
64.6	1.12	1.03	1.20
69	0.99	1.06	1.19
90	1.00	1.00	1.00

Table 34.  $K_0$  range for different weir widths

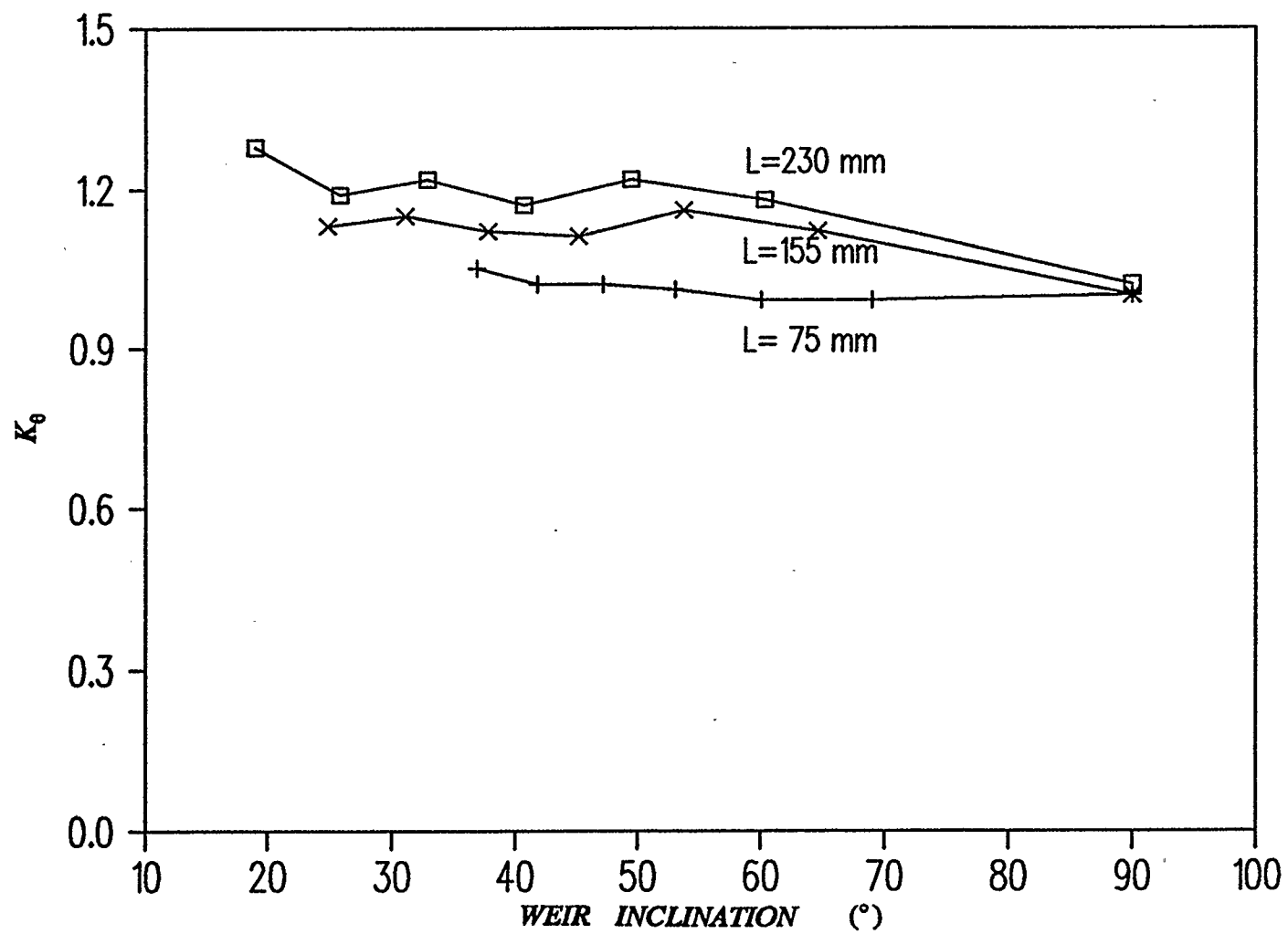


Fig.60  $K_\theta$  vs  $\theta$  for weir width 270 mm

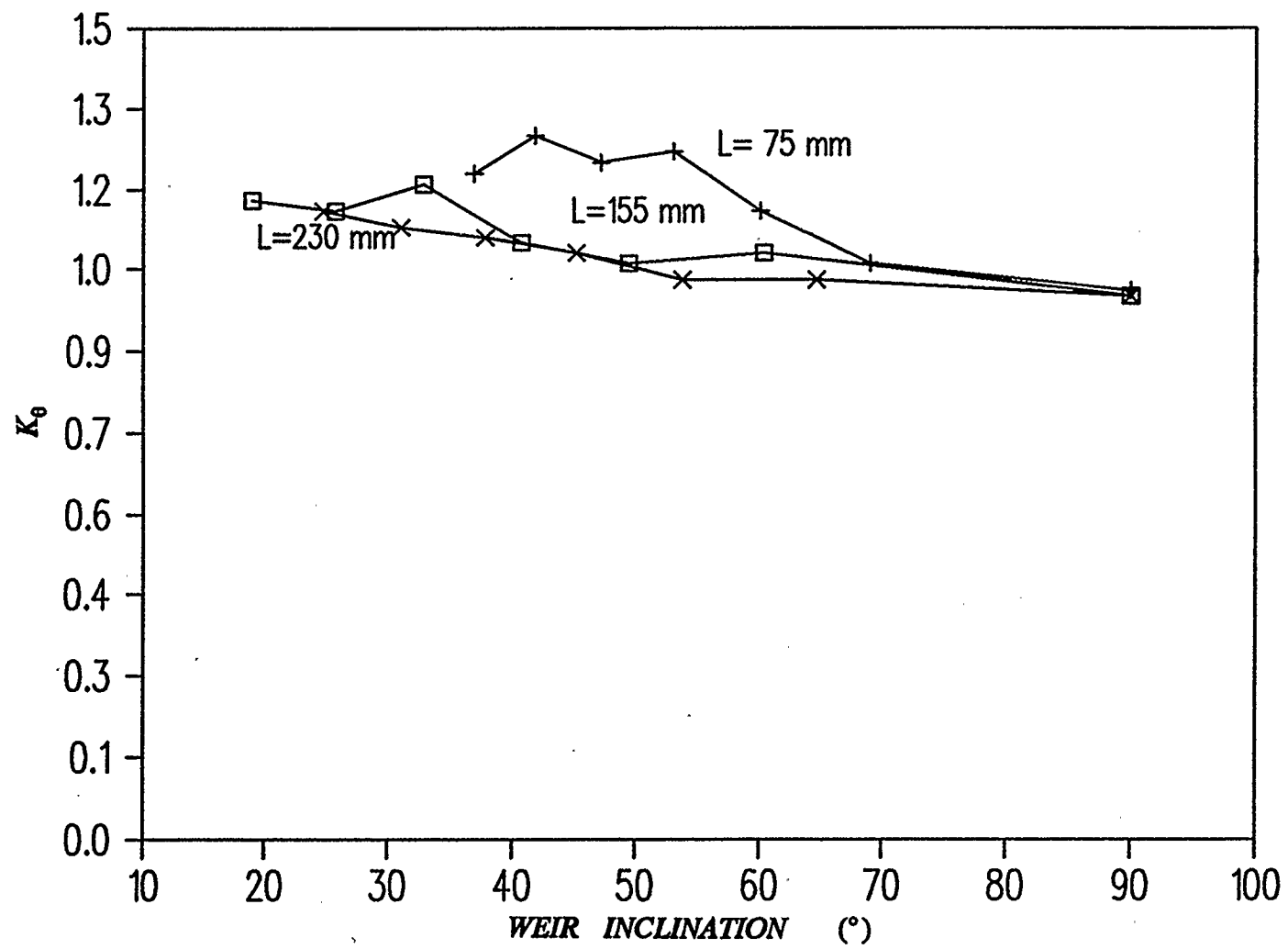


Fig.61  $K_\theta$  vs  $\theta$  for weir width 420 mm

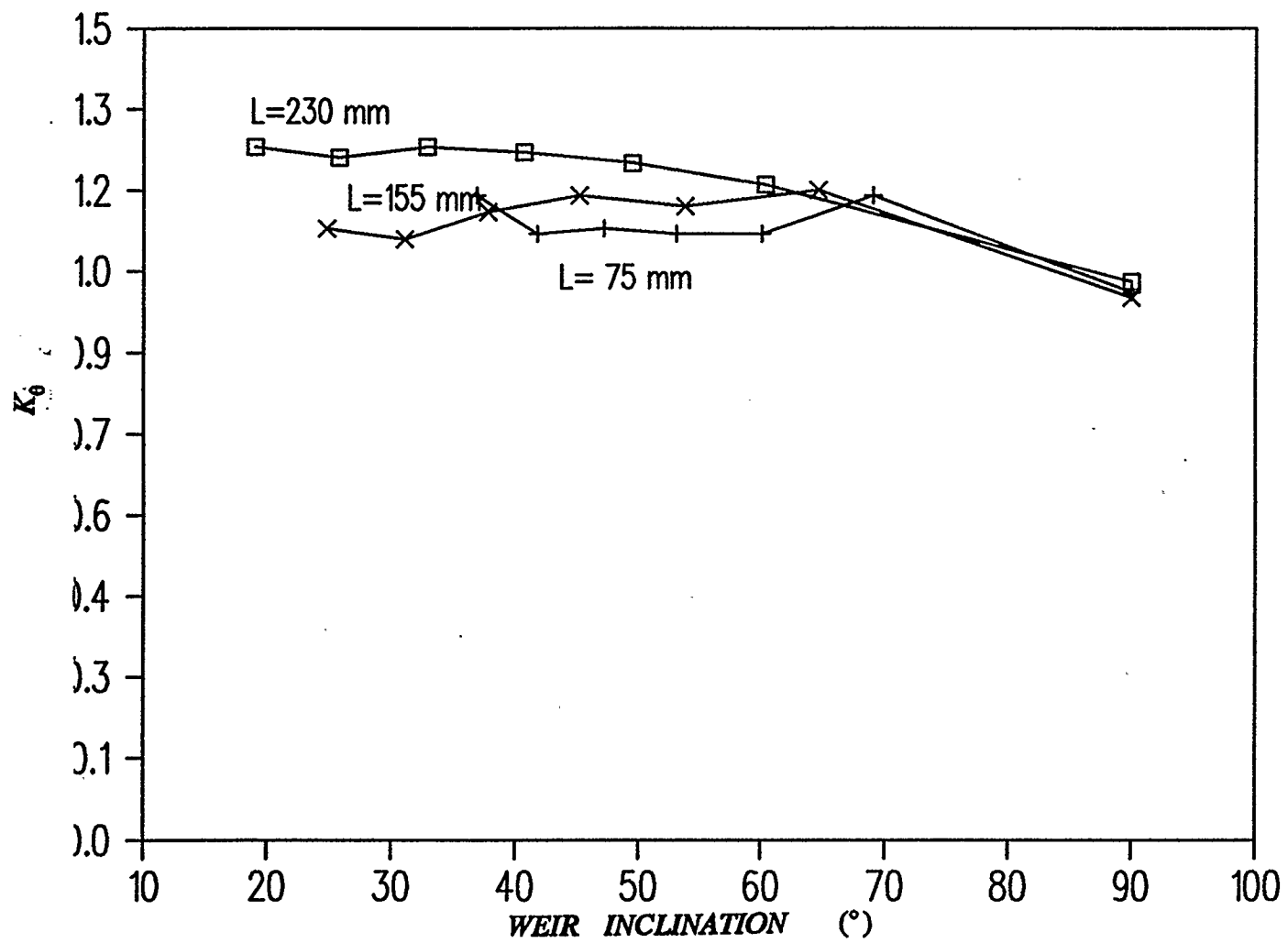


Fig.62  $K_\theta$  vs  $\theta$  for weir width 570 mm



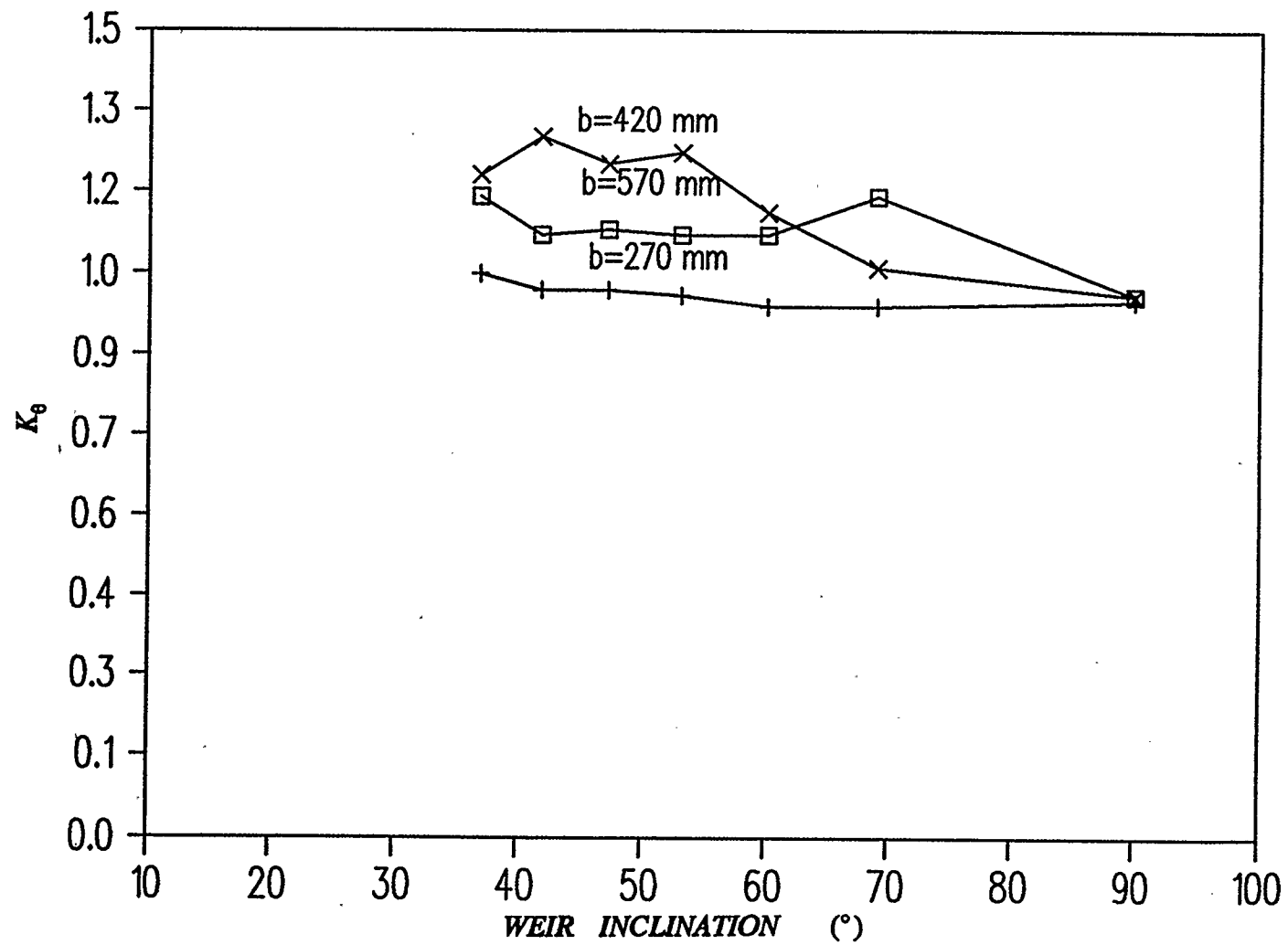


Fig.63  $K_\theta$  vs  $\theta$  for weir length 75 mm

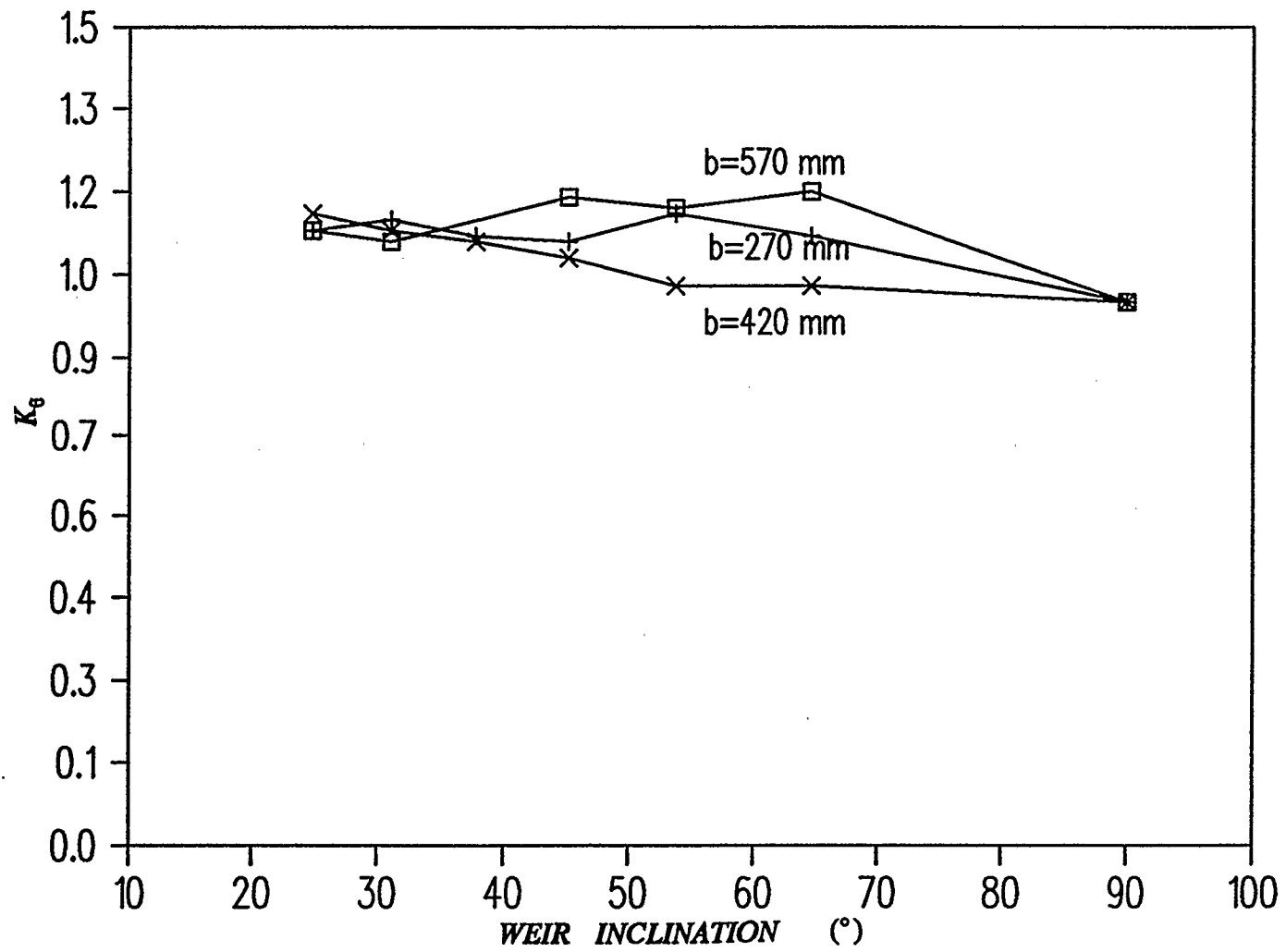


Fig.64  $K_\theta$  vs  $\theta$  for weir length 155 mm

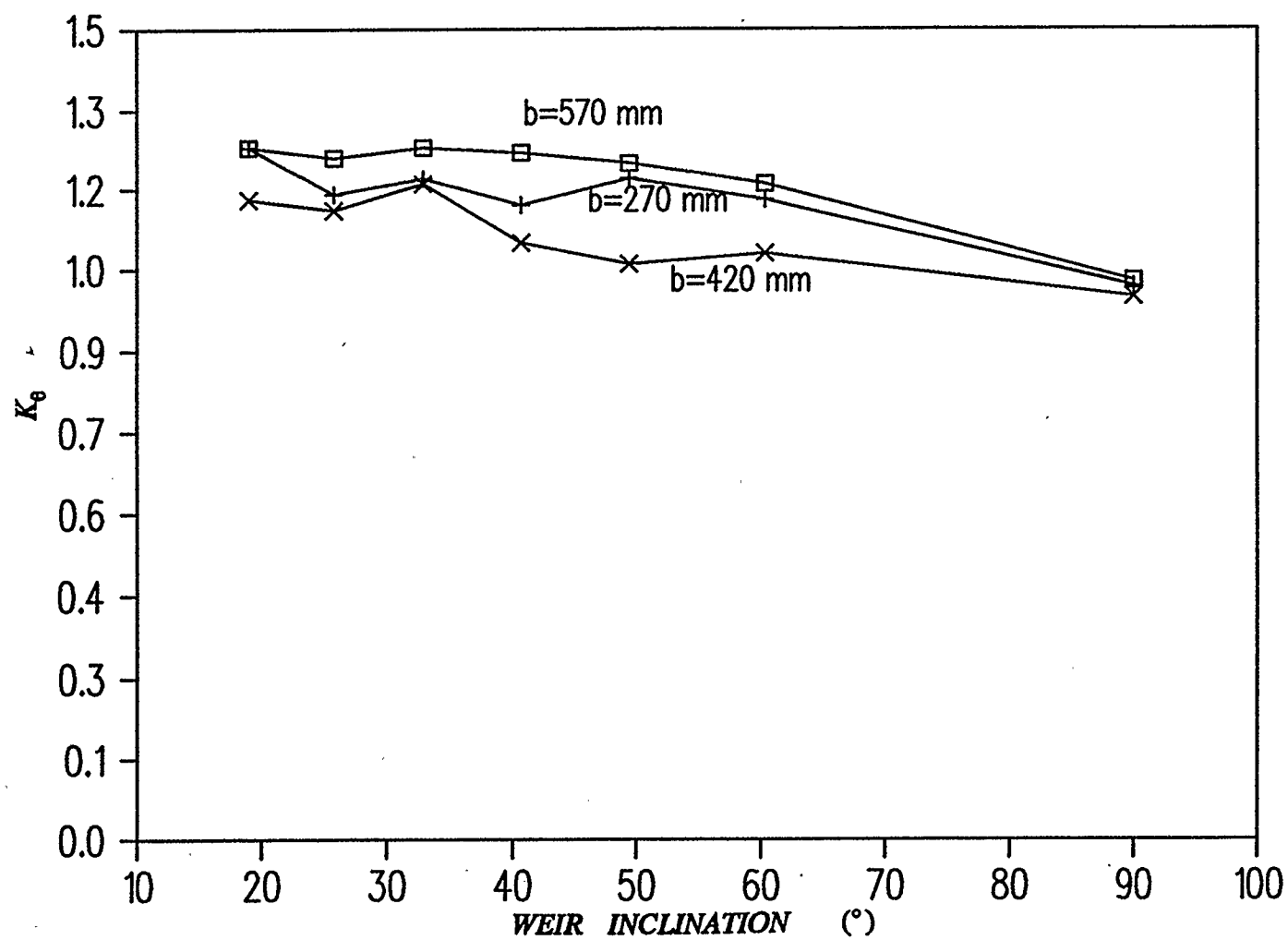


Fig.65  $K_\theta$  vs  $\theta$  for weir length 230 mm

For submerged flow over weir, the values of  $m$  and  $b$  were determined as discussed in Chapter 3, and the submerged flow coefficient  $K_2$  calculated using the Villamonte's equation<sup>(30)</sup>. When the downstream water level is at the weir crest or rises just above the crest and the weir is just slightly submerged, the calculated submerged coefficient is equal to unity or very close to unity. For that case the submergence does not affect the discharge over weir. As the degree of submergence ( $H_2/H_1$ ) increases, the values of  $K_2$  decrease and the discharge becomes more affected by the submergence of the weir. When the weir is deeply submerged, ( $H_2/H_1 > 0.9$ ) the values of  $K_2$  are as low as 0.10, which means that the actual discharge over weir is only 10% of what the flow rate would be if the weir were unsubmerged.

The values of the exponent  $m$  and intercept  $b$  are given in Tables 26 to 32. The values of intercept are very close to zero and the small deviation from zero has probably occurred due to the experimental error. Hence the equation 35 seems to apply rather than Equation 36 to determine  $K_2$ .

The values of  $m$  vary from 0.27 to 0.49. The value of  $m$  published elsewhere is 0.38. The values of  $m$  greater than the published value were obtained for small length weirs ( $L = 75$  mm) while the exponent was smaller than published value for weirs of lengths 155 mm and 230 mm. It should be noted, however, that using the described experimental procedure, it was possible to complete the study for only one weir of length 230 mm.

study for only one weir of length 230 mm.

For weirs of same length and different widths, the values of  $m$  are increasing in relation to the width of the weir.

Values of  $m$  change with the angle of weir inclination, but the steady pattern of the change could not be observed.

One of the objectives of this study was to comment on and advise the applicability of the Equation 18.

Equation 18 considers the combined effects of weir and channel geometry, weir inclination and submergence on a discharge over weir<sup>(16)</sup>. It does not, however, consider the mode of weir operation. When the weir is inclined, contraction develops at the entrance of the weir and the weir is neither suppressed nor contracted.

Apparently, the Eq.18 gives good results when used to predict flow over vertical unsubmerged or submerged weir. In the case of inclined weir, however, some error could be expected. The equation itself does not appear to solve the difficulties associated with the design of the inclined weirs. The extent of possible error can be determined if the effect of the contraction at the weir entrance on the flow over weir are further investigated.

Further investigation should be conducted before the Eq.18 can be safely used, as the hydraulics of the inclined weir seem to be more complex than it is possible to explain using only Eq. 18.

## 5.2 Recommendations

Apparently further research on this topic is necessary. The following suggestions might help future work.

In the future experimental work, surface jet development should be avoided or at least lessened, so that better submerged flow data could be obtained.

In this study the case of rectangular channel was observed. Data were also collected for a trapezoidal channel with sides set at slope 2:1, and preliminary analysis shows that the results are similar to those presented in this study. The next step would be to collect the data for channel with sides set at slope 1:1 and study how the coefficients change with the slope of side walls and whether any pattern could be observed.

As the analysis conducted in this study did not give expected results, the flow pattern at the entrance of the inclined weir should be investigated further. Knowing the characteristics of the flow in that section is necessary to explain why the inclination coefficient  $K_\theta$  and exponent  $m$  have such values and do not follow an identifiable pattern, as was expected. There is a possibility of separation in front of steeply inclined weirs and that might well be the reason that the pattern of inclination coefficient is scattered. In future experimental work the visualization technique should be used in order to determine the exact pattern of flow in that section.,

## REFERENCES

1. Ackers, P., 1978. Weirs and Flumes for Flow Measurement, Wiley Interscience, Toronto, 327 pp.
2. Anderson, V. A., and McLean, R. A., 1974. Design of Experiments - A Realistic Approach, Marcel Dekker, New York
3. Bauzil, V., 1952. Traité d'Irrigation, Éditions Eyrolles, Paris
4. Bendat, J. S., and Piersal, A. G., 1971. Random Data: Analysis and Measurements Procedures, Wiley Interscience, New York
5. Bos, M. G., 1976. Discharge Measurement Structures, Publication No. 20, International Institute for Land Reclamation and Improvement, Wageningen, The Netherlands, 464 pp.
6. Bozic, L., 1987. Uticaj lokalnih fenomena na formiranje linija nivoa u otvorenim tokovima, Research Report No. 87-23, Faculty of Civil Engineering, The University of Belgrade, Yugoslavia
7. Chugaev, R. R., 1972. Гидравлика, Стройиздатель, Москва
8. Daries, M. G., 1943. Hydraulique, Quatorzième Edition, Editions Léon Eyrolles, Librairie de l'Enseignement Technique, Paris
9. Denning, W. E., 1943. Statistical Adjustment of Data, Wiley Interscience, New York

10. Irrigation Systems for the 21st Century, Proceedings of Conference sponsored by the Irrigation and Drainage Division of ASCE, Portland, Oregon, July 28-30, 1987.
11. Kisilev, P. G., 1960. Гидравлика - Специальный Курс, Гл. 5, Водосливы, Стройиздать, Москва (MIS USSR)
12. Leliavsky, s., 1981. Design Textbook in Civil Engineering, Volume V, Weirs, Chapman and Hall, London
13. Majcherek, H., 1985. Modeling of Flow Velocity Using Weirs, Journal of Hydraulic Engineering, Vol 111, No.1, ASCE Jan.1985, 64 pp.
14. Majcherek, H., 1985. Submerged Weirs, Journal of Hydraulic Engineering, Vol 111, No.1, Jan 1985, ASCE, 163 pp.
15. Manz, D. H., 1988. Computer Simulation of Irrigation Conveyance Systems Using the ICSS Model, Proceedings of the Third International Conference on Computing in Civil Engineering, August 1988, Vancouver, B.C., Canada, 605 pp.
16. Manz, D.H., 1988. Preliminary Investigation of the hydraulics of pivoting sharp crested rectangular weirs, Proceedings of the Annual Conference of the Canadian Society for Civil Engineering, St. John's, Newfoundland, June 7-10, 1988.
17. Merriman, M., 1889. A Treatise on Hydraulics, Fourth Edition, John Wiley and Sons, New York



18. Mikhail, E. M., and Ackerman, F., 1976. Observations and Least Squares, IEP Series in Civil Engineering, A Dun-Donnelley Publisher, New York
19. Nakasone, H., 1987. Study of Aeration at Weirs and Cascades, Journal of Environmental Engineering, Vol 113, No.1, Jan. 1987, ASCE, 64 pp.
20. Planning Now for Irrigation and Drainage in the 21st Century, 1980. Proceedings of the conference sponsored by the Irrigation and Drainage Division of the ASCE, Co-sponsored by the Nebraska Section of ASCE, Lincoln, Nebraska, July 18-21, 1980.
21. Planning, Operation, Rehabilitation and Automation of Irrigation Water Delivery Systems, 1987. Proceedings of the Symposium sponsored by Irrigation and Drainage Division of the ASCE and the Oregon Section, ASCE, Portland, Oregon, July 28-30, 1987.
22. Rajaratnam, N., and Muralidhar, D., 1968. Flow Below Deeply Submerged Weirs, Proceedings of ASCE, J. Hydraulic Division, Vol 94, HY3, 663 pp.
23. Rajaratnam, N., and Subramanian, S., 1983. An Experimental Study of Plane Turbulent Buoyant Surface Jets and Jumps, Water Resources Engineering, Report 83-3, Dept. of Civil Engineering, The University of Alberta, Edmonton, Alberta, Canada
24. Ramakrishnan, C. R., 1979. Flow Characteristics of Rectangular and Trapezoidal Finite Crest Width Weirs and Triangular Profile Weirs,

a Thesis submitted to the Department of Civil Engineering, Indian Institute of Science, Bangalore, India

25. Ramamurthy, A. R., Tim U. K., Roo, M. U., 1987. Weir -Orifice Units for Uniform Flow distribution, ASCE Journal of Environmental Engineering, Vol 115, Issue No.1, Feb. 1987, 155 pp.
26. Reese, A. J., and Maynard, S. T., 1986. Design of Spilway Crests, ASCE Journal of Hydraulic Engineering, Vol 113, No.1, Jan. 1985, 163 pp.
27. Sreetharan, M., 1988. Discharge Characteristics of Rectangular Profiled Weirs, Proceedings of the National Conference on Hydraulic Engineering sponsored by ASCE, 969 pp.
28. Swamee, P. K., 1988. Generalized Rectangular Weir Equations, ASCE Journal of Hydraulic Engineering, Vol 114, No.8, Aug. 1988, 945 pp.
29. Vennard, J. K., and Weston, R. F., 1943. Submergence Effect on Sharp crested weirs, Engineering News Record, June 1943, 118 pp.
30. Villemonte, J. R., 1947. Submerged Weir - Discharge Studies, Engineering News Record, May 1947, 54 pp.

## APPENDIX A

### Surface Jet Phenomenon

In the course of experimental work, the surface jet phenomenon was observed downstream of the weir operating under submerged flow conditions (see Fig. 66 to Fig. 69)

For model weirs of length 230 mm and widths 570 mm and 420 mm, which are the largest structures used in the experimental program, the surface jet development was very prominent (Figs. 58 and 59) and the experimental procedure could not be completed. For smaller structures, the surface jet eddies were not so large. Apparently, the size of the surface jet eddies depend largely on the weir geometry and the relative size of the weir to downstream channel.

The degree of submergence also appears to be an important factor which determines the development of the surface jet. The degree of submergence is determined by the submergence ratio  $H_2/H_1$ . In cases where the ratio  $H_2/H_1$  was greater than 0.9 or less than 0.1, the submerged jet did not occur. The largest jet eddies were noticed for values of  $H_2/H_1$  around 0.5.

The angle of the weir inclination is another factor that apparently affects the occurrence of a surface jet and the size of jet eddies. As the weir angle decreased, the size of turbulent eddies increased, particularly for angles less than  $45^\circ$ .

The size of eddies also depend on the flow region in which they develop. In

a flow development region ( the region just downstream of the weir of length approximately  $P$ ) the eddying was very prominent, while in a fully developed flow region the eddies were subsiding and much smaller.

The surface jet phenomenon was observed for weirs operating in both suppressed and contracted mode.

The scatter of the unsubmerged flow data can be explained by a surface jet development, which substantially decreased the accuracy of measurements.



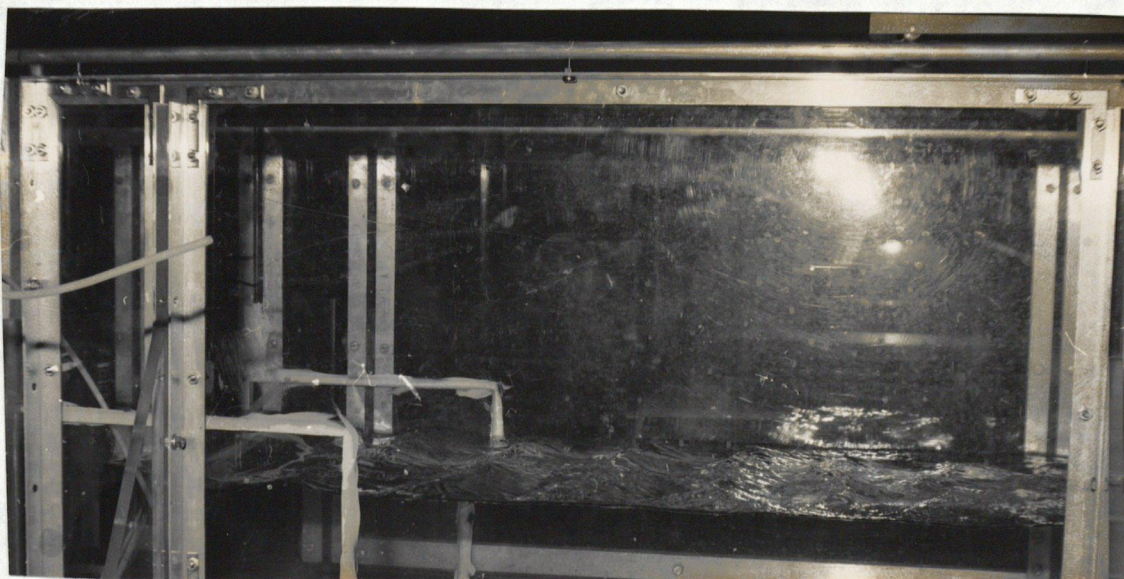


Fig. 66 Surface jet observed on submerged weir  
of length 155m, and width 420 mm

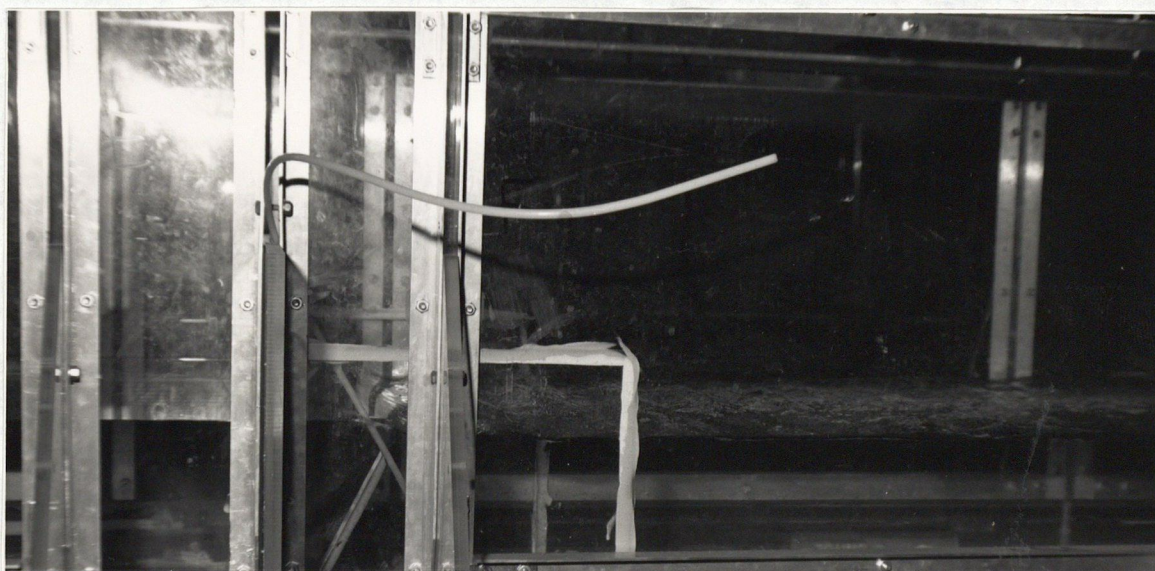


Fig. 67 Surface jet observed on submerged weir  
,  
of length 155 mm, and width 570 mm



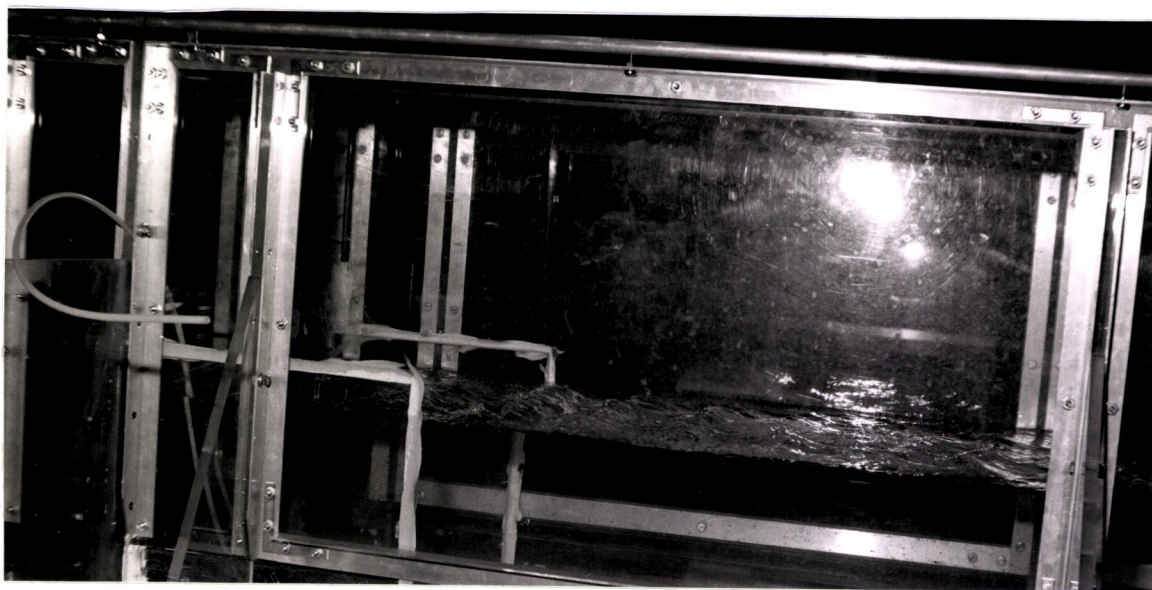


Fig. 68 Surface jet observed on submerged weir  
of length 75 mm, and width 420 mm

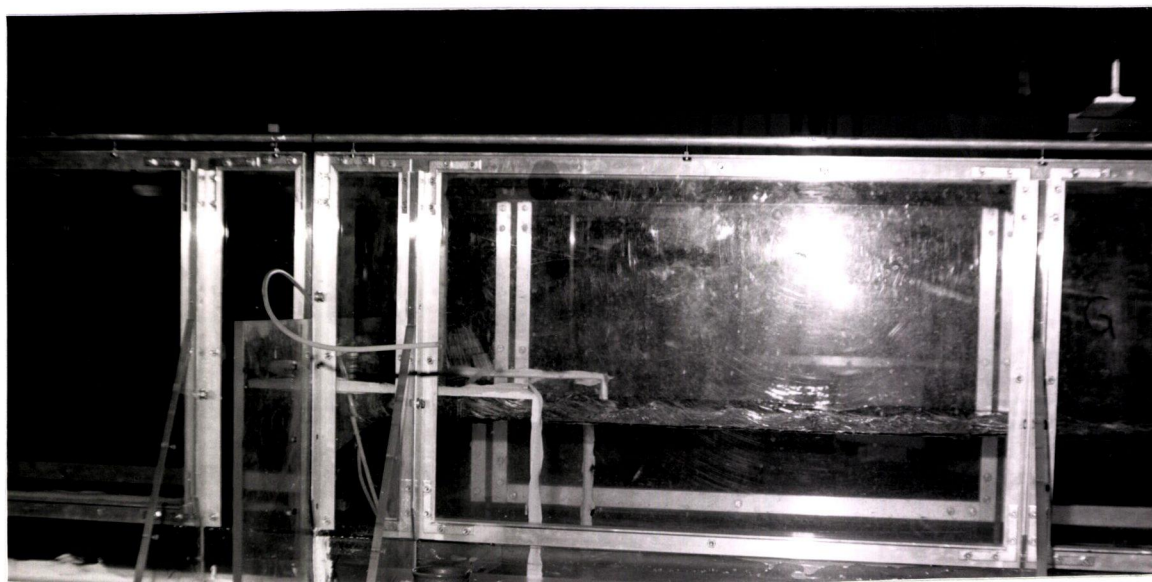


Fig. 69 Surface jet observed on submerged weir  
of length 155 mm, and width 270 mm

## APPENDIX B



### Derivation of Bazin's Equation

The flow pattern over a weir is very complex. The streamlines of the flow over weir are curved and thus there is no cross-section of the flow where the pressure is uniform. Hence it is very difficult to determine the variation of the velocities within the stream. There are also turbulence, surface tension and friction effects affecting the flow over weir. Therefore a rather drastic simplifications of weir hydraulics were necessary in order to derive the relationship between the flow rate and the depth of flow at the weir.

A sharp-crested, rectangular weir is considered. The weir crest is horizontal and normal to the direction of the flow. The necessary assumptions are as follows:

1. The velocities of particles in the stream upstream of weir are uniform and parallel and the pressure varies according to the hydrostatic law.
2. All flow particles passing through the weir move horizontally, and perpendicular to the plane of the weir. The water surface is horizontal as far as the plane of the weir.
3. The weir nappe well aerated and under the atmospheric pressure.
4. The effects of viscosity of the fluid and surface tension are neglected.
5. The flow over weir is steady and irrotational.

According to these assumptions, the flow over weir is idealized and the

actual weir hydraulics simplified, thus making it possible to derive the basic weir equation.

For a typical streamline, with the datum taken to be in the plane of the weir crest, and with section 1 taken to be upstream of the weir and section 2 at the weir crest, the Bernoulli's equation gives:

$$\frac{p_1}{\rho g} + \frac{u_1^2}{2g} + z_1 = 0 + \frac{u_2^2}{2g} + z_2 \quad (41)$$

where:  $z_1$  and  $z_2$  - distance from the datum to the flow particles in sections 1 and 2

$u_1$  and  $u_2$  - velocities of the flow particles in sections 1 and 2

It is apparent that at section 1:

$$\frac{p_1}{\rho g} + z_1 = H \quad (42)$$

where H is a height of the free surface.

Equation (41) can further be written as:

$$u_2 = [2g(H - z_2 + \frac{u_1^2}{2g})]^{0.5} \quad (43)$$

This shows that  $u_2$  varies with  $z_2$ .

The idealized total discharge is now:

$$Q_{ideal} = b \int_0^H u_2 dz_2 \quad (44)$$

$$Q_{ideal} = b\sqrt{2g} \int_0^H \left(H - z_2 + \frac{u_1^2}{2g}\right)^{0.5} dz_2 \quad (45)$$

$$Q_{ideal} = \frac{2}{3} b\sqrt{2g} \left[ \left(H + \frac{u_1^2}{2g}\right)^{1.5} - \left(\frac{u_1^2}{2g}\right)^{1.5} \right] \quad (46)$$

Solution of Eq.(46) is only possible by trial and error procedure, as  $u_1$  depends on  $Q$ . If we assume that the approach velocity  $u_1$  equals zero, the Eq.(46) becomes:

$$Q_{ideal} = \frac{2}{3} Kb\sqrt{2g} H^{1.5} \quad (47)$$

where  $C$  is a discharge coefficient that had to be inserted to account for all the assumptions made.